Klinik und Poliklinik für Neurologie

HABILITATIONSSCHRIFT

Diagnostic and experimental applications of cortico-muscular and intermuscular frequency analysis

zur Erlangung der Lehrbefähigung im Fach Neurologie

Charité-Universitätsmedizin Berlin, Campus Virchow-Klinikum

Pascal Grosse

Prof. Dr. med. Paul Martin

Gutachter: 1. Prof. Dr. med. Benecke

2. Prof. Dr. med. Deuschl

eingereicht: September 2003

Datum der Habilitation: 17.5.2004

Table of contents

Publications of work incorporated in this thesis

Grosse P, Cassidy M, Brown P. EEG-EMG, MEG-EMG and EMG-EMG Frequency Analysis: Physiological Principles and Clinical Applications. *Clinical Neurophysiology* 2002;113:1523-1531.

Grosse P, Guerrini R, Parmiggiani L, Bonanni P, Pogosyan A, Brown P. Abnormal corticomuscular and intermuscular coupling in high frequency rhythmic myoclonus. *Brain* 2003;126:326-342

Grosse P, Kühn A, Cordivari C, Brown P. Synchronising influences in the myoclonus of corticobasal degeneration. *Movement Disorders* 2003;18:1345-1350.

Grosse P, Brown P. The acoustic startle evokes bilatarally synchronous oscillatory EMG activity in the healthy human. *Journal of Neurophysiology* 2003;90:1654-1661.

Grosse P, Edwards M, Tijssen MAJ, Schrag A, Lees AJ, Bhatia KP, Brown P. Patterns of EMG-EMG coherence in limb dystonia. Movement Disorders, *in press*

Abbreviations

1DI	First dorsal interosses muscle
ANOVA	Analysis of variance
APB	Abductor pollicis brevis muscle
CBD	Corticobasal degeneration
CBZ	Carbamazepine
CLB	Clobazam
CZP	Clonazepam
DPH	Phenytoin
EEG	Electroencephalogram
EMG	Electromyogram
ESM	Ethosuximide
FE	Finger extensor muscle
FF	Finger flexor muscle
FFT	Fast Fourier transform
GC	Gastrocnemius muscle
GLM	General linear model
LEV	Levetiracetam
MAR	Multivariate autoregressive model
MEG	Magnetoencephalogram
PB	Phenobarbitone
Pir	Piracetam
PRM	Primidone
SEM	Standard error of the mean
TA	Tibialis anterior muscle
VPA	Valproic Acid

1. Introduction

Since the synchronisation of muscle through the central nervous system had first been demonstrated in humans (McLachlan and Leung, 1991; Farmer et al., 1993) and other primates (Murthy and Fetz, 1992; Murthy and Fetz 1996a; Murthy and Fetz 1996b; Sanes and Donoghue, 1993) about a decade ago frequency analysis of the motor system has increasingly received recognition as a new tool to investigate the human motor system. However, the fact that muscle discharge tends to be rhythmic has been known for almost 200 years. William Wollaston, using a precursor of the stethoscope, was the first to describe this in 1810 (Wollaston, 1810). He determined the rhythm to be in the beta-frequency band by comparing the pitch of the sound picked up over his muscles with that from a horse drawn carriage driven over the cobbled streets of London at different speeds. A century later, the pioneering German neurophysiologist, Hans Piper (Fig. 1), delineated a further modulation of motor unit discharge in the low gamma-frequency band at around 40 Hz (Piper, 1907; Piper, 1912). But only the past decade the has seen steadily growing interest in this field, with specific attention being turned to whether specific patterns of oscillatory drives to muscle may be of pathophysiological and/or diagnostic significance.

Fig. 1

Fig. 1: Hans Edmund Piper, German physiologist, born 1877, died 1915. Read biology in Kiel, Munich, Berlin and Freiburg; PhD in Freiburg in 1902. Research assistant at the Institute of Physiology in Berlin, later in Kiel. In 1908 he became head of the department for physics at the Institute of Physiology in Berlin, 1909 promotion to professor. Initially he focussed his research on embryology, his later work encompassed mostly physiological topics, in particular optics, acoustics. the physiology of muscles and nerves and a theory on electrical currents in the retina where he developed the "Piper's law". (From: Abeßer, Elke/Schubert, Ernst. Das Berliner Physiologische Institut der Humboldt-Universität. 100 Jahre nach seiner Gründung. Wissenschaftliche Schriftenreihe der Humboldt-Universität zu Berlin. Berlin 1977, p. 29)

This line of inquiry is being taken up in the following experiments both in diseased patients and healthy subjects to further assess the relevance of frequency analysis of the motor system. Thus, this work aims at delineating the usefulness of the technique for diagnostic purposes and at providing some new insights into the pathophysiology of some movement disorders such as cortical myoclonus (Chap. 3), dystonia (Chap. 4), and the myoclonus of corticobasal degeneration (Chap. 5). Particular attention is being paid as to whether intermuscular frequency analysis is an asset to the spectrum of methodologies within the scope of frequency analysis of the motor system. Further, it is explored in healthy subjects whether intermuscular frequency analysis is helpful in assessing physiological subcortical oscillations, such as those elicited by the acoustic startle response, as an innovative means to identify non-invasively subcortcal drives within the motor system (Chap. 6).

1.1. Physiological drives to muscle

Frequency analysis is a useful way of analysing neuronal synchrony and is based on the cross-correlation between two separate signals in the time and frequency domain. The principal measure of the linear dependence or correlation between two signals in the frequency domain is coherence. It is mathematically bounded between zero and one, where one indicates a perfect linear relationship and zero indicates that the two signals are not linearly related at that frequency. Thus oscillatory coupling between motor elements of the central nervous system and EMG discharge is most clearly measured as coherence between the motor cortex and muscles whereas the phase informs on the temporal relationship between the two signals.

The human central nervous system drives muscle discharges at a number of frequencies and, although the physiological function of these oscillations is far from clear (Farmer, 1998a; Brown, 2000; Brown and Marsden, 2001), one of the interests from the clinical point of view is that these different activities may be characteristic of functional activities in distinct circuits. The different physiological oscillatory drives to spinal motoneurones

are summarised in table 1.1.

Table 1.1: Physiological oscillatory drives synchronising motor units in humans

frequency range [Hz]	origin	task in which manifest	detection	References
~2 ("common drive")	unknown	isometric contraction, slow movements	EMG-EMG	DeLuca and Erim, 1994; Kakuda et al., 1999
6-12	unknown	isometric contraction, slow movements	MEG-EMG, EMG-EMG	Vallbo and Wessberg, 1993; Conway et al., 1995b; Marsden et al., 2001a
12-18	brainstem	galvanic stimulation of the inner ear	EMG-EMG	Sharott et al. 2003
15-30	motor cortex	submaximal voluntary contraction	MEG-EMG EEG-EMG	Conway et al., 1995b, Halliday et al., 1998
30-60 ("Piper rhythm")	motor cortex	strong voluntary contraction, slow movements	MEG-EMG	Brown et al., 1998
60-90	brainstem	eye movements	EMG-EMG	Brown and Day, 1997; Spauschus et al., 1999
60-100	brainstem	respiration	EMG-EMG	Carr et al., 1994

The first is a low frequency drive at 2-3 Hz, that has been, in retrospect, rather confusingly termed "common drive," even though there are many such drives (DeLuca et al., 1982). This rhythm can be picked up during isometric contraction or slow movements, even in muscles without muscle spindles (Kamen and DeLuca, 1992; DeLuca and Erim, 1994). The site of its generation is unclear. As it is preserved in patients with cortical or capsular strokes (Farmer et al., 1993) it is not likely to have an origin within the corticospinal system.

Oscillations in the 6-12 Hz range have been related to the pulsatile organisation of slow movements at ~10 Hz (Vallbo and Wessberg, 1993) - identical to physiological action tremor - and to the central component of physiological postural tremor (force tremor) (Conway et al., 1995a) as they prove to be unaffected by alterations of the limb mechanics (Halliday et al., 1999; Vallbo and Wessberg, 1996). The olivary-cerebellar system has been

suggested as a possible generator for the 6-12 Hz oscillations (Llinàs and Pare, 1995) based on findings in the animal harmaline-tremor-model (Llinàs and Volkind, 1973). Consistent with this, some studies have failed to show a cortical correlate at ~10 Hz (Kilner et al., 1999; Mima et al., 2000a). Nevertheless, the exclusivity of the subcortical generation of this drive has been challenged as other studies have detected significant cortico-muscular coherence at this frequency (Mima, 1999; Raethjen et al., 2000a; Salenius et al., 1997a) indicative of sensorimotor cortex involvement. In part, this variability in findings may be accounted for by task-dependency. Thus a recent MEG-EMG study found coherence at 6-12 Hz in force tremor with a source unequivocally originating in the primary motor cortex but no such coherence in action tremor (Marsden et al., 2001a).

In contrast, there is general agreement that motor unit synchronisation in the beta (15-30 Hz) and low gamma (30-60 Hz) bands is predominantly driven from the primary motor cortex, with less influential contributions possibly from supplementary motor and premotor cortices (Feige et al., 2000; Marsden et al., 2000a). Coupling between primary motor cortex and muscle has been demonstrated by both MEG (Conway et al., 1995b; Salenius et al., 1997a; Salenius et al., 1997b; Brown et al., 1998c; Gross et al., 2000) and surface EEG (Halliday et al., 1998; Mima et al., 1998a), although coherence in the gamma band is best seen with the former technique due to the low pass filtering charactaristics of the skull and scalp. Cortico-muscular coherence seems ubiquitous and is even demonstrated by those muscles with small representation in the motor cortex such as the paraspinal and abdominal wall muscles (Murayama et al., 2001). The coherence in the beta band appears during weak tonic contraction and is abolished by movement, whereas that in the gamma band is more obvious in strong contractions and may persist during slow movements (Baker et al., 1997; Brown et al., 1998c; Kilner et al., 1999). Oscillatory drives of motor cortex origin above 60 Hz have also been described through electrocorticographic recordings from the motor cortex (Marsden et al., 2000a) as an indication that the conduction properties of the scull prevents the full range of cortico-muscular coherence from being demonstrated when scalp EEG recordings are used.

Cortical oscillations coupled to motor unit discharge may arise intrinsically within the

cortex or may be under extrinsic, subcortical influence. The intrinsic generation of cortical oscillations may involve pacemaker cells, such as the "chattering cells" (Jefferys et al., 1996; Steriade et al., 1993), which fire rhythmically and may drive neuronal networks (Conners and Amitai, 2001) or result from network properties. The latter include recurrent circuits between excitatory and inhibitory cells and circuits involving the mutual inhibition of inhibitory neurons (Wilson and Bower, 1992; Jefferys et al., 1996).

Striking evidence in favour of a subcortical influence on cortical rhythmicity was initially found non-invasively in patients with Parkinson's disease through muscle sound recordings using a stethoscope. In untreated patients the normal sound due to the Piper (around 40 Hz) rhythm of muscle was replaced by a 10 Hz rhythm, although the Piper drive could be restored by treatment with levodopa (Brown, 1997a). The implication was that the pattern of cortical drive to muscle was critically dependent on the effects of the basal ganglia on the motor areas of the cerebral cortex. This hypothesis was recently been confirmed by MEG-EMG studies (Salenius et al., 2002).

Further, through EMG-EMG frequency analysis in the striated ocular muscles (Brown and Day, 1997b; Spauschus et al., 1999) and respiratory muscles (Carr et al., 1994) high frequency drives >60 Hz have been idenfied which are of brainstem origin. On the other hand low frequency drives between 12 and 18 Hz of brainstem origin could be demontrasted by using galvanic stimulation of the inner ear (Sharott et al., 2003).

1.2. Frequency analysis in pathological conditions

Pathological oscillatory drives manifest themselves either by a shift of the physiological peak(s) and/or by an the inflation of coherence at a given frequency. Usually, both aspects of pathological coherence coincide. In a few disorders of the motor system frequency analysis has already identified the abnormal features of the oscillatory drive from the central nervous system to muscle.

1.2.1. Cortical myoclonus

Frequency analysis shows the most diagnostic potential in cortical myoclonus. To date, the diagnosis of cortical myoclonus has relied on the detection of giant cortical sensory evoked potentials, which are not always present, and of a cortical correlate upon back-averaging (Shibasaki and Kuroiwa, 1975). Frequency analysis may, however, have several advantages over the time domain technique of back-averaging. High frequency myoclonic discharges with low amplitudes, such as in high frequency myoclons ("minipolymyoclonus", Wilkins et al., 1985), do not preclude analysis as no arbitrary trigger level has to be chosen so that jitter is less, statistical evaluation of the results is possible and the technique is quick and automated, so that long sections of data may be analysed. Thus in a recent study it was possible to demonstrate cortical activity related to myoclonic jerking through frequency analysis in eight patients in whom classical back-averaging failed to show a cortical correlate in five (Brown et al., 1999). Three of the patients in this study also showed exaggerated coherence that encompassed not only the physiological frequency range between 15 and 60 Hz, but also much higher frequencies. This report described patients with large amplitude jerks of low frequency typical of post-anoxic myoclonus and progressive myoclonic epilepsy and ataxia. Recently significant coherence between EEG and EMG has also been reported in high frequency rhythmic myoclonus (Guerrini et al., 2001). Regardless of aetiology, phase spectra confirm that cortical activity precedes EMG by a delay appropriate for conduction in the fast conduction pyramidal pathway. However, it should be noted that occasional exceptions to this rule are met at low frequencies, where the cortical activity lags (Marsden et al., 2000b).

Patients with cortical myoclonus also have exaggerated coherence between ipsilateral muscles co-activated by myoclonic jerks (Brown et al., 1999). Thus, it has been suggested that EMG-EMG coherence analysis can be used as a surrogate marker of coherence between motor cortex and EMG, which will be analysed in chapter 3.

1.2.2. Tremor

Cortico-muscular coherence in tremor with maximal coherence at the frequency of the tremor was first demonstrated in parkinsonian rest tremor using MEG (Volkmann et al., 1996). This finding has since been confirmed in studies of MEG/EEG-EMG coherence (Hellwig et al., 2000; Salenius et al., 2002), but the time delays between cortex and muscle are very variable, suggestive of efferent and afferent cortico-muscular drives in different patients (Hellwig et al., 2000). Some of this variability may be explained by the presence of two types of parkinsonian tremor with differing pathophysiological mechanisms (Lance et al., 1963). In higher frequency (7-10 Hz) parkinsonian action tremors cortical signals tend to lead EMG, whereas during low frequency (3-6 Hz) parkinsonian rest tremor EMG activity in the forearm precedes cortical activity, consistent with peripheral re-afference (Volkmann et al., 1996; Salenius et al., 2002).

Findings in essential and exaggerated physiological tremor have been more contradictory. A single channel MEG-EMG study failed to demonstrate cortico-muscular coherence at tremor frequency in essential tremor (Halliday et al., 2000). In contrast, a recent EEG-EMG study with extensive head coverage showed coherence between the contralateral sensorimotor cortex and the tremulous arm (Hellwig et al., 2001). The same authors could not, however, demonstrate EEG-EMG coherence at tremor frequency in enhanced physiological postural tremor although this is at odds with studies on physiological tremor using EMG-EMG coherence analysis in patients with mirror movement (Köster et al., 1998; Mayston et al., 2001) and with MEG-EMG coherence studies in physiological postural tremor (Marsden et al., 2001a).

In summary, there have been conflicting reports of coherence between cortex and tremor and at present EEG-/MEG-EMG coherence studies do not help differentiate different tremor types.

1.2.3. Parkinson's disease

Parkinson's disease is characterised by a reduction in the normal cortical oscillatory drive to muscles in the beta and gamma band. Instead, in untreated Parkinson's disease MEG-EMG coherence tends to be at $\leq$10Hz. Such synchronisation of muscle discharge at rest and action tremor frequencies leads to a sub-optimal unfused pattern of muscle activation, thereby slowing the onset of voluntary actions and decreasing contraction strengths (Brown et al., 1998a). Treatment with L-Dopa or therapeutic stimulation of the subthalamic nucleus restores the normal cortical drive and enables cortical motor elements to oscillate at higher frequencies (Salenius et al., 2002; Marsden et al., 2001b). Muscles can then be activated at high frequencies, improving bradykinesia and weakness. Motor cortical elements are also freer to form dynamic patterns of synchronised activity at frequencies above 20 Hz that might be important in higher-order aspects of motor control (Brown and Marsden, 1998b).

1.2.4. Dystonia

Patients with upper limb dystonia show abnormal coherence between extensor carpi radialis and flexor carpi radialis over 1-12 Hz and 14-32 Hz leading to the suggestion that cortical drives may be responsible for the co-contraction of antagonistic muscles in this condition (Farmer et al., 1998b). In contrast, in writer's cramp the only abnormality was a discrete peak in EMG-EMG coherence at 11-12 Hz when tremor was present.

EMG-EMG frequency analysis has been used to distinguish idiopathic dystonic torticollis from voluntary torticollis in agonistic muscles. Patients with dystonic torticollis exhibit an abnormal synchronised drive in agonistic sternocleidomastoid and splenius capitis muscles between 4 and 7 Hz (Tijssen et al., 2000). The same common 4-7 Hz drive can also be found in complex cervical dystonia (Tijssen et al., 2002).

1.2.5. Stroke

Transcranial magnetic stimulation and imaging studies have suggested that the ipsilateral motor cortex may show compensatory activity in stroke patients after recovery. Mima et al. explicitly tested this hypothesis in six patients with longstanding subcortical lacunar, pure motor strokes, but failed to find coherence between muscle and ipsilateral motor cortex (Mima et al., 2001b). Coherence between EMG and contralateral EEG was smaller for distal but not proximal muscles on the affected side, in line with the view that pyramidal pathways are differently organised to proximal and distal muscles (Turton and Lemon, 1999; Marsden et al., 1999).

1.2.6. Functional neurosurgery

In the future a specific clinical application of frequency analysis in patients with movement disorders treated with deep brain stimulation might be to identify the optimal electrode contact for stimulation. It has recently been shown that the degree of coherence between the local potential picked up by contacts on subthalamic nucleus macroelectrodes and EEG recorded over the midline scalp is correlated with the degree of clinical improvement derived from stimulation at that contact (Marsden et al., 2001b). A comparable finding for coherence between GPi and EEG in dystonia would be particularly useful as stimulation effects may be delayed for many months in this condition.

2. Methodology

Frequency analysis provides a few parameters whose knowledge is crucial to adequately interpret the results. This chapter will describe the methodological and analytical techniques that are in common to the experiments presented in Chapters 3–6. Specific methodological aspects of each experimental set up will be detailed at the start of each chapter. For all experiments cortico-muscular and intermuscular frequency analysis was performed off-line using a program written by J. Ogden and D. Halliday (Division of Neuroscience and Biomathematical Systems, University of Glasgow, UK) based on methods outlined by Halliday and colleagues (1995).

The very basis of all measurements in the frequency domain is the divison of the signal into discrete spectra. Spectra are usually determined using the fast Fourier transform (FFT), which was used in all the following experiments. A schematic summary of the different frequency analysis techniques is shown in Figure 2.1. In the FFT appraoch data are divided into serial, usually non-overlapping windows, transformed and then averaged. The basic trade-off to be considered in the FFT approach is between frequency resolution and spectral variance. As the size of the windows decrease, the variance goes down, but the spectral resolution becomes poorer. Spectra derived from a FFT approach are defined pointwise, and the frequency difference between two adjacent points is given by the sampling rate divided by the FFT window size (in samples).

Alternatively, spectra could be determined using MAR models. The latter have the desirable property of representing the characteristics of a signal with just a few coefficients, which can then be used to calculate the relevant spectra. Because of this property, MAR models are often useful for modelling short data sets. In addition, MAR spectra are continuous functions of frequency, and thus avoid the spectral resolution problems encountered with the FFT approach. In practice, however, the calculation of true confidence limits is

Fig. 2.1

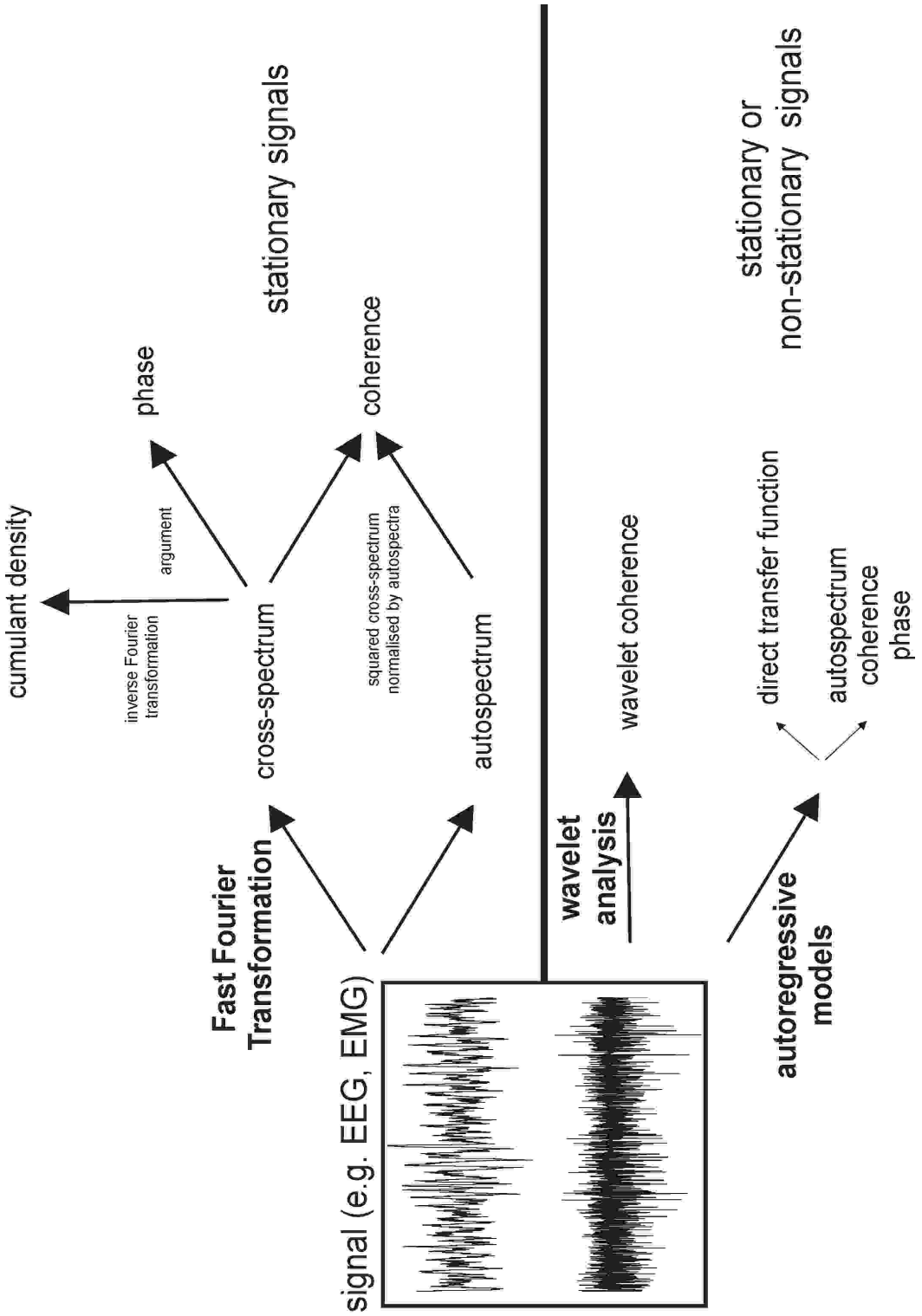

Fig. 2.1.: Schematic overview of the different methodological approaches to signal analysis in the frequency domain. Note that FFT based models can only be applied with signals assumed to be stationary whereas wavelet analysis and autoregressive models can additionally analyse non-stationary signals. For details see text

problematic and the approximate limits that can be calculated are generally wider than their FFT counterparts. (Cassidy and Brown, 2002). Also, the computation time for FFT methods is much faster than for MAR modelling. The MAR representation can also be embedded into more complex non-stationary models, which are often necessary in the analysis of signals whose statistical properties change substantially over time.

Finally, coherence estimation can also be achieved using wavelet analysis. The major advantage of this technique is that, different to FFT based analysis, the data has not to be stationary and that it can detect short, significant episodes of coherence (Lachaux et al., 2001). Whichever technique is used autospectra and cross-spectra may be derived, and from these coherence and phase are determined. For a general introduction to coherence see Challis and Kitney (1991), and for a more detailed discussion of the measures derived from frequency analysis to Rosenberg et al. (1989) and Halliday et al. (1995) for FFT approaches, Cassidy and Brown (2002) for MAR approaches and Lachaux et al. (2001) for wavelet analysis.

The main parameters deriving from the division of signals into spectra are as follows:

2.1. Coherence

The coherence between signals a and b at frequency λ is an extension of Pearson's correlation coefficient and is defined as the absolute square of the cross-spectrum normalised by the autospectra:

$$\left|R_{ab}(\lambda)\right|^2 = \frac{\left|f_{ab}(\lambda)\right|^2}{f_{aa}(\lambda)\, f_{bb}(\lambda)}$$

In this equation, *faa*, *fbb* and *fab* give the values of the auto and cross-spectra as a function of frequency λ and are assumed to be realisations of stationary zero mean time series. Coherence is a measure of the linear association between 2 signals. It is a bounded measure taking values from 0 to 1 where 0 indicates that there is no linear association (that is signal

a is of no use in linearly predicting signal b) and 1 indicates a perfect linear association between the two. Here, coherence was considered to be significant if it exceeded the 95% confidence level.

Because coherence ranges between 0 and 1, its variance must be stabilised by transformation before statistical comparison for scientific purposes in larger studies. In practice this makes relatively small difference to small coherences, but is important with coherences of more than 0.6. The variance of the coherence is usually normalised by transforming the square root of the coherence (a complex valued function termed coherency) at each frequency using the Fisher transform:

Var {arctan(Rab)}=1/2L

This results in values of constant variance for each record given by 1/2L where L is the number of segment lengths used to calculate the coherence (Rosenberg et al., 1989), which can then lead to coherences greater than 1.

2.2. Phase

Phase, $\phi_{ab}(\lambda)$, is expressed mathematically as the argument of the cross-spectra:

$$\phi_{ab}(\lambda) = \arg \{f_{ab}(\lambda)\}$$

It comprises two factors, the constant time lag given by the slope of the phase spectrum, when linear, and a constant phase shift, which is reflected in the intercept and is due to differences in the shapes of the signals (Mima and Hallett, 1999a). To calculate the temporal delay between the two signals the following equation is used (where the phase is in radians):

$$\frac{\Delta\phi}{\Delta frequency x 2\pi}$$

The phase estimate from a single point is ambiguous (Gotman, 1983). Measuring phase relationships that are linear over a band of frequencies reduces this ambiguity. Under these circumstances the temporal delay between the signals can be calculated from the gradient of the line. A negative gradient indicates that the input/reference signal leads.

2.3. Cumulant density estimate

The cumulant density, equivalent to the cross-correlation between signals, is calculated from the inverse Fourier transform of the cross-spectrum. When the input/reference signal is EMG this cumulant density estimate resembles a back-averaged EEG record.

2.4. Surrogate measures of cortico-muscular coupling: EMG-EMG frequency analysis

The recording of scalp EEG is not always easy, for example in children, and in movement disorders, in particular, the signal can be marred by muscle artefact. Thus it is fortunate that the same drive that leads to coherence between cortex and muscle also leads to coherence between the EMG signals of agonist muscles coactivated in the same task (Kilner et al., 1999). EMG-EMG coherence analysis can be performed using single or multi-motor unit intramuscular needle recordings or surface EMG. Studies of single units tend to be less informative (smaller signal to noise ratio in coherence spectra) than multi-unit needle or surface recordings (Christakos, 1997). Surface EMG is more practical but may be limited by volume conduction between muscles. The latter can be ruled out if there is a constant phase lag between the two EMG signals in the range of significant coherence. Thus it is generally best to chose muscle pairs that are separated (such as forearm extensors and intrinsic hand muscles), where one would expect physiological coupling to involve a phase difference. Alternatively, volume conduction can be limited by appropriate levelling of both signals and analysing the coherence between the resulting point processes. The

principle that intermuscular coherence may give comparable information about descending cortical drives as cortico-muscular coupling has been validated in cortical myoclonus (Brown et al., 1999).

Nevertheless, it should be remembered that oscillatory presynaptic drives to spinal motoneurons other than those of cortical origin will also be reflected in the synchronisation of motor unit discharge, where these contribute to muscle activity. Thus EMG-EMG coherence may afford an additional insight into subcortical motor drives.

2.5. General problems of recording and interpretation

This section considers some specific problems of recording and interpretation relevant to the investigation of corticomuscular coupling.

2.5.1. The signal and its collection

The first problem is the signal itself and the question of how closely it matches the activity to be modelled. For example, the skull and scalp act as a low pass filter so that scalp EEG may not reflect cortical activities at higher frequencies which are otherwise evident in electrocorticographic or MEG recordings. Another factor is the focality of the cortical area sampled by scalp EEG. This can be increased by Laplacian derivations such as the current source density and Hjorth transformation (Hjorth, 1975; Horth 1980). The latter also tend to give higher EEG-EMG coherence estimates, whereas common average references and balanced non-cephalic references may give misleading results because of possible EMG contamination (Mima and Hallett, 1999b). In addition, it is necessary to sample the signal at a rate that is greater than twice the low-pass filter setting so as to avoid aliasing and the identification of spurious spectral elements.

Additionally, filter settings deserve specific consideration. In all experiments EMG was

band pass filtered between 53 and 1000 Hz. The high-pass filter was chosen to limit contamination by movement artifact (see Fig. 2.2.), which otherwise would have lead to greatly inflated coherence estimates.

Fig. 2.2.

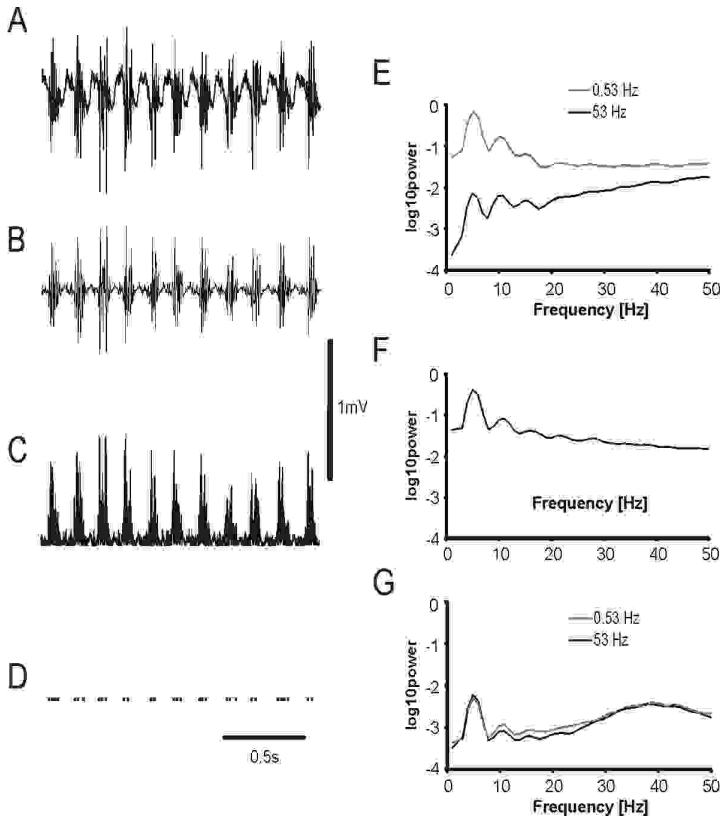

Fig. 2.2.: Example of data processing. (**A**) Raw EMG from 1DI high-pass filtered at 0.53 Hz and recorded during self-paced movement at ~5 Hz. Note prominent movement artefact between EMG bursts. (**B**) Simultaneously recorded raw EMG high-pass filtered at 53 Hz. Movement artefact is much reduced. (**C**) EMG as in (B) but full-wave rectified. (**D**) Product of levelling signal in (C) to give a point process. (**E**) Power spectra corresponding to EMG in (A) and (B). Power between the two differs by a factor of ~100 (note logarithmic scale), although qualitatively the autospectra are similar. The difference in power is most marked at the tremor frequency of 5 Hz and is largely due to the presence of movement artefact with a high-pass filter of 0.53 Hz. (**F**) Power spectrum of rectified high-pass filtered EMG from (**C**). Rectification increases power and emphasises the tremor peak at 5 Hz. (**G**) Spectra of point processes derived from levelling rectified EMG filtered at 0.53 Hz and 53 Hz. Power spectra are almost identical, confirming that high pass filtering at 53 Hz does not diminish information about interspike intervals in the multi-unit EMG record. It is the spike timing information that is important in determining the coherence between different EMG signals. Levelling, however, diminishes the effects of low-level signals such as movement artefact or volume conduction.

2.5.2. Coherence

An most important point is that as coherence is a measure of linear dependence between two signals in the frequency domain, any artefact common between channels leads to high coherence values over the relevant frequency band. This is most commonly evident in the case of mains artefact, but any volume conduction of signals between electrodes or cross-talk within leads or amplifiers will also lead to inflated coherences. Such artefacts occur with zero phase delay, and are reasonably obvious in paradigms in which biologically related signals would be expected to demonstrate phase differences, such as when investigating the coupling between EEG and EMG or EMG and tremor.

2.5.3. Phase

Two confounding factors must be remembered when the temporal delay between two signals is calculated from the phase. First, low pass filters, such as the skull and scalp, may introduce phase shifts that may underestimate real conduction delays (Lopez da Silva, 1989). Second, it is possible that more than one coherent activity may overlap in the same frequency band, in which case the phase estimate will be a mixture of the different phases. This may help explain why the temporal differences calculated between EEG or MEG and EMG are often shorter than those predicted from transcranial stimulation of the motor cortex (Brown et al., 1998c; Mima et al., 1998b; Salenius et al., 1997a), as both efferent and afferent cortico-muscular coupling may occur in overlapping frequency bands (Mima et al., 2001a). Co-existing bi-directional oscillatory flows between neural networks can be separated through application of the directed transfer function (Kaminski and Blinowska, 1991), although so far there has been only one report of the use of this in the motor sphere (Mima et al., 2001a).

3. Frequency analysis in high frequency rhythmic myoclonus

The analysis of the coherence between scalp EEG and surface EMG has shown promise as a new tool in delineating the functional coupling between oscillatory activity in the motor cortex and that in muscle in patients with cortcial myoclonus (Brown et al, 1999). In this conditaion EEG-EMG frequency analysis may have methodological advantages in detecting a cortical correlate over the classical neurophysiological repertoire of back-averaging and the detection of a giant cortical sensory evoked potential. Many myoclonic patients do not have reflex myoclonus and giant cortical evoked potentials and the identification of a cortical correlate that precedes jerks in back-averages relies on the absence of myoclonic events just prior to the trigger EMG burst. Yet many patients with cortical myoclonus have rhythmic EMG bursts at relatively high frequency (Thompson et al., 1994; Brown and Marsden, 1996), especially those with minipolymyoclonus (Wilkins et al., 1985; Hallett and Wilkins, 1986), as in cortical tremor (Toro et al., 1993; Terada et al., 1997), Angelman Syndrome (Guerrini et al., 1996) or autosomal dominant cortical myoclonus and epilepsy (Guerrini et al., 2001). In contrast, the increased signal content with repetitive myoclonic jerks favors detection using frequency analysis. In addition, the latter technique introduces no arbitrary trigger level so that jitter is less, statistical evaluation of the results is possible and the technique is quick and automated, so that long sections of data may be analysed. Thus in a recent study, EEG-EMG coherence and a cortical correlate in the cumulant density estimate were demonstrated in eight patients with a variety of conditions associated with cortical myoclonus, whereas only three had a time-locked EEG correlate upon back-averaging (Brown et al., 1999).

Nevertheless the determination of EEG-EMG coherence still requires a relatively artefact free EEG recording and EEG recording itself can be difficult and time-consuming in patients with involuntary jerks, some of whom are children. There is growing evidence that corticomuscular coupling is reflected in the pattern of coherence between muscles (Farmer et al., 1993; Kilner et al., 1999). This leads us to hypothesise that EMG-EMG coherence

may also be used to identify pathological cortical drives to muscle, and if so, this technique may have practical advantages over the assessment of EEG-EMG coherence. Certainly there is preliminary evidence of a close correspondence between the pattern of EEG-EMG coherence and that of EMG-EMG coherence in cortical myoclonus (Brown et al., 1999).

The interpretation of the results of frequency analysis in myoclonus is, however, bedevilled by the sensitivity of this technique. This has two consequences. First, even healthy subjects may be found to have EEG-EMG and EMG-EMG coherence and corresponding features in cumulant density estimates (Halliday et al., 1998; Kilner et al., 1999; Mima and Hallett, 1999b). To date studies have failed to address which aspects distinguish the pathological cortico-muscular coupling found in cortical myoclonus from the physiological state. Second, afferent activities will be detected as well as efferent discharges, but so far there has been the tacit assumption that the results of frequency analysis in patients with myoclonus may be satisfactorily interpreted solely in terms of descending drives from the motor cortex to muscles.

Here the results of back-averaging to those of frequency analysis in patients with high frequency rhycthmic myoclonus are compared. Further, the extent to which EMG-EMG coherence can provide a practical alternative to EEG-EMG coherence, the factors that distinguish pathological from normal corticomuscular and intermuscular coupling and whether coupling is always the product of cortical efferent activity are systematically explored. The assessments was based on minimal interventions that would lend themselves to incorporation into routine clinical neurophysiological practice and studied patients with the clinical syndrome of high frequency rhythmic myoclonus, as these are the cases that are most difficult to diagnose using standard back-averaging techniques. The results confirm the clinical utility of both EEG-EMG and EMG-EMG coherence estimates in the assessment of myoclonus, but indicate that interpretation must take into account the physiological complexity of cortical myoclonus, which does not solely involve efferent cortico-muscular pathways.

3.1. Patients and methods

3.1.1. Patients and healthy subjects

Nine patients (mean age 43 years; range 14-80 years) with jerks due to a variety of non-progressive syndromes associated which cortical myoclonus (table 3.1) were examined. All had high-frequency, low-amplitude myoclonus consistent with minipolymyoclonus (Wilkins et al., 1985). Case 9 also had some additional infrequent and less regular larger amplitude jerks. Three patients of a pedigree (cases 1-3) had multifocal myoclonus in relation to the recently described and genetically defined syndrome of autosomal-dominant cortical reflex myoclonus and epilepsy linked to chromosome 2 (Guerrini et al., 2001). Three patients (cases 4-6) had Angelman syndrome with different genetic defects (one with 15q11-13 deletion [case 4], one with uniparental disomy for chromosome 15 [case 5], and one with UBE3A mutation [case 6]). They exhibited continuous multifocal, high frequency myoclonic jerks associated with dystonic limb posturing as previously described in this syndrome (Guerrini *et al.*, 1996). One patient (case 7) had myoclonus in relation with Lennox-Gastaut-syndrome. In one patient (case 8) the diagnosis of familial cortical tremor was made. Cortical tremor is a type of minipolymyoclonus consisting of cortical reflex myoclonus, often associated with epilepsy and posture and/or action induced jerks at high-frequencies and low amplitudes showing the neurophysiological features of cortical myoclonus (Ikeda et al., 1990; Toro et al., 1993; Terada et al., 1997). The last patient (case 9) had myoclonus related to coeliac disease. More than half of the patients (cases 1, 2, 4, 6, and 7) had epilepsy with focal and/or generalised seizures besides cortical myoclonus. All patients except two (cases 3 and 8) received a variety of antimyoclonic and/or antiepileptic medication with different modes of action at the time of the neurophysiological examination. Ten healthy subjects (mean age: 40, range: 27-74) were also studied.

Table 3.1. Patient's clinical details

case	sex	age	features of myoclonus	epilepsy	clinical syndrome	drugs
1	f	47	multifocal, rest<posture	yes	autosomal-dominant cortical reflex myoclonus and epilepsy	VPA, PRM
2	f	71	multifocal, rest<posture	yes	autosomal-dominant cortical reflex myoclonus and epilepsy	PB, DPH, ESM
3	m	80	multifocal, rest<posture	1 seizure	autosomal-dominant cortical reflex myoclonus and epilepsy	None
4	f	17	multifocal, rest>posture	yes	Angelman syndrome	VPA, CLB
5	m	21	multifocal, rest>posture	no	Angelman syndrome	CLB, Pir
6	f	14	multifocal, rest>posture	yes	Angelman syndrome	VPA
7	m	26	multifocal, rest>posture	yes	Lennox-Gastaut syndrome	VPA, CBZ
8	m	45	forearm, hand, posture	no	cortical tremor	None
9	f	68	multifocal, posture, action-induced	no	coeliac disease	CZP, LEV, Pir, L-Dopa

3.1.2. EEG and EMG recording

Surface EMG and EEG were recorded with 9mm diameter silver-silver chloride electrodes. We opted for a bipolar EEG derivation rather than a Laplacian derivative, as the latter requires considerably more channels, limiting its utility in the setting of a routine clinical neurophysiological service. Both montages avoid the use of a common reference although bipolar electrodes may degrade phase information (Mima and Hallett, 1999b). Electrodes were positioned according to the 10-20 system at C3-F3 and C4-F4. EMG was recorded bilaterally from deltoid, finger extensor and intrinsic hand muscles (APB and 1DI). EMG electrodes were placed 2 cm apart on the muscle belly (except for intrinsic hand muscles where one electrode was sited over the metacarpo-phalangeal joint). EMG and EEG were bandpass-filtered at 16-300 and 0.53-300 Hz, respectively. The high pass filter for EMG was chosen so as to limit movement artefact. Signals were amplified and digitised with 12-bit resolution by a CED 1401 analogue-to-digital converter. The sampling rate was 1000 Hz. Signals were displayed and stored on a PC by a software package (CED Spike 3).

Patients were recorded either at rest (cases 4-7), so that no voluntary drive to muscles was present, or while posturing voluntarily (shoulder abduction, wrist extension, thumb adduction; cases 1-3, 8, 9). Record lengths averaged 183 ±21 s (SEM). Within individual subjects data lengths were kept fixed. Healthy subjects were asked to co-activate recorded muscles over 4 periods of about 60 seconds. Sixty-180s rest was given between co-activations. Total data lengths used were fixed at 200 s in healthy subjects.

3.1.3. Analysis

Frequency Analysis

EEG-EMG and EMG-EMG coherence were analysed as outlined in chapter II. The discrete Fourier transform and parameters derived from it were estimated by dividing the records into a number of disjoint sections of equal duration (1024 data points), and estimating spectra by averaging across these discrete sections. For comparison between groups, muscles and across signals the area under the curve of transformed coherence was calculated for each subject over the band at which coherence was significant. Data were then pooled for each group and the 95% confidence limits of the mean calculated.

Phase was assessed only where coherence was significant and extended over at least 5 data points. The constant time lag between the 2 signals was calculated from the slope of the phase estimate after a line had been fitted by linear regression, but only if a linear relationship accounted for > 80% of the variance. In some instances coherence and phase spectra appeared to consist of more than one component. In these cases the limits of individual components were defined by the turning points of the best-fit second or third order polynomial fitted to all contiguous plotted points at which coherence was significant. The polynomials accounted for > 80% of the variance and had $\geq$ 8 data points per model order.

Back-averaging

Back-averaging was performed off-line in Spike 2. EMG was rectified and myoclonic EMG bursts identified using a level of 100 μV (sufficient to exclude volume conduction or mains artefact) to produce a series of digital events. EEG and EMG signals were then re-aligned to these events and averaged. The dominant frequency of cortico-muscular coupling was determined from the interval between the peak positivities of the largest serial cortical correlates in the back-averaged contralateral EEG. The interval with which EEG lead or lagged EMG was determined as the latency of the peak positivity in the contralateral EEG with respect to the time of the digital events, after subtraction of the latency of the EMG response with respect to the same events. This was only performed where a single positive-negative cortical correlate was unequivocally larger (> 10%) than others.

3.2. Results

3.2.1. Raw EMG

The raw EMG consisted of rhythmic EMG bursts of short duration with minimal or no pre-innervation between myoclonic bursts. Thus in each case the rectified EMG level between myoclonic bursts was less than 40 μV in over 95% of interburst intervals. Fig. 3.1A is a representative example of the signal recorded in a patient with autosomal-dominant cortical reflex myoclonus and epilepsy linked to chromosome 2 (case 3). Brief myoclonic bursts are evident at a frequency of ~13-15 Hz.

3.2.2. Frequency analysis

Fig. 3.1B-E illustrates the results of frequency analysis in the same patient as above. Coherence between APB and the contralateral motor cortex is significant at frequencies

between 6 and 19 Hz (Fig. 3.1C) with a linear phase slope between the two signals (Fig. 3.1D) and a delay of 15.7 ms with EEG preceding EMG. The corresponding cumulant density estimate is shown in Fig. 3.1E.

Fig. 3.1.

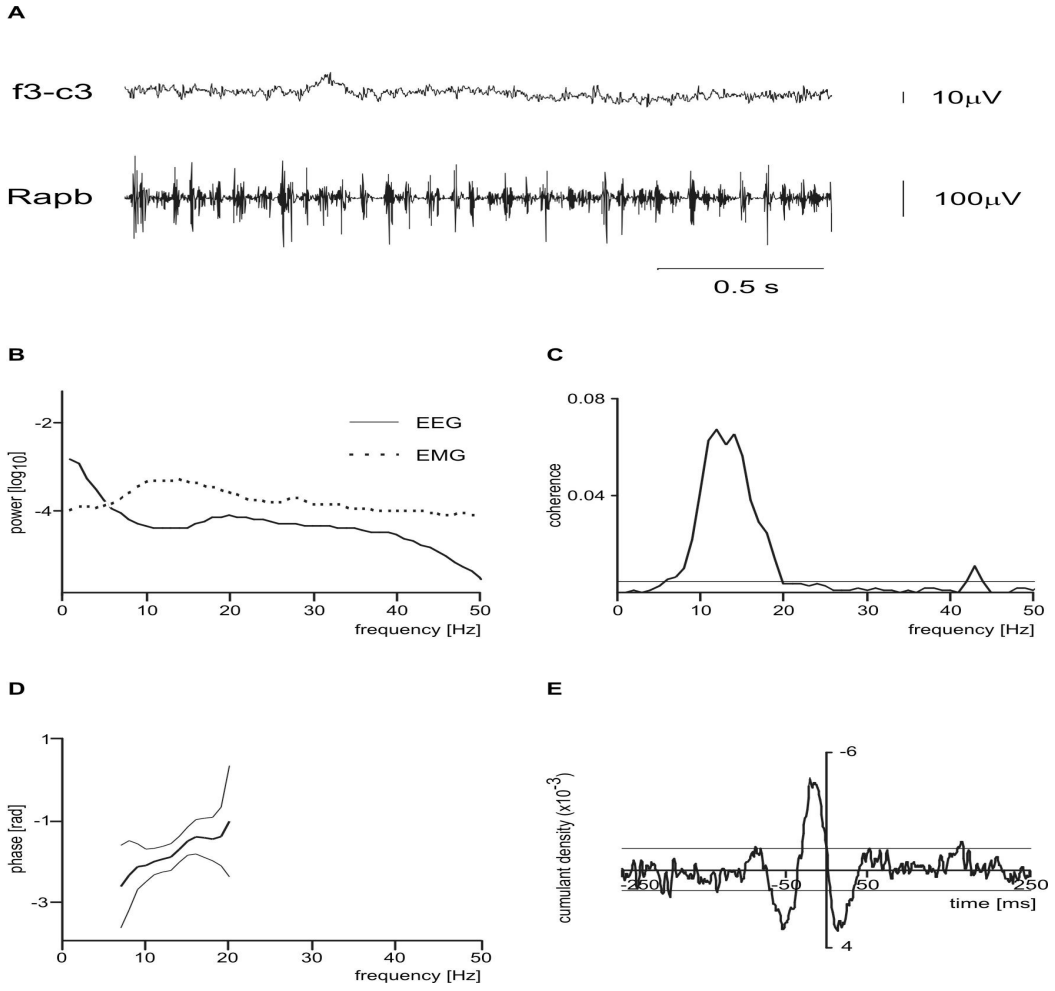

Fig. 3.1: Frequency analysis in case 3. (**A**) Left scalp EEG and EMG from right-sided deltoid, finger extensors and APB. EMG shows myoclonic bursts at high frequency (~13-15 Hz). (**B**) Autospectrum of right APB and F3-C3. (**C**) Coherence between right APB and F3-C3 showing exaggerated EEG-EMG coherence in the range 6 - 19 Hz. The thin horizontal line is the 95% confidence level. (**D**) Phase between right APB and F3-C3. The thin lines either side of the phase estimate (thick line) are the 95% confidence levels. EEG precedes EMG. Regression analysis gave a time lag between the two signals of 15.7 ms (± 2.8 ms 95% confidence limits**)**. (**E**) Cumulant density function showing a negative EEG deflection with a peak about 15 ms before the EMG. EMG was the input. Thin horizontal lines are 95% confidence levels.

Fig. 3.2, taken from the same patient, gives an example of the typical difference between EEG-EMG and EMG-EMG coherence for both proximal and distal muscles. The data are drawn from the same recording. While the frequency at which coherence peaks remains constant, centered around 13 Hz, the frequency content is broader and the extent of coherence is higher for EMG-EMG coherence than EEG-EMG coherence.

Fig. 3.2.

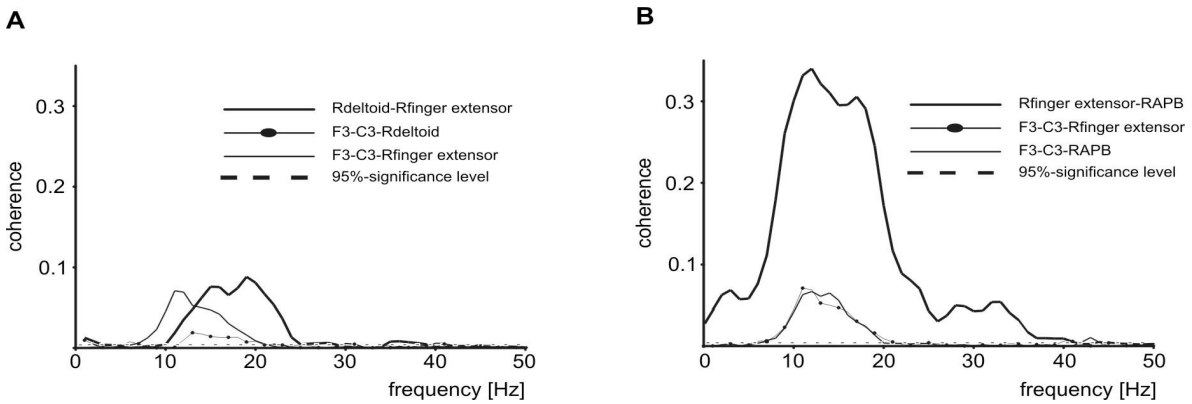

Fig. 3.2: Comparison of frequency content and degree of coherence between EEG-EMG and EMG-EMG for proximal (**A**) and distal (**B**) muscle pairs in case 3.

EEG-EMG coherence

Fig. 3.3A-C summarises the area of significant transformed coherence between EEG and EMG in the spectra from individual subjects for deltoid, finger extensors and intrinsic hand muscles. Both right and left sided muscles are included. Note the logarithmic scale. Transformed coherences showed substantial overlap between patients and controls. Thus on an individual basis EEG-EMG coherence using a simple bipolar montage had limited sensitivity.

Nevertheless there were clear differences at the group level. Fig 3.3D summarises the mean transformed coherence area and its 95% confidence limits across all patients and all healthy subjects for the different muscles. The mean transformed coherence area in the patient group is higher by a factor of 3 to 9 compared to normal values (Fig. 3.3D). Note too that coherences are considerably higher for distal muscles.

Fig. 3.3.

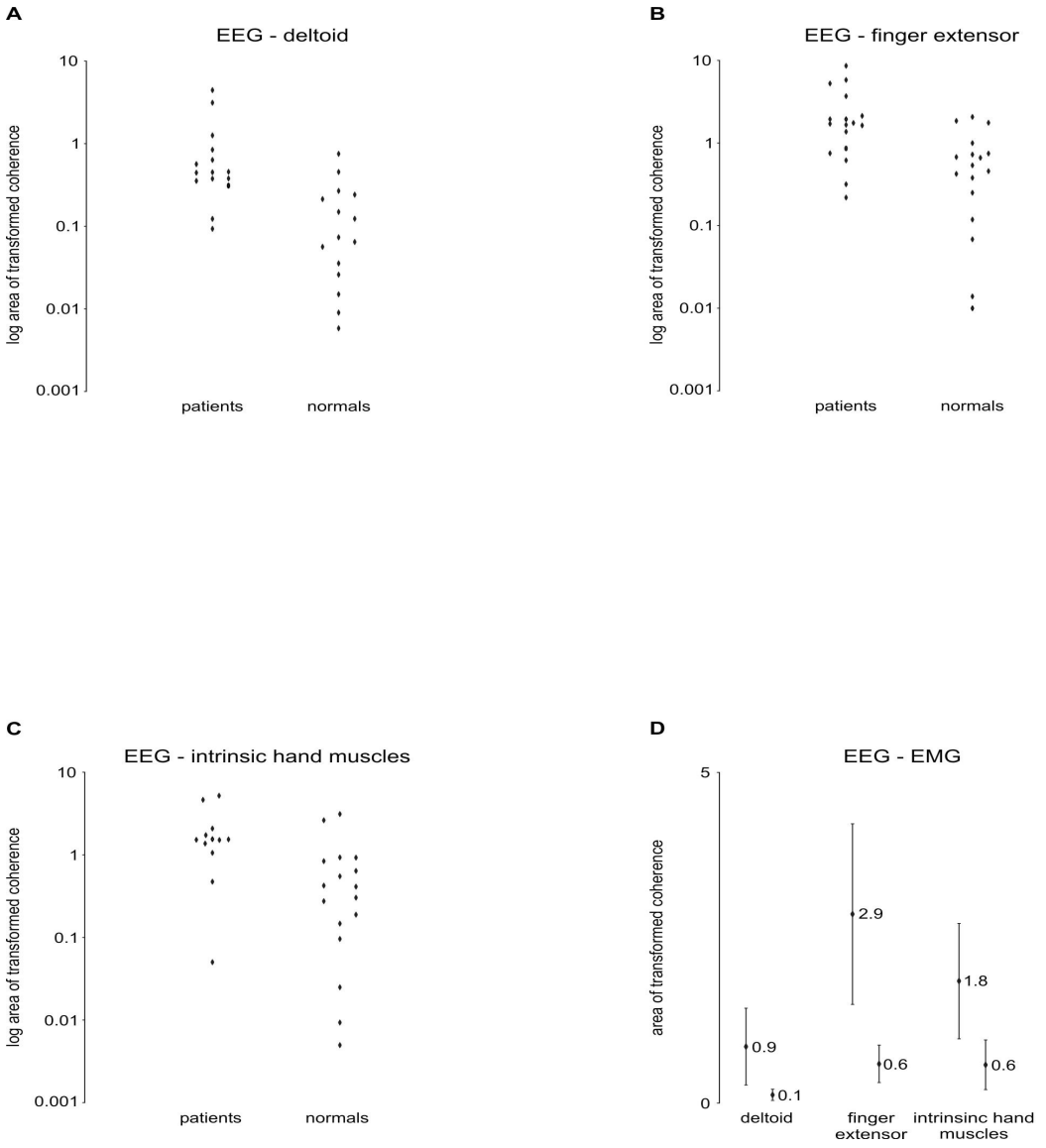

Fig. 3.3: Areas of transformed EEG-EMG coherence, taken from above the 95% confidence level, in each patient for deltoid (**A**), finger extensor (**B**) and intrinsic hand muscles (**C**). Transformed coherence is plotted on a log scale; overlap is evident between individual patients and healthy subjects. (**D**) Transformed coherence areas averaged across patients and healthy subjects (asterixed) with 95%-confidence level of each mean.

Fig 3.4 compares the distribution of transformed EEG-EMG coherence across frequencies for the different muscles. For this purpose the individual spectra, rather than the cumulative area, have been pooled. Healthy subjects only show a discrete peak in the pooled spectra for the forearm and intrinsic hand muscles centred around 15 Hz. This is slightly

Fig. 3.4.

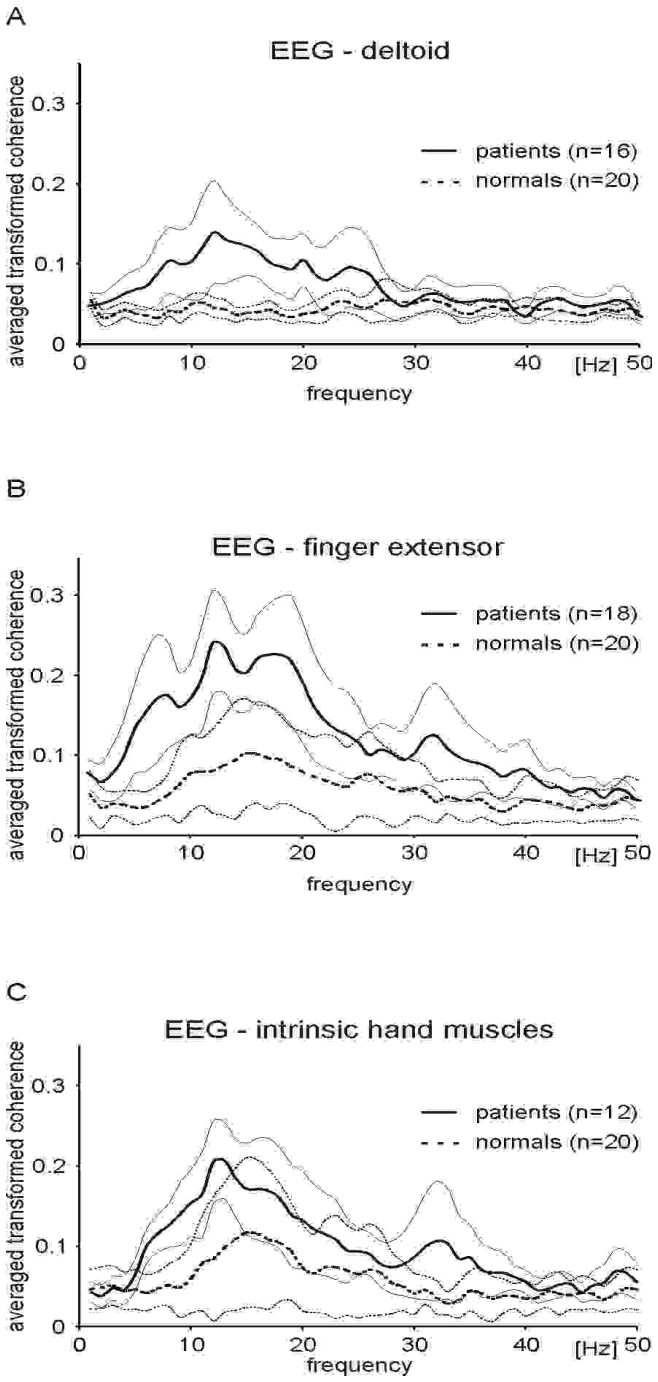

Fig. 3.4: Averaged transformed EEG-EMG coherence spectra in patients and normal subjects for deltoid (**A**), finger extensor (**B**) and intrinsic hand muscles (**C**). The level of averaged transformed coherence is higher in paients compared to healthy subjects in all three muscles (bold lines), but with overlap of the 95%-confidence limits of the mean (thin lines) between the two groups.

lower than in a previous study of physiological cortico-muscular coupling (Brown et al., 1998) and may be partly due to the use of EEG (which is affected by the low-pass filter characteristics of the skull and scalp) rather than magnetoencephalograpy in the current study. The frequency range in the present study is comparable to that found in other electroencephalographic studies of corticomuscular coherence (Mima and Hallett, 1999b), where coherence in the alpha band is not uncommon (Mima and Hallet, 1999a). Patients also had a peak in the pooled spectrum for deltoid, while their mean transformed coherence area was mostly above the 95% confidence limits for the healthy subjects in all three muscles. The peak frequency was similar in the different spectra, although peaks were broader in the patient group, where there was also a subsidiary peak at just above 30 Hz in the spectra for distal muscles.

EMG-EMG coherence

Similar analyses were performed for EMG-EMG coherence. Fig. 3.5 A and B summarise the area of significant transformed coherence between finger extensor and deltoid and between finger extensor and intrinsic hand muscle EMG in the spectra from individual subjects. Transformed coherences show overlap between patients and controls, although compared to EEG-EMG coherence (Fig. 3.3) this overlap is modest.

Fig: 3.5

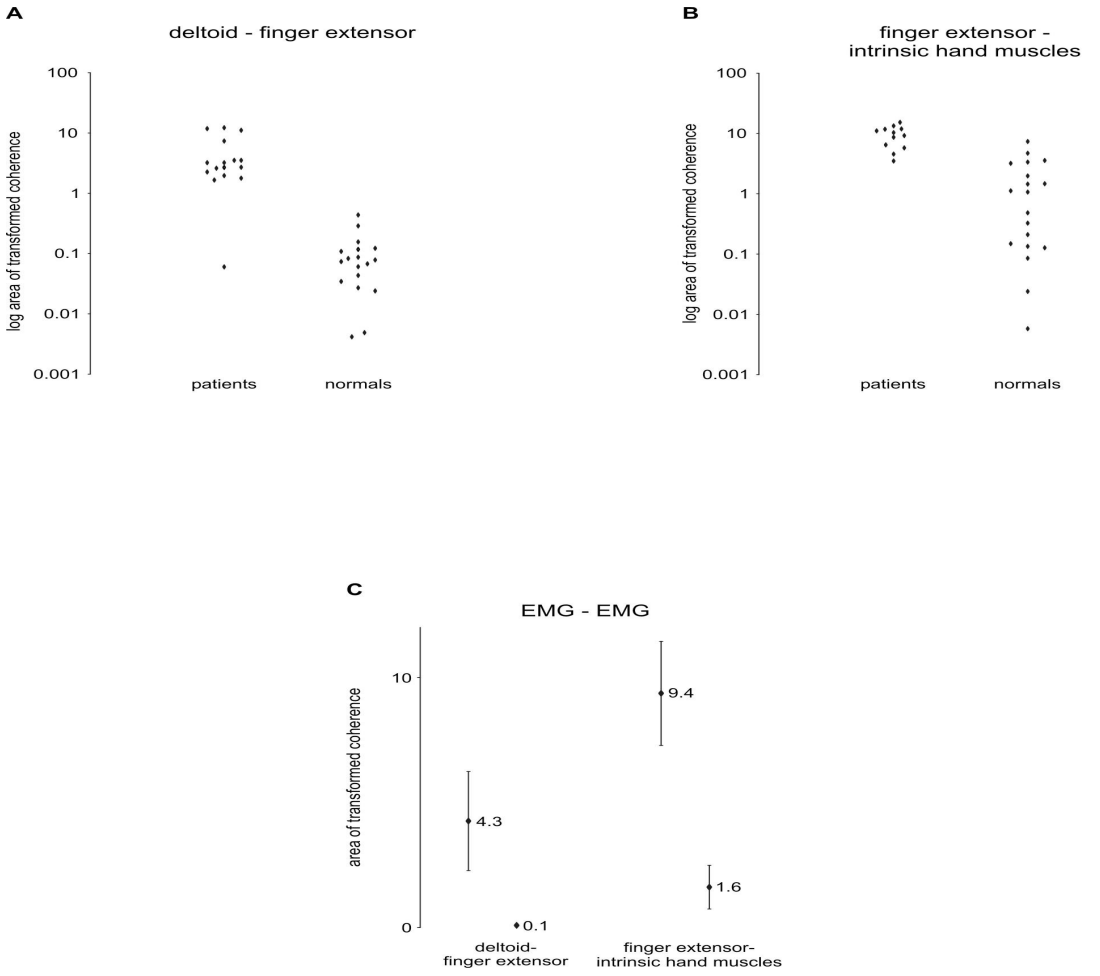

Fig. 3.5: Areas of transformed EMG-EMG coherence, taken from above the 95% confidence level, in each patient for deltoid-finger extensor (**A**) and finger extensor-intrinsic hand muscles (**B**). Transformed coherence is plotted on a log scale. In comparison to respective transformed EEG-EMG coherences (fig 3) there is less overlap between patients and healthy subjects. (**C**) Transformed coherence areas averaged across patients and healthy subjects (asterixed) with 95%-confidence level of each mean.

The differences were even clearer at the group level. Fig 3.5 C summarises the mean transformed coherence and its 95% confidence limits across all patients and all healthy subjects for the different muscle pairs. The mean transformed coherence in the patient group is very much greater than in normals and greater than the mean transformed coherence between EEG and muscles in the patients (Fig 3.3D). Note too that coherences are considerably higher for the distal muscle pair.

Fig 3.6 compares the distribution of transformed EMG-EMG coherence across frequen-

Fig. 3.6.

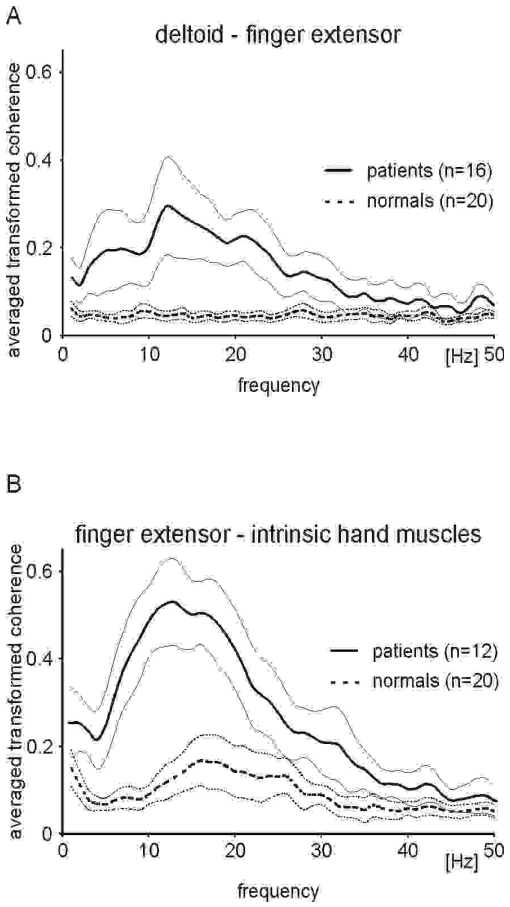

Fig. 3.6: Averaged transformed EMG-EMG coherence spectra in patients and normal subjects for deltoid-finger extensor (**A**) and finger extensor-intrinsic hand muscles (**B**). The level of averaged transformed coherence is higher in patients compared to normals, but unlike fig 4 there is no overlap of the 95%-confidence limits of the mean (thin lines) between the two groups over the 6-30 Hz band. Data were smoothed with a 3 point moving average.

cies for the different muscle pairs. Healthy subjects only show a peak in the pooled spectra for the distal muscle pair. Patients have a peak in both proximal and distal muscle pairs and transformed coherences for both are clearly above the 95% confidence limits of the mean for the healthy subjects. The peak frequency in the spectrum for finger extensor-intrinsic hand muscles is similar in controls and patients, although the peak is broader in the patient

group.

In every single patient the coherence between muscle pairs, be they proximal or distal, as measured by the area of transformed coherence exceeded the coherence between the EEG and respective muscles. In addition, EMG-EMG coherence between finger extensor and intrinsic hand muscles was able to establish abnormal coupling in every case, whereas abnormal coupling could only be demonstrated in less than 90 % of cases of EEG-EMG coherence (Table 3.2).

Table 3.2.

	back-averaging			frequency analysis				
	cortical correlate	frequency [Hz]	temporal delay	signif. EEG-EMG coherence†	peak frequency [Hz]	temporal delay‡	EEG-EMG coherence >95%-CL of control group*	EMG-EMG coherence >95%-CL of control group*
Deltoid	50%	17.6 ± 3.8	31%	88%	14.4 ± 3	63% (31%)	88%	94%
finger extensor	77%	16.9 ± 2.4	56%	100%	14.1 ± 2.4	94% (67%)	89%	100%
intrinsic hand muscles	75%	16.3 ± 2	42%	100%	14.4 ± 2.6	83% (67%)	75%	
deltoid-finger extensor	—		—	—		—	—	94%
finger extensor-intrinsic hand muscles	—		—	—		—	—	100%

†above 95%-confidence limit
‡ at least 5 contiguous data points in the frequency of significant coherence with $p<0.05$
*at least 2 data points above the highest point of upper 95%-confidence limit irrespective of frequency

Phase

Hand muscles

The temporal difference between EEG and EMG calculated from phase spectra demonstrated a uniform pattern in the intrinsic hand muscles. EEG systematically lead EMG by 8.3 to 18.8 ms (Fig 3.7A). The mean EEG lead was 14.8 ± 2.3 ms (95% confidence limits), being shorter than the mean MEP latency in active 1DI following transcutaneous magnetic stimulation of the motor cortex of 20.4 (Eisen and Shtybel, 1990). A comparable pattern was seen for the temporal difference between forearm extensor and intrinsic hand muscle EMG. The former lead by 3.3 to 11.2 ms (Fig. 3.7B). The mean lead of the forearm extensors was 6.7 ± 1.4 ms and was therefore compatible with the difference of 5.2 ms between MEP latencies for forearm extensors and 1DI following TMS of the motor cortex in normal controls (Eisen and Shtybel, 1990).

Proximal muscles

In contrast, phase differences between EEG and EMG for more proximal muscles and between deltoid and finger extensor EMG were more complicated. In some cases EEG lead EMG but in others EMG lead EEG (Fig. 3.7C-E). The latter suggests an afferent drive from muscle to cortex. Although the picture varied between subjects, phase estimates concurred within each subject in every case in whom estimates were available for deltoid and forearm extensors on the same side. Thus, phase estimates were of the same sign in cases 2, 5 and 9 (see fig. 3.7C and D). This suggests that variations in the temporal difference between EEG and proximal muscles across patients were due to physiological differences rather than chance. In some subjects EEG-EMG coupling for proximal muscles was dominated by a corticomuscular efferent drive as with 1DI, whereas in others coupling was dominated by an afferent drive from the periphery.

When delays were compatible with an efferent system they were somewhat shorter than

the latency of TMS induced MEPs to the respective active muscle, as was the case for the intrinsic hand muscles. For example, in the one patient (case 2) in whom EEG lead deltoid EMG, this was by 9.6 ms (fig 3.7C). In cases 2, 3 and 8, in whom EEG lead forearm extensor EMG, this was by around 10 ms (fig 3.7D).

On the other hand, when delays were compatible with an afferent system they were seldom consistent with the latency of evoked potentials from the region of the respective muscle recorded in healthy subjects. For example, in cases 5, 7 and 9 in whom deltoid EMG lead EEG this lead varied between -24.1 to -76.9 ms (fig 3.7C). In cases 1, 4, 5, 6 and 9, in whom finger extensor EMG lead EEG, the mean delay between the two signals exceeded 25 ms (fig 3.7D). EMG leads were therefore greater than the expected delay for an afferent loop, even allowing 10 or so ms for electromechanical delay (McCauley *et al.*, 1997). This variation in the temporal delays was not systematically related to the semiology of the myoclonus or the clinical syndrome associated with it.

A similar pattern was observed in the temporal delay between deltoid and finger extensor EMG. In cases 6, 7, and cases 2 and 5 on the right, deltoid EMG lead that in the finger extensor, as would be expected for a simple efferent system. However, in cases 1, 3 and case 2 on the left, forearm extensor EMG lead by 20.1 ± 12.1 ms, compatible with an afferent loop, in which afferent activity from the distal upper limb drove a reflex response in deltoid.

Fig. 3.7.

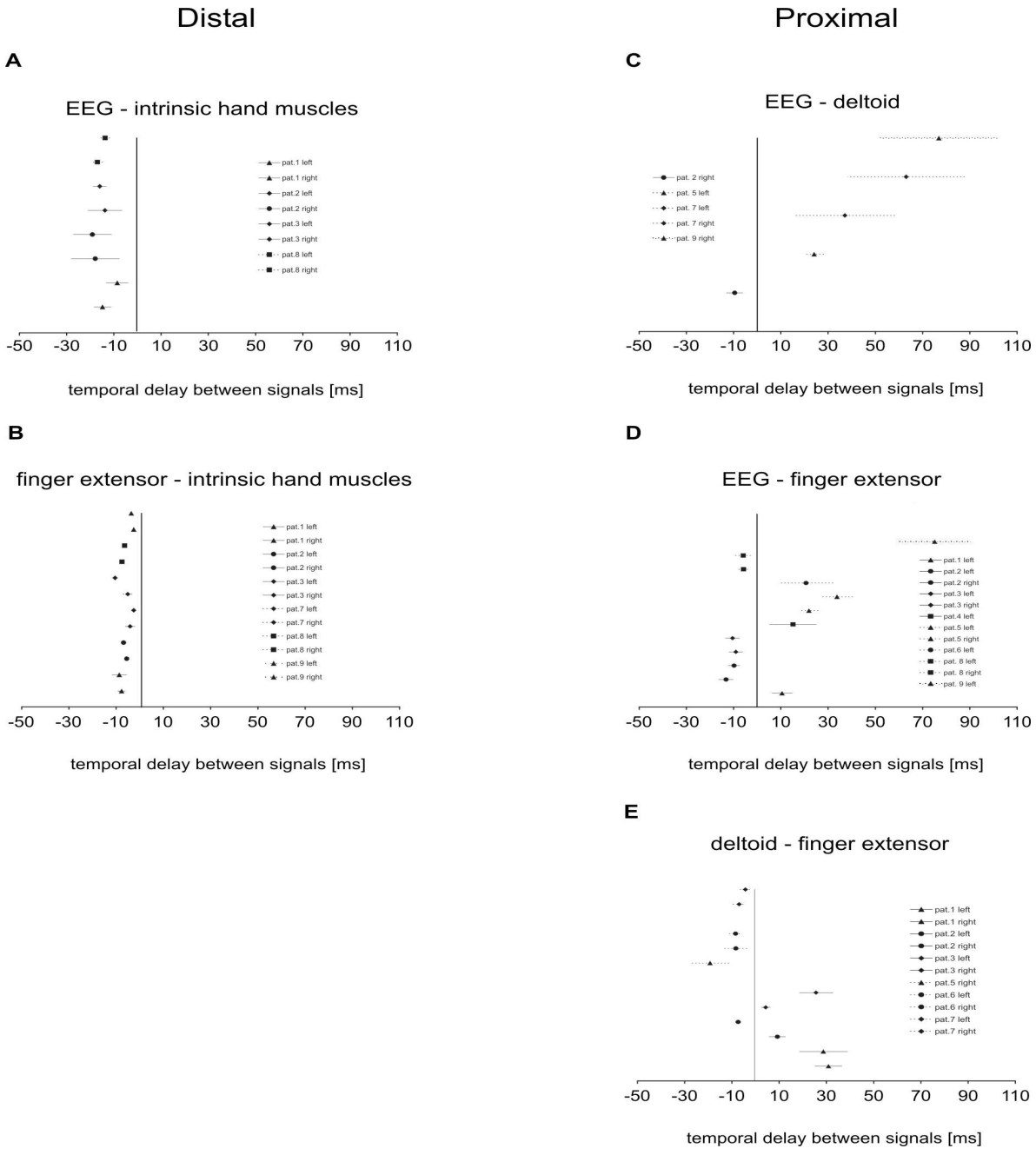

Fig. 3.7: Phase relationships in patients for proximal and distal muscles. Only patients meeting our criteria for calculation of temporal delays (see methods) are included. Horizontal lines are the 95%-confidence limit of the temporal delay in each subject. A positive sign for EEG-EMG (**A, C, D**) indicates that EEG leads EMG. When negative EMG leads EEG. A positive sign for EMG-EMG (**B, E**) indicates that the more proximal muscle leads the more distal muscle. Note that for distal muscles (**A, B**) the phase relation indicates a dominant efferent drive between cortex and muscle as well between muscles. For proximal muscles (**C-E**) phase suggests efferent and afferent drives in individual patients.

3.2.3. Back-averaging

Back-averaging was performed in all 9 patients (table 3.2). A back-averaged cortical correlate could be discerned in only 50to 77 % of muscles, but cortico-muscular coherence was above the significance level in 100% of cases for finger extensors and intrinsic hand muscles and in 82% of cases for deltoid. For those muscles in which back-averaging was successful the back-averaged EEG consisted of a rhythmic series of cortical correlates , and was similar in nature to the cumulant density estimate(Fig. 3.8B-D).

Fig. 3.8.

Fig 3.8: Examples of back-averaged contralateral EEG. (**A**) Back-averaged EEG (black line) of left finger extensor of case 3 fails to disclose a cortical correlate, although the cumulant density estimate (grey line) shows a maximal positive deflection that follows EMG onset and exceeds the 95%-confidence limits (dotted grey lines). (**B**) Back-average and cumulant density estimate compared in case 3 (same as Fig 1). Note that positive deflections are symmetrical and therefore the temporal difference between EEG and EMG was ambiguous with these time domain measures. In contrast, phase spectra (Fig 1 d) in the same patient clearly showed that EEG lead EMG. (**C**) Back-average in case 1. The peak positive deflection is ambiguous, but the oscillatory nature of the back-averaged EEG can be seen at a frequency of 14 Hz. (**D**) Unambiguous back-average in case 2. The peak positive deflection in the EEG precedes EMG onset in the right finger extensors by 23 ms. Note the oscillatory nature of the back-averaged EEG at a frequency of 22 Hz. In each case EMG is rectified and the same data were analysed to give the back-average and cumulant density estimate.

The frequency of back-averaged cortical correlates was around 16 Hz, while the peak frequency upon frequency analysis was about 14 Hz. However, there were no statistically significant difference between the peak frequency derived from back-averages and that derived from coherence spectra in those patients in whom both estimates were available. When areas under the curve were considered sensitivity for EMG-EMG coherence was greater than for EEG-EMG coherence (table 3.2) with a specificity which was better than values for sensitivity.

A single positive-negative EEG correlate exceeded others in peak-to-peak amplitude in a given series by > 10% in 31 to 56 % of muscles examined. Accordingly, we were only able to measure unambiguous time differences between EEG correlates and EMG onset in these patients. Examples of uninformative/negative (3.8A), ambiguous (3.8B and C)and unambiguous (3.8D) back-averages are illustrated in Fig. 3.8. Temporal differences measured from unambiguous back-averages are summarised in Fig. 3.9.EEG lead EMG in the intrinsic hand muscles in all but one case. In contrast, EEG could lead or lag EMG in the forearm extensors. EEG's lead or lag over EMG was always the same in direction in those muscles where temporal delays could be calculated from back-averages and frequency analysis, suggesting that variability was physiological rather than technique dependent.

Fig. 3.9.

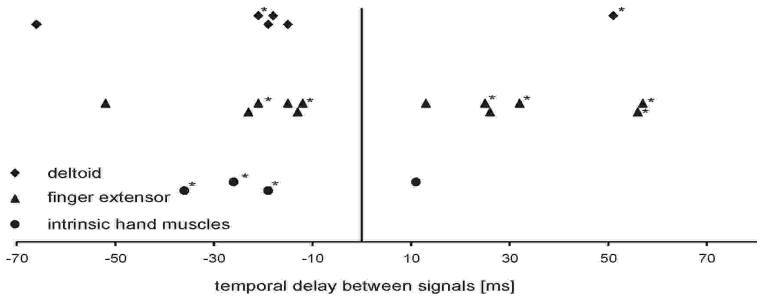

Fig. 3.9: Time lag between EEG and EMG based on back-averaged EEG where a negative sign indicates that EEG leads EMG and a positive sign suggests that the EMG signal precedes the EEG. Note that results are comparable to phase estimates calculated by frequency analysis (fig. 7), although deriving partly from different individuals (asterixes indicate identical cases represented in fig. 7). In particular, there is a wide variation of time lags suggestive of afferent and/or efferent conduction. Except in one case, EEG always leads EMG in the hand, while there is a mixed pattern of efferent and afferent conduction between EEG and finger extensor EMG.

3.3. Discussion

It could be shown that the exaggerated functional cortico-muscular coupling in patients with cortical myoclonus is not only reflected in an exaggerated coherence between EEG and EMG, but also in an abnormally strong coherence between the EMGs of muscles co-activated by myoclonic jerks. In addition, the results demonstrate that the phase relationship between EEG and EMG and between pairs of EMG signals is complex, reflecting both efferent and afferent drives between cortex and muscles.

Clinical utility of frequency analysis in myoclonus

Hitherto the electrophysiological characterisation of cortical myoclonus has largely depended on the results of back-averaging, in which a positive result requires the demonstration of a cortical correlate that precedes myoclonic EMG bursts. As stated in the introduction, frequency analysis of myoclonic activity has several potential advantages over back-averaging when myoclonic EMG bursts are frequent as in minipolymyoclonus. This was borne out by the present study in which the symmetry of cortical correlates upon back-averaging meant that unambiguous estimates of the temporal difference between cortical correlate and myoclonic EMG could only be made for 31 to 56 % the muscles examined, and a cortical correlate could not be discerned for around 40% of muscles. In contrast, frequency analysis demonstrated abnormal EEG-EMG coherence for 75 to 89 % of muscles and was able to establish a temporal delay in the majority of cases.

It must be stressed that back-averaging and frequency analysis emphasise different aspects of the data. The results of frequency analysis reflect the coupling between motor cortex and muscle and that between muscles due to common drive averaged over time. Here we have characterised how this coupling deviates from normal in patients with high frequency myoclonus. All signals within a recording are analysed, so there is the methodological concern that the index of coupling reflects both myoclonic activity and any pre-innervation. In practice this was not a problem in our data sets, where EMG levels were very

low between myoclonic bursts. However, had this not been the case then only back-averaging would have demonstrated the cortical correlate exclusively linked to myoclonic EMG bursts. In addition, non-reflex myoclonic bursts can be relatively infrequent in some conditions. In these instances current frequency analysis techniques would be inappropriate as local data stationarity is not approximated and back-averaging would offer the only possibility of documenting a cortical origin. Thus frequency analysis of myoclonus has advantages when myoclonic jerks occur at high frequency, as in minipolymyoclonus, but back-averaging is the analytical technique of choice when myoclonic bursts occur at low frequency.

The present study also suggests that the assessment of EMG-EMG coherence may be more useful in the future than EEG-EMG coherence in the routine neurophysiological evaluation of patients with myoclonus. As EEG is not required the technique is less time-consuming and applicable when movement artefact or cranial EMG activity are likely to prevent satisfactory EEG recordings. More importantly, the technique appears to be more sensitive in distinguishing abnormal and normal common drives, and for this purpose the simultaneous assessment of the coherence between the forearm extensor and ipsilateral intrinsic hand muscles can be recommended. The greater sensitivity of EMG-EMG coherence may relate to the increased coherence levels seen between these signals compared to EEG and EMG. Importantly, the increased coherence levels found between EMG signals did not seem to relate to volume conduction, as coherence occurred over relatively narrow bands and did not involve zero phase delays between EMG signals. It is possible that other forms of recording of cortical activity, such as MEG or Laplacian derivatives of EEG may provide more sensitive measurements of EEG-EMG coherence, but these techniques are not universally available or are time consuming and require multiple EEG channels.

Attention should also be drawn to the question of specificity of an elevated EEG-EMG or EMG-EMG coherence with regard to other pathologies. Inflated EEG-EMG coherences have also been reported in Parkinson's disease (Hellwig et al., 2000) and essential tremor (Hellwig et al., 2001), but here coherence is narrow band in nature and centred on a tremor frequency of $\leq$10 Hz. Thus EEG-EMG coherence occurs at generally lower frequencies in

these tremor disorders, but a comparative study of coherence in tremor and high frequency rhythmic myoclonus is necessary to establish whether there is any significant overlap in the frequency of peak coherence in these entities.

Possible homology between EEG-EMG and EMG-EMG coherence

If EMG-EMG coherence is to be useful in the clinical evaluation of cortical myoclonus then it should be a faithful marker of the functional coupling between cortex and muscle. This may not necessarily be the case as the coherence between EMG signals reflects sub-cortical and spinal inputs as well as oscillatory cortical drives to α-motoneurones. In practice, however, the pattern of EEG-EMG and EMG-EMG coherence was similar, suggesting that the major oscillatory influence on spinal motoneurones, at least in this pathological state, involves the sensorimotor cortex. The one notable difference between EEG-EMG and EMG-EMG coherences was the wider frequency band of the latter. However, this band was still centered on similar peak frequencies and may simply be the product of the improved signal to noise ratio and greater coherence between pairs of EMG signals.

Preferential projection of the oscillatory corticomuscular system to the distal limb

EEG-EMG coherence was greater distally than proximally in the upper limb. This was evident in patients, but also in healthy controls, where there was no detectable coherence in deltoid using bipolar EEG electrodes. It is tempting to interpret these observations as evidence in favor of the preferential projection of pyramidal pathways to distal upper limb muscles (Colebatch and Gandevia, 1989; Rothwell et al., 1991; Ferbert et al., 1992; Palmar and Ashby, 1992; Marsden et al., 1999; Turton and Lemon, 1999).

However, we must first consider an alternative suggestion, that it was our use of a bipolar EEG lead drawn form over the hand area of the motor cortex that lead to the greater coherences for intrinsic hand muscles. Isocoherence maps of the coherence between cortical and muscle activity in studies using magnetoencephalography or surface EEG (Salenius et

al., 1997; Hellwig et al., 2001) and a further study examining the distribution of coherence by Mima et al. (2000b) would suggest that the source of cortical activity coupled to EMG activity is relatively focal. On the other hand the Laplacian derivations used in many of these studies have been criticized as applying an excessively high spatial filter (Srinivasan et al., 1998), and many MEG studies start from the assumption of a point source responsible for activity (Salenius et al., 1997; Brown et al., 1998). Studies using electrocorticography or tomographic modelling of EEG sources suggest a much more distributed source for the cortical inputs responsible for EEG-EMG coherence even in healthy subjects (Marsden et al., 2000a; Feige et al., 2000; Ohara et al., 2000).

In considering the possibility that our use of a bipolar EEG lead over the hand area may have contributed to the apparent preferential projection of fast conducting pyramidal pathways to distal upper limb muscles we are fortunate in having a further measure of common inputs to motoneurones that is independent of the EEG. Importantly, EMG–EMG coherence in the upper limb was also greater for a distal muscle pair compared to a proximal muscle pair.

Afferent loops in proximal muscles

A previous frequency analysis of data from patients with cortical myoclonus (Brown et al., 1999) suggested that EEG consistently lead EMG. This study limited itself to consideration of distal upper and lower limb muscles. Our frequency analysis and back-averaging results in the distal upper limb were in accord with this. However, here it was also demonstrated that the temporal relationships between EEG and the EMG of more proximal upper limb muscles and between pairs of EMG signals from more proximal muscles is more complex, regardless of whether relationships are calculated from time or frequency domain estimates. In many patients temporal relationships were inverted so that EMG lead EEG or a distal muscle lead a proximal muscle. In these instances an afferent loop is implicated and the myoclonic bursts in such proximal muscles may be the product of a complex interaction of cortical, subcortical and spinal influences. It is worth noting that despite the

differences in phase relationships between proximal and distal muscles, coherence did not involve activity over systematically different frequency bands.

It is also notable that not all patients demonstrated temporal relationships in proximal muscles suggestive of afferent loops. The consistency of findings for different proximal muscles within the same subject argues that this is likely to represent biological variation. A variability similar to ours has been reported in the phase differences between cortex and forearm muscles in the physiological action tremor of healthy subjects (Marsden et al., 2001) and in patients with tremor due to Parkinson's disease. Here estimated phase delays between cortex and forearm muscles were widely distributed with cortex leading or lagging by as much as 76 ms (Hellwig et al., 2000; Salenius et al., 2002). The implication is that individual variation in the organisation and dominance of afferent and efferent loops to upper limb muscles occurs outside the hand. Some of this individual variation may be pathological, although in our patients there seemed no consistent correlation between the variation in phase and either the semiology of the myoclonus or the presence of concomitant epilepsy or drugs. On the other hand physiological inter-individual variation in the organisation of motor pathways to proximal muscles is increasingly recognised and may underlie the variability in recovery following stroke (Hamdy and Rothwell, 1998; Turton and Lemon, 1999).

The finding of prolonged delays between EMG and EEG when estimates indicated afferent conduction may, at least in theory, be due to conduction delays of somatosensory pathways as documented in some myoclonic syndromes, such as Angelman's syndrome (Guerrini et al., 1996). However in the patients the N1-latency was within normal limits (mean 18.6 ms ± 1.6, 95% confidence limits; value not available in case 9). Neither do delays due to cortico-cortical spread of afferent triggered cortical activity (Brown et al., 1991c) seem sufficient to account for the very excessive delays found in some of the patients. One possibility is the involvement of afferent pathways with indirect projections to cortex.

Delays to distal muscles

Although cortical activity lead EMG in distal upper limb muscles, the sensorimotor cortex's lead over muscle was, in our patients, slightly shorter than expected from the TMS-induced MEP latency in the respective active muscle, recorded in healthy controls. Similar observations have been made in studies of myoclonic patients using back-averaging (Cantello et al., 1997) and in healthy subjects regardless of whether EEG was recorded with bipolar electrodes as here (personal observations), Laplacian or current source derivations (Mima and Hallett, 1999a and b). There may be several explanations for this, including the additional synaptic delay during cortical activation by (submaximal intensity) TMS, the way in which delay is calculated from a single point rather than the whole EMG waveform in TMS and back-averaging studies and the low-pass filtering (with phase delay) of EEG by the skull (Pfurtscheller and Cooper, 1975). However, these factors are alone unlikely to explain the shorter cortical lead in the present patients as in earlier studies, using similar analytical techniques, we found that the phase differences between EEG and EMG in distal muscles were consistent with TMS-induced MEP latencies (Brown et al., 1999; Marsden et al., 2000b). Our earlier studies involved patients with large amplitude multifocal jerks rather than high-frequency myoclonus. These differences in phase relationship could be reconciled if we were to assume mixed afferent and efferent loops to the distal muscles of the upper limbs, with activity in these loops occupying overlapping frequency bands, as for proximal muscles. In patients with large amplitude cortical myoclonic jerks the efferent system might dominate, so that phase differences mirrored closely those expected from TMS. In patients with minipolymyoclonus, there may be mixed afferent and efferent influences on distal muscles. The latter still dominate, so that cortex still leads, but the lead will be an underestimate as it reflects two processes occurring over the same frequency range.

4. EMG-EMG-frequency analysis in limb dystonia

Dystonia is a syndrome characterised by prolonged muscle contractions causing sustained twisting movement and abnormal mobile and/or fixed postures often along with tremor or myoclonus. It may be generalised or focal and is usually classified into primary and secondary causes. Dystonia of the extremities presents a particular problem with major functional limitation and different aetiologies and occurs in patients with primary and secondary dystonia. Limb dystonia is a hallmark of idiopathic torsion dystonia, with mutations in the DYT1 gene representing the commonest genetic basis (Németh, 2002). However, it may also be seen with structural lesions involving the basal ganglia due to trauma, stroke and malignancy (Marsden et al., 1985; Pettigrew and Jankovic, 1985; Kostic et al., 1996; Nardocci et al., 1996) and in the syndrome of fixed dystonia (Marsden et al., 1984; Jankovic and van der Linden, 1988; Bhatia et al., 1993), which can also occur in the context of reflex sympathetic dystrophy (Schwartzmann and Kerrigan, 1990) or the causalgia-dystonia syndrome (Bhatia et al., 1993).

Here it was investigated whether the character of EMG discharge may provide a clue to both pathophysiology and diagnosis in patients with dystonia in whom upper and lower limbs are affected. Some EMG features have been previously reported in dystonic patients (Yanagisawa and Goto, 1971), but these accounts remain largely descriptive and provide relatively little insight into pathophysiology or diagnosis. Thus dystonia is associated with sustained EMG activity of co-contracting muscles lasting up to a few seconds. In addition, shorter regular or irregular bursts of muscle activity in the range from 50 to 200 ms can give rise to additional clinical symptoms such as tremor or myoclonus, depending on the frequency, rhythmicity and duration of these bursts (Yanagisawa and Goto, 1971; Obeso et al., 1983; Jedynak et al., 1991). In the case of fixed dystonia, EMG-bursts between 4 and 8 Hz have also been reported (Marsden et al., 1984; Jancovic and van der Linden, 1988).

Recently, attention has focussed on more sophisticated analyses of EMG discharge in dystonia. These have the potential to disclose the character of the descending discharges

responsible for the abnormal muscle activity. For example, frequency analysis can differentiate idiopathic dystonic torticollis from voluntary torticollis, as patients with dystonic torticollis exhibit an abnormal synchronised drive to agonistic sternocleidomastoid and splenius capitis muscles with a frequency of 4-7 Hz (Tijssen et al., 2000). The same abnormal 4-7 Hz drive has also been reported in patients with complex cervical dystonia (Tijssen et al., 2002) and the report of coherence between pallidal oscillations and dystonic neck muscle activity at similar frequencies in a patient with familial myoclonic dystonia (Liu et al., 2002) serves to highlight the saliency of EMG-EMG coupling in this frequency band. Nevertheless, the extent to which this abnormal descending drive characterises involuntary dystonic limb contraction remains unkown. In the upper limb, for example, the available evidence points to an abnormal corticomuscular drive in the 15-30 Hz band leading to co-contraction between antagonistic muscles, with the exception of writer's cramp where a discrete peak in EMG-EMG coherence may be seen at 11-12 Hz (Farmer et al., 1998), while, in the absence of tremor, EMG-EMG coherence between agonist muscles is normal (Cordivari et al., 2002)

The above observations lead to the hypothesis that the nature of the descending drive to muscles in dystonia may vary depending on aetiology and the muscles under consideration. Hence, in this study the pattern of EMG-EMG coherence in the dystonic upper and lower limb are being investigated in patients with dystonia due to a variety of known aetiologies to establish whether an abnormal 4-7 Hz drive is present in any or all of these conditions.

4.1. Patients and methods

4.1.1. Patients

Frequency analysis of EMG from the lower limb was performed in three groups of patients: 12 symptomatic carriers of the DYT1-gene (5 men, 7 women; mean age 41 yrs, range 21-63 yrs; table 4.1), three patients with symptomatic dystonia due to trauma or in-

farct leading to structural brain lesions (3 women, mean age: 36 yrs, range: 28-44 yrs; table 4.2) and 11 patients with the syndrome of fixed dystonia (2 men, 9 women; mean age: 38 yrs, range: 22-61 yrs; table 4.3). The findings were compared to those in 15 healthy subjects (6 men, 9 women; mean age: 36 yrs, range: 23-60 yrs). In addition, the results in symptomatic carriers of the DYT1-gene were compared to those in four asymptomatic gene carriers (2 men, 2 women; mean age: 51 yrs, range: 43-57 yrs; table 4.1). To compare coherence patterns between upper and lower extremities six out of the 12 symptomatic DYT1 patients and a further three patients with symptomatic dystonia (giving a total of 1 man, 5 women; mean age: 36yrs, range: 24-53 yrs, table 4.2) were investigated. All subjects gave written informed consent and the study was approved by the Joint Research Ethics Committee of the National Hospital for Neurology and Neurosurgery and the Institute of Neurology.

The 12 symptomatic carriers of the DYT1 gene had generalised dystonia, although in two patients clinical manifestations were exclusively task specific (cases 9 and 10). The four carriers of the DYT1 gene had no clinically apparent involvement (Burke-Fahn-Marsden scale score = 0; Burke et al., 1985). Some cases were related (cases 2, 3 and 13; cases 6, 9 and 15). The six patients with symptomatic dystonia had cerebral lesions, of whom four had imaging evidence of involvement of the basal ganglia (table 4.2), but only three had major leg involvement. The majority of the 11 patients with fixed dystonia had a history of peripheral trauma and complex regional pain syndrome (table 4.3). All of the latter patients presented with one leg affected, except case 33 in whom all four limbs were in a fixed dystonic posture. Three of these patients had clinically apparent regular or jerky tremor. All patients with fixed dystonia were DYT1 gene negative.

Table 4.1: Clinical details of the DYT1 gene carriers

Case	Sex	Age (yrs)	Disease duration (yrs)	Burke-Fahn-Marsden rating scale-score	Drugs
symptomatic					
1	F	57	46	40	Clonazepam
2	F	36	11	12	Benzhexol
3	M	34	30	41	Benzhexol, Baclofen
4	F	22	14	40	none
5	M	45	35	45	Botulinum toxin
6	F	21	15	43	Baclofen, Sertraline, Botulinum toxin
7	F	33	22	29	none
8	M	31	15	29	none
9	M	54	~45	6	none
10	F	63	~50	5	none
11	M	41	31	48	Botulinum toxin, Trihexyphenydil
12	F	51	35	37	none
asymptomatic					
13	F	56	-	0	none
14	M	57	-	0	none
15	M	49	-	0	none
16	F	43	-	0	none

Table 4.2: Clinical details of patients with symptomatic dystonia

Case	Sex	Age (yrs)	Aetiology	Imaging abnormalities**	Drugs
17*	F	28	perinatal ischemia	head of caudate nucleus, lentiform nucleus (MRI)	Botulinum toxin
18*	F	44	perinatal ischemia	inferior parietal lobe (MRI)	Botulinum toxin
19*	F	37	postpartal ischeamia	globus pallidus, putamen (MRI)	Botulinum toxin
20	M	30	posttraumatic	globus pallidus (MRI)	Botulinum toxin
21	F	53	perinatal	parietal atrophy (CT)	Botulinum toxin
22	F	24	posttraumatic	lentiform nucleus; frontal and parietal white matter (MRI)	Botulinum toxin

*patients in whom both the upper and lower extremities were studied
**MRI signal change unless otherwise stated

Table 4.3: Clinical details of patients with fixed dystonia

Case	Sex	Age (yrs)	Disease duration (yrs)	History of peripheral trauma	Drugs
23	F	61	11	yes	Botulinum toxin, Paroxetine
24	M	34	12	yes	Botulinum toxin
25	F	41	5	yes	Botulinum toxin
26	F	46	6	yes	Botulinum toxin
27	F	45	8	yes	Botulinum toxin
28	F	40	6	yes	none
29	F	23	2	yes	none
30	F	45	5	yes	none
31	M	37	7	yes	Botulinum toxin
32	F	22	8	yes	Benzhexol, Gabapentin
33	F	29	14	no	Botulinum toxin, Tetrabenazine, Buprenorphin, Baclofen, Lorazepam, Fluoxetine

4.1.2. Recordings

The core assessment was the determination of EMG-EMG coherence between the proximal and distal parts of TA. TA was chosen as it is a superficial muscle that can easily be recorded using surface electrodes and the resulting EMG-EMG coherence has proven a robust measure (Hansen et al., 2002). Additionally, in eight symptomatic DYT1 patients, five patients with fixed dystonia and five healthy subjects TA EMG was recorded simultaneously with needle EMG from both heads of the ipsilateral GC. GC was chosen instead of the soleus muscle as e.g. in Hansen et al. (2002) because the former is more accessible compared to the latter. In the upper limb surface EMG was recorded from triceps, biceps, finger extensor, finger flexor, 1DI and APB.

EMG in TA was recorded using pairs of surface (Ag-Ag, 9mm diameter) electrodes placed 2 cm apart in the horizontal plane on the muscle belly of the proximal and distal portions of the muscle. Electrode pairs were separated by a distance of ~8-10 cm depending

on the subject's height. To study GC concentric needle-EMG electrodes were placed in the lateral and medial heads of the muscle. For upper extremity muscles surface electrodes were placed at a distance of 2 cm on the muscle belly (except for 1DI and APB where one electrode was sited over the metacarpo-phalangeal joint).

Signals were amplified and digitised with 12-bit resolution by a CED 1401 analogue-to-digital converter. The sampling rate was 5000 Hz. Signals were displayed and stored on a PC by a software package (CED Spike 2, version 4). Needle EMG form GC was levelled at > 50uV, off-line to convert the multi-unit analogue EMG signal to a point process, which was then used for subsequent frequency analysis. Concentric needle recordings and levelling were performed so as to avoid contamination of GC signals by volume conduction from TA and movement artefact.

To record lower limb EMG subjects were asked to sit on a chair with the hip and knee flexed at an angle of 90° and to perform sustained submaximal dorsiflexion of the ankle joint with the heel on the ground. All healthy controls, asymptomatic DYT1 carriers and most symptomatic DYT1 patients and patients with cerebral lesions were able to perform this task. The remainder and those patients with fixed dystonia found difficulty in performing the task due to existing back-ground contraction. Similarly, many of the dystonic patients could not exert a maximal voluntary contraction (MVC) of TA that was comparable to that in healthy subjects or asymptomatic DYT1 carriers due to additional co-contraction. In addition, there was no certain equivalence of mean rectified EMG voltage between subjects given the very different interference pattern in some subjects. Accordingly, it was not possible to accurately quantify and compare the % of MVC exerted by each subject. EMG autospectra were therefore expressed as a percentage total EMG power prior to comparison between subjects.

Some patients were asked to perform specific activation tasks (knee extension along with dorsiflexion of the ankle, standing, writing). To record upper limb EMG patients were asked either to write or to perform extension of the elbow, wrist extension and thumb abduction. Both tasks provoked dystonia in the arm.

4.1.3. Analysis

Analysed record lengths were kept constant at 200 s for all muscles and all tasks. Signals were down-sampled to 1 kHz and EMG was rectified. Rectification emphasises tremor peaks in spectra (Fig 1 F) and accentuates firing rate information, thereby improving EMG-EMG coherence estimates (Myers et al., 2003). The discrete Fourier transform and parameters derived from it were estimated as outlined in chapter II by dividing the records into a number of disjoint sections of equal duration (1024 data points).

Phase was formally assessed only where coherence was significant and extended over at least 5 consecutive data points in the frequency spectrum. The constant time lag between the 2 signals was calculated from the slope of the phase estimate after a line had been fitted by linear regression. The time lag was only calculated from the gradient if a linear relationship accounted for (r^2) $\geq$ 71% of the variance ($p < 0.05$).

4.1.4. Statistics

To compare transformed EMG-EMG coherences between groups a repeated measures General Linear Model was performed using frequency as the main effect. Transformed coherences were averaged across 4-7 Hz, 8-13 Hz and 14-30 Hz. These bands were selected as they have been associated with dystonia (Tijssen et al., 2000; Liu et al., 2002; Tijssen et al., 2002), physiological tremor (Vallbo and Wessberg, 1993; Halliday et al., 1999; Vallbo and Wessberg, 1996) and corticomuscular drives (Conway et al., 1995; Salenius et al., 1997; Brown et al., 1998; Halliday et al., 1998; Mima et al., 1998b; Gross et al., 2000), respectively. Where results were non-spherical, a Greenhouse-Geisser correction was used and when differences were significant at the group level post-hoc pair-wise comparison with Scheffé correction was carried out.

4.2. Results

4.1.2. Clinical appearance and raw EMG in the lower limb

The 12 symptomatic DYT1 patients had varying degrees of clinical lower limb involvement. Four patients had periodic leg spasms along with a regular or jerky tremor (jerky because of the appearance of additional non-rhythmic, sometimes myoclonic elements) upon voluntary contraction, five had only a tremor and one patient had leg spasms but without clinically evident tremor. Two patients only had an abnormal gait (Table 1), which was not related to involuntary contractions in the lower leg.

Examples of the raw EMG recorded during active dorsiflexion of the ankle are shown in fig.4.1. Ten out of the 12 (83 %) DYT1 patients with leg involvement exhibited regular bursts in TA that ranged in duration from 50 (Fig. 4.1A) to 200 ms (Fig. 4.1B) in surface EMG. Burst frequency varied from 4 and 7 Hz between subjects. This clinically evident tremor was neurogenic and not due to mechanical resonance phenomena. Simultaneous needle EMG recordings from TA and GC indicated similar rhythmic bursts that were co-contracting with TA activity (Fig. 4.1A). Rhythmic EMG bursting was invariably accompanied by a clinically evident regular or jerky tremor in seven out of the 10 DYT1 patients with this EMG pattern when they performed dorsiflexion of the ankle while sitting. In cases 9 and 10 TA EMG showed a rhythmic bursting pattern, but this was only accompanied by clinically evident tremor when performing specific activation tasks (extension of the hip and knee, with dorsiflexion of the ankle joint and standing, respectively). In case 7 EMG bursts in TA only occurred when the patient wrote and these were not accompanied by clinically evident tremor. EMG had a normal interference pattern when case 7 performed other tasks. The only evidence of dystonia in the lower limb was an abnormal gait due to axial and thigh involvement in cases 11 and 12. Both these patients had a normal interference pattern in TA (Fig. 4.1C).

Conversely, asymptomatic DYT1 carriers, patients with symptomatic dystonia and six of the 11 patients with fixed dystonia had unremarkable EMG interference patterns. Five

patients with fixed dystonia (cases 23, 26, 29, 31, 32) had rhythmic EMG bursts in TA, with a frequency of ~8-10 Hz and an average duration of ~60 ms (Fig. 4.1D). These EMG bursts could be distinguished from those in the symptomatic DYT1 patients by their higher frequency.

Fig. 4.1.

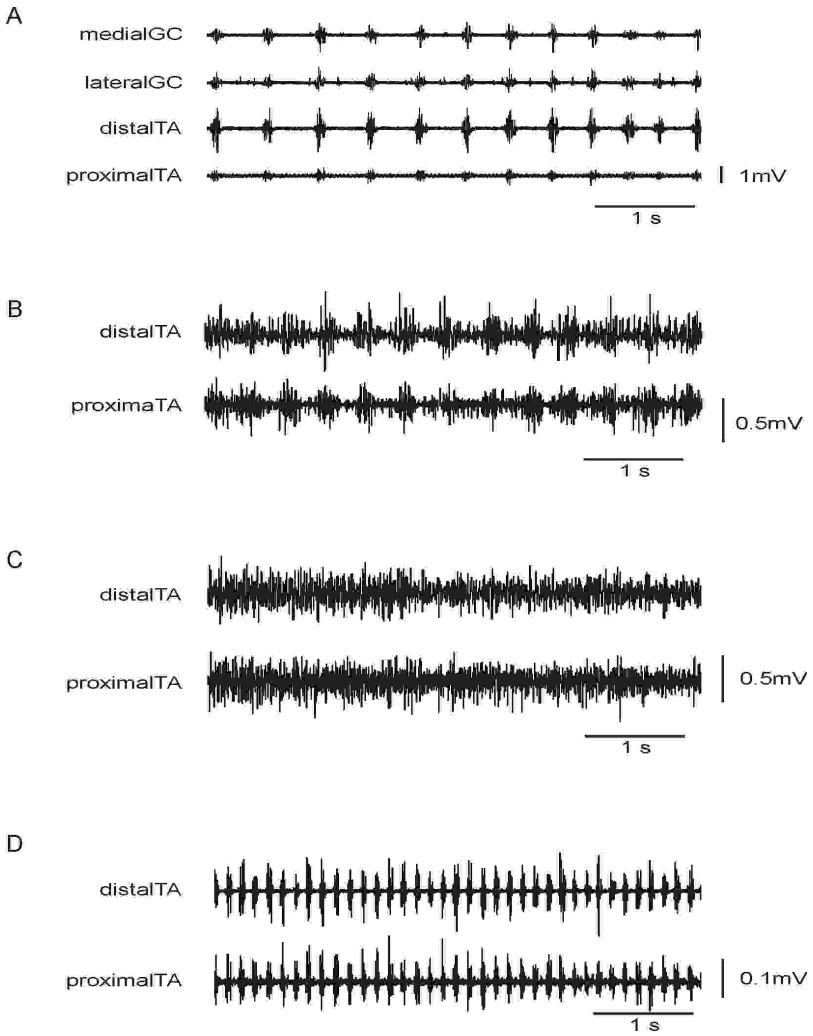

Fig. 4.1: Raw EMG recordings of lower leg muscles in different patient groups. Patients sitting with the ankle actively dorsiflexed. (**A**) and (**B**) symptomatic DYT1 patients with synchronous muscle bursts of 50 (**A**, case 2) and 200 ms (**B**, case 3) duration at 4 Hz. Note that in A antagonistic muscles (GC, TA) are co-contracting. (**C**) Symptomatic DYT1 patient (case 11) with no involvement of the lower leg. The interference pattern is normal. (**D**) Patient with fixed dystonia (case 31) with a ~8 Hz bursting pattern. Patient had a fixed posture with the ankle joint plantar-flexed at ~50° and was asked to try to dorsiflex the ankle. All recordings are surface EMGs, except for GC.

4.2.2. Frequency analysis in the lower leg

The results from frequency analysis of TA EMG averaged across the subjects in each group are presented in Fig. 4.2. The power spectra of rectified TA EMG are dominated by a distinct peak at 4-7 Hz, only present among symptomatic DYT1 patients (Fig. 4.2A). This 4-7 Hz peak was present in all cases in whom the lower leg was clinically affected, but not the those cases (11 and 12) without leg involvement. Note that there is a distinct, but smaller peak at 8-10 Hz in patients with fixed dystonia that relates to the high frequency EMG bursting evident in five out of the 11 cases.

The averaged transformed EMG-EMG coherence in TA is illustrated in Fig. 4.2B. Again, the spectra are dominated by a distinct peak at 4-7 Hz, only present among symptomatic DYT1 patients. The remaining groups, including the healthy controls, show a broad band of increased coherence over 8-30 Hz. That over the 15-30 Hz band is most likely due to rhythmic synchronised discharging in the corticospinal neurones (see Farmer, 1998; Brown, 2000 for reviews). Fig. 4.2C illustrates individual coherence spectra from a symptomatic DYT1 patient. Note that this patient (case 9) only had clinical evidence of leg tremor during a specific task (extension of the hip and knee, with dorsiflexion of the ankle joint), which occasionally alternated with spasms without tremor. Nevertheless, an abnormal 4-7 Hz peak was seen regardless of task. None of the individual coherence spectra from asymptomatic DYT1 patients, patients with dystonia due to focal cerebral lesions, patients with fixed dystonia nor healthy controls showed a peak in the 4-7 Hz band.

Transformed coherences were entered into a general linear model with frequency band (3 levels: 4-7 Hz, 8-13 Hz and 14-30 Hz) as a main effect and grouped according to disease (5 groups: symptomatic DYT1 carriers, asymptomatic DYT1 carriers, symptomatic dystonia with structural lesions, fixed dystonia and healthy controls). There was a significant group x frequency interaction ($F[8,80] = 6.566$, $p < 0.001$). Post-hoc tests indicated that the latter interaction was due to the coherence in the 4-7 Hz band which was greater in symptomatic DYT1 carriers than in patients with symptomatic dystonia and, more importantly, healthy subjects (Fig. 4.2D). In addition, if cases 11 and 12 were excluded (the two patients

whose only lower limb manifestation was an abnormal gait), then coherence in this group was significantly different from any other group including asymptomatic DYT1 carriers and patients with fixed dystonia.

Similarly, when power spectra were entered into a general linear model with the same frequency bands and disease groups there was a significant frequency x group interaction ($F[8,170] = 8.133$; $p < 0.001$; not shown). Here, post-hoc tests revealed significant differences between symptomatic DYT1 and asymptomatic DYT1 carriers and healthy subjects in the 4-7 Hz band. Again, if cases 11 and 12 were excluded, then DYT1 significantly differed from any other group in the 4-7 Hz band. Further, there was no significant frequency x group interaction between symptomatic DYT1 carriers on medication and those without when entered into a separate general linear model.

The time differences between the EMG signals recorded at the rostal and caudal TA electrodes were calculated from phase spectra and are summarised for all subjects in Fig. 4.2E. The estimated delay for conduction between the proximal and distal portion of TA across the subject groups was 2-3 ms. This delay excludes a significant contribution from volume conduction to the observed coherence.

In simultaneous recordings of surface and needle EMG made from TA and GC, respectively, all but one of the symptomatic DYT1 patients showed strong coherence between the antagonistic muscles, with a peak at 4-7 Hz. Fig. 3F is a representative example showing a peak at 4-7 Hz that merged with a broader band of activity extending to 20 Hz. Coherence between TA and its partial antagonists over 8-30 Hz can be a normal finding (Hansen et al., 2002), but that at 4-7 Hz is pathological. Cumulant density estimates of TA-GC activity (not shown) confirmed that EMG was co-contracting among the patients. Note that fast voluntary alternating plantar and dorsi-flexion of the ankle may reach 5 Hz but is associated with out-of-phase coupling between TA and calf muscles (Hansen, 2002).

Fig. 4.2.

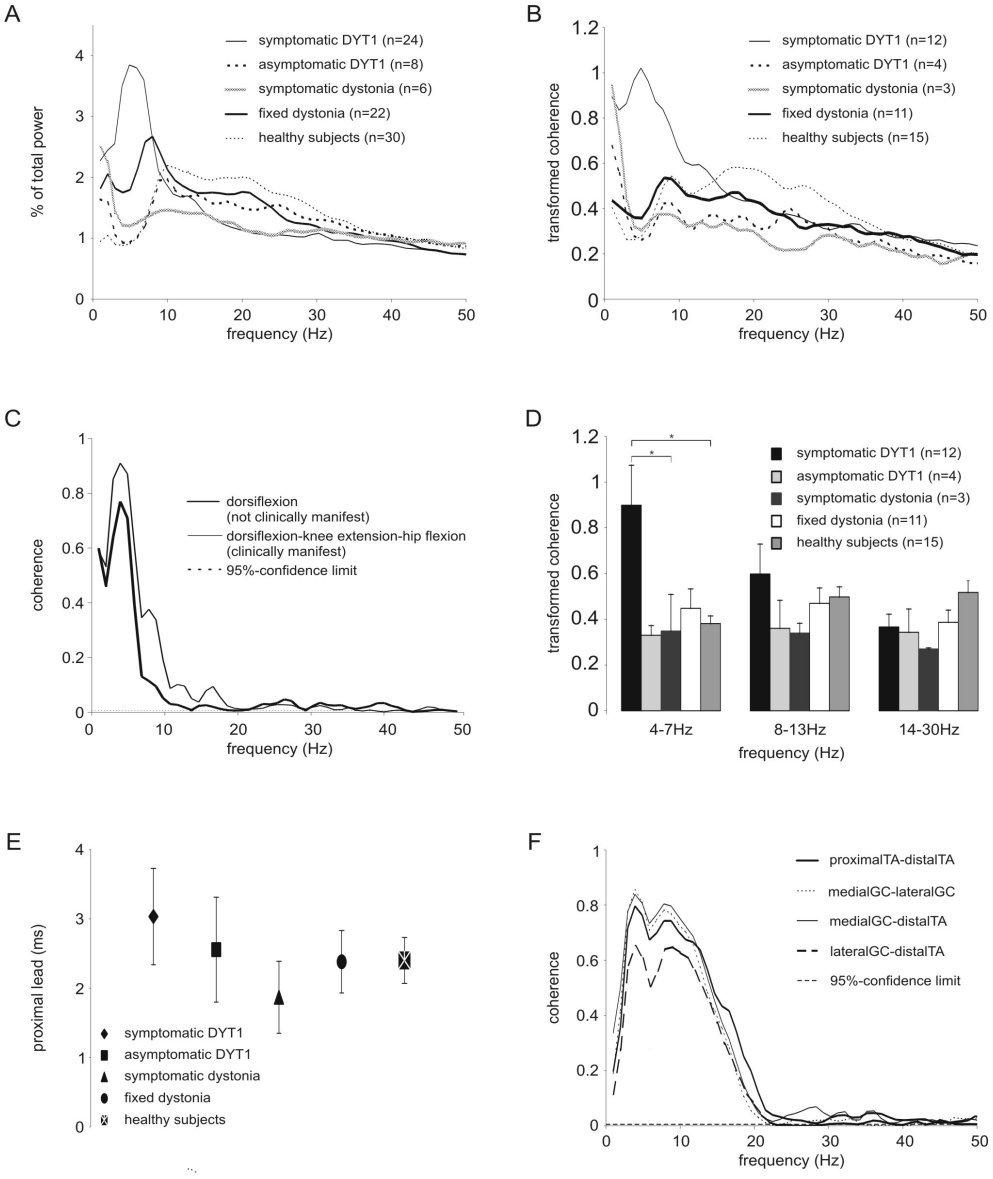

Fig. 4.2: Frequency analysis in the lower leg muscles. (**A**) Averaged %-power spectra of proximal and distal aspects of TA show a peak for symptomatic DYT1 patients at 4-7 Hz. (**B**) Averaged transformed EMG-EMG coherences for TA in the different groups. Note the distinct peak centred at ~5 Hz in the symptomatic DYT1 patients, which is absent in the other groups. (**C**) Individual coherence spectra in case 9 (symptomatic DYT1). Coherence at 4-7 Hz is present regardless of whether tremor was clinically evident or not. (**D**) Averaged transformed coherences in the 3 frequency bands. The 4-7 Hz activity was greater in symptomatic DYT1 patients (asterix = $p<0.05$). (**E**). Time delay estimates (**G**) between proximal and distal aspects of TA, confirming conduction delay. Bars are 95%-confidence limits. (**F**) Abnormal coupling between TA and GC with a distinct peak at ~4 Hz in the same patient as Fig. 1A (levelled EMG). Error bars indicate the standard error of the mean.

4.2.3. EMG-EMG Coherence in the upper extremity

The prominence of EMG-EMG coherence at 4-7 Hz in the lower limb of symptomatic patients carrying the DYT1 gene raised the question of whether this activity also dominated in the upper limb. This was studied in six of the symptomatic DYT1 patients. Only two of these patients showed a 4-7 Hz pattern in arm muscles similar to that in their lower limbs. These patients also had peaks in EMG-EMG coherence at 4-7 Hz both for TA and for selected muscle pairs of the upper limb (Fig. 4.3A), but there was no significant coherence between ispilateral upper and lower extremity muscles. Both patients had clinically manifest tremor in the upper limbs. The coherence pattern in the remaining four patients differed between upper and lower limbs. Despite EMG-EMG coupling at 4-7 Hz in the lower limb these patients only had irregular low frequency spasms in the upper limb leading to EMG-EMG coherence < 3Hz (Fig. 4.3B). A similar pattern was found in the six patients with symptomatic dystonia due to focal cerebral lesions who had dystonic upper limbs.

Fig. 4.3.

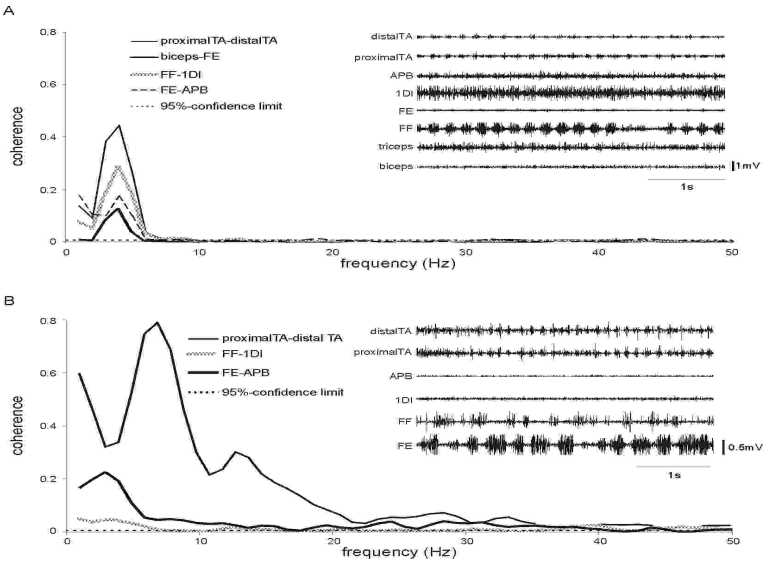

Fig. 4.3: Coherence patterns in upper extremity muscles in symptomatic DYT1 patients. (**A**) Case 1. Inset: regular bursting pattern in TA and forearm flexors (FF). Coherence spectra confirm exaggerated EMG-EMG coherence in the 4-7 Hz range in upper and lower limb. FE = finger extensor. (**B**) Case 5. Inset: 7 Hz bursting pattern in TA is not reflected in upper extremity muscles. Instead alternating bursts prevail in FF and FE at ~2-3 Hz. Coherence spectra confirm exaggerated EMG-EMG coherence in the 4-7 Hz range in lower but not upper limb.

4.3. Discussion

It can be shown that different patterns of EMG-EMG coherence prevail in different aetiological groups of patients with dystonic limbs. In addition, the pattern of coupling between muscles may differ between the upper and lower extremities in patients with the same aetiology. Differences in the pattern of synchronisation within and between muscles of the upper and lower limbs have been previously noted in healthy subjects (Nielsen and Kagamihara, 1994; Hansen et al., 2002). In so far as EMG-EMG coherence reflects the common drives to spinal motoneurones these observations imply that the nature of EMG-EMG coherence in dystonia may be constrained by the character of descending motor systems, both in terms of their anatomical distribution and their frequency characteristics.

The most striking finding was an abnormal drive synchronising motor unit discharge at 4-7 Hz in the distal lower limb of symptomatic patients with the DYT1 gene mutation, irrespective of whether patients were related with each other or not. This drive involved agonist and antagonist muscles leading to co-contracting EMG bursts. In most patients the pathological drive was manifest clinically as a jerky or regular tremor, though there were instances where EMG indicated an abnormal 4-7 Hz drive in the absence of clinical tremor. The advantage of frequency analysis was that it confirmed the homology of the tremor in the tremolous subjects, demonstrated that the same oscillatory drive could be subclinical, permitted quantitative assessment and comparison with other aetiological forms of dystonia and showed that EMG activity in symptomatic DYT1 carriers is dominated by a drive that leads to pathological synchronisation of motor unit discharge at 4-7 Hz. Coherence rather than power spectra were particularly important in demonstrating the latter.

The coherence at 4-7 Hz was not caused by electrical cross-talk. When detected in recordings from the proximal and distal aspects of TA it was associated with a phase difference that was appropriate for axonal conduction. When detected in recordings from TA and GC this was despite the use of concentric needles in GC and levelling of EMG discharge to select the largest amplitude EMG activity, both of which would have minimised the effects of cross-talk. In addition, whether detected within TA or between TA and GC,

coherence occurred in a discrete band, whereas cross-talk would have lead to more extensively elevated coherence.

The study did, however, have one particular limitation. For a variety of clinical reasons outlined in the Results we were unable to accurately match contraction strengths across patients. To limit the impact of this we compared normalised EMG power spectra. Nevertheless, it must be acknowledged that the strength of contraction can change the relative distribution of EMG power and also the pattern of EMG-EMG coherence. The best documented change with strong contractions is an increase in EMG activity in the Piper range of 40-60 Hz, due to increased corticomuscular drive in this band (Brown et al., 1998). However, differences in power and coherence in this band were not apparent between groups. Further, synchronisation at 4-7 Hz has not been demonstrated in lower leg muscles in healthy subjects, even when different levels of muscle contraction were assessed (Hansen et al., 2002). Another way in which task execution may have altered the pattern of EMG is through fatigue. As discussed later this may have contributed to the altered interference pattern in some patients with the syndrome of fixed dystonia, but is unlikely to account for the segmented 4-7 Hz EMG pattern in the lower limb of symptomatic DYT1 carriers which was present when contractions were made from rest.

The abnormal drive was found in over 80 % of symptomatic DYT1 patients and in all of those with leg dystonia if gait abnormalities due to axial and proximal leg involvement were excluded. The 4-7 Hz activity was manifest in raw EMG and coherence spectra whether or not accompanied by a clinically evident regular or jerky tremor. However, it was absent in patients with leg dystonia due to other aetiologies. Together, these factors indicate that simple surface EMG recordings from TA may be helpful in suggesting a DYT1 mutation in patients with lower limb dystonia. Of course, a rhythmic synchronising of motor unit discharges at 4-7 Hz is not exclusively seen in dystonia, but may also be seen in Parkinson's disease.

The abnormal 4-7 Hz drive to the dystonic lower limb in patients with the DYT1 gene mutation is similar to that previously reported in patients with idiopathic dystonic torticollis (Tijssen et al., 2000; Tijssen et al., 2002). This, together with the coupling between

pallidal oscillations and dystonic neck muscle activity at a similar frequency in a patient with familial myoclonic dystonia (Liu et al., 2002) suggests that there is an abnormal synchronising drive in the theta (4-7 Hz) range in dystonia which may involve the globus pallidus. But whether this theta drive is exclusive to some types of dystonia rather than suggestive of extrapyramidal involvement per se seems unlikely. Strong coherence between activity in globus pallidus internus and arm muscles at tremor frequency (3-6 Hz) has also been reported in patients with Parkinson's disease (Hurtado et al., 1999; Lemstra et al., 1999), so that the globus pallidus might be generally involved in different movement disorders associated with tremor and pathological synchronisation at 4-7 Hz. The implication here is that the 4-7 Hz drive is not necessarily responsible for dystonia, at least by itself, as similar drives may occur without dystonia, as for example in the resting leg tremor of Parkinson's disease, and dystonia may occur in the upper limbs of patients with the DYT1 gene in the absence of a 4-7 Hz drive to the affected muscles. Rather, the abnormal 4-7 Hz drive may be one product of basal ganglia, and particularly pallidal, dysfunction that is closely related to the aspect of basal ganglia dysfunction that causes dystonia, but which is not one and the same. Nevertheless, it is likely that the 4-7 Hz drive was closely associated with the development of dystonia in patients with the DYT1 gene as it was absent in asymptomatic carriers and present in nearly all affected carriers. The hypothesised relationship between the theta drive to muscle and the pallidum is particularly interesting given the greater success of pallidal stimulation in DYT1 dystonia compared to dystonia of other aetiologies (Coubes et al, 2000).

The exaggerated synchronising drive to lower leg muscles between 4 and 7 Hz in symptomatic patients with DYT1 dystonia and clinical involvement of the affected leg was distinct from the EMG-EMG coherence over 8-10 Hz evident in the lower leg of healthy subjects controls (Hansen et al., 2002) and exaggerated in some of our patients with fixed dystonia. The latter exaggeration may simply reflect the fact that this drive becomes more prominent with more prolonged contraction of lower leg muscles. Under this condition even healthy subjects may show a sufficiently pronounced burst-like EMG activity with a frequency of around 10 Hz that it becomes evident as a clear tremor (Hansen et al., 2002).

The finding of an abnormal common drive to spinal motoneurones innervating the lower limb in symptomatic patients with DYT1 but not in other forms of leg dystonia should also be placed in context of the other electrophysiological abnormalities identified in dystonia (see Berardelli et al., 1998 for review). Abnormalities in cortical (Ridding et al., 1995; Ikoma et al., 1996), brainstem (Berardelli et al., 1985; Tolosa et al., 1988; Nakashima et al., 1989) and spinal inhibition (Panizza et al., 1990; Deuschl et al., 1992) have been found in dystonia, but these too cannot alone be responsible for the abnormal movement pattern as they may be seen outside of the clinically involved area, and, like the 4-7 Hz drive, may not be limited to patients with dystonia (Berardelli et al., 1998). However, these abnormalities of inhibition do not serve to distinguish different aetiological forms of dystonia.

It seems likely that frequency analysis may be able to differentiate between some aetiologies in dystonia. We have shown that symptomatic DYT1 leg dystonia is associated with an abnormal 4-7 Hz drive to spinal motoneurones, that is not present in asymptomatic DYT1 carriers, patients with symptomatic dystonia or patients with fixed dystonia, while Farmer et al. (1998) have previously shown that an 11-12 Hz drive may distinguish some cases of writer's cramp from symptomatic hemidystonia or primary segmental dystonia in the upper limb. The difference in pathophysiological mechanisms in different aetiologies of dystonia is not limited to the pattern of common drive to muscles. Differences between idiopathic torsion dystonia (which includes DYT1) and symptomatic dystonia have also been reported in some PET studies (Ceballos-Baumann et al. 1995a; Ceballos-Baumann et al. 1995b). Whereas in patients with idiopathic dystonia the sensorimotor cortex is under-activated during voluntary movements, the reverse is seen in those with symptomatic dystonia. Both groups, however, show over-activity of other frontal lobe regions. Further studies are required to define pathophysiological differences between different dystonic aetiologies, especially when phenotypes may be so similar.

5. Coherence analysis in the myoclonus of corticobasal degeneration

Myoclonus is a common finding in corticobasal degeneration (CBD), with more than half of patients exhibiting jerks during the course of the disease (Kosmopoliti et al., 1998). It has features in common with cortical myoclonus as it is predominantly distal, action-induced and stimulus sensitive with a rostro-caudal spread of the myoclonic bursts along the affected limb (Thompson et al., 1994). However, classical neurophysiological techniques have generally failed to confirm a cortical origin for the myoclonus in CBD. Only one patient has been reported in whom back-averaged surface EEG disclosed a time-locked cortical correlate (Tanosaki et al., 1999) and a further patient has been reported in whom a cortical correlate was identified upon magnetoencephalography Mima et al., 1998a). Similarly, in a large study comprising 14 patients a giant sensory evoked potential was only found in one case (Thompson et al., 1994). The rarity of electrophysiological evidence of a cortical origin could be due to methodological difficulties, pathological involvement of the sensorimotor cortex (Brunt et al., 1995; Lu et al., 1998) or a subcortical origin for the myoclonus.

The myoclonus of CBD tends to be of high frequency and low amplitude. Under these circumstances we expected frequency analysis to have some advantages over time-domain methods, such as back-averaging, in the detection of a cortical correlate as shown in other conditions associated with cortical myoclonus (Guerrini et al., 2001, Brown et al., 1999).

5.1. Patients and methods

5.1.1. Patients

Five patients (table 5.1) who fulfilled the criteria of clinically probable CBD (Riley and Lang, 2000) were examined. All patients exhibited unilateral action-induced and stimulus sensitive myoclonus in the upper extremity except case 5 who had bilateral myoclonus. 4

healthy subjects (mean age: 62 years, range: 55-65 years) were also studied. Patients and healthy subjects gave their informed consent to the study, which was approved by the local ethics committee.

Table 5.1.

Case	Sex	Age (yrs)	Disease duration (yrs)	Peak frequency of myoclonic bursts [Hz]	Clinical features	Drugs
1	F	66	4	14	unilateral asymmetric akinetic-rigid syndrome; limb apraxia, dystonia, dysarthria	L-Dopa, Baclofen, Sodium Valproate
2	F	65	6	17	unilateral asymmetric akinetic-rigid syndrome; dystonia, pain	Morphine, Gabapentin
3	F	57	N/A	10	unilateral asymmetric akinetic-rigid syndrome; dystonia, pain	Sodium Valproate
4	F	66	6	20	unilateral asymmetric akinetic-rigid syndrome; painful limb dystonia, numbness	None
5	F	66	5	8	unilateral asymmetric akinetic-rigid syndrome; dystonia, dysphasia	Amantadine

5.1.2. Recordings

Surface EMG and EEG were recorded with 9 mm diameter silver-silver chloride electrodes. Bipolar EEG was recorded from FC3/4-C3/4. EMG was recorded bilaterally from finger extensor and first dorsal interosseous (1DI) muscles in cases 1 and 2 and from the affected finger extensors and 1DI in cases 3-7. EMG and EEG were amplified, band-pass filtered and sampled at 600 Hz (cases 1-2) or 2 kHz (cases 3-7). Signals were displayed and stored on a PC using CED Spike 2, version 4 software. Patients were recorded during postural contraction which would trigger the myoclonus. Healthy subjects were asked to co-activate recorded muscles over 4 periods of about 60 seconds with 60 seconds rest between contractions.

5.1.3. Frequency analysis and back-averaging

Analysed record lengths were kept constant at 200 seconds in all subjects. The EEG and rectified EMG were assumed to be realisations of stationary zero mean time series. EEG-EMG and EMG-EMG coherence were analysed using methods outlined in chapter II. Signals were interpolated or down-sampled to a sampling rate of 1 kHz and block size was 1024 data points. The phase was only assessed where coherence was significant and extended over at least 5 consecutive data points.

First-order partial coherence functions were also estimated to assess whether 'partialisation' with a third process (the 'predictor') accounted for the relationship between two other processes (Halliday et al., 1995; Rosenberg et al., 1998). As used here, partial coherence can be viewed as representing the fraction of coherence between EMG signals that is not shared by EEG (Halliday et al., 1995; Rosenberg et al., 1998; Spauschus et al., 1999). Thus, if sharing of the signal between the different EMG signals and EEG were complete, then partialization of the coherent activity between the EMGs with contralateral EEG as the predictor would lead to zero coherence. It follows that if EEG had no influence on the coupling between EMGs then partialization with EEG would have no effect on EMG-EMG coherence.

Back-averaging was performed off-line in Spike 2. EMG was rectified and myoclonic EMG bursts identified using a level of 100 μV to produce a series of digital events. EEG and EMG signals were then re-aligned to these events and averaged.

5.1.4. Statistics

The power in each bin of autospectra was expressed as the relative percentage of the total power of each autospectrum. The variance of the coherence was normalised by transforming the square root of the coherence (a complex valued function termed coherency) at each frequency using the Fisher transform. This results in values of constant variance for

each record given by 1/2L where L is the number of segment lengths used to calculate the coherence.

To compare autospectra and coherences between patients and normals repeated measures ANOVA (analysis of variance) was performed. When a significant difference was present, post-hoc pair-wise comparison with Scheffé correction was carried out.

5.2. Results

Fig 1A is an example of the raw EMG, showing high frequency myoclonic bursts in both finger extensor and 1DI at a rate of ~12 Hz, together with the accompanying EEG. Note the absence of a normal interference pattern in Fig 5.1A, with no pre-innervation between myoclonic bursts. Fig 5.1B shows the corresponding autospectra of EEG and EMG and Fig 5.1C is the coherence between finger extensor and 1DI, all in the same patient (case 1). Intermuscular coherence is excessively exaggerated up to ~60 Hz. Partial coherence between between finger extensor and 1DI with the EEG as predictor shows only a slight reduction of coherence in the frequency range between 6 and 11 Hz.

Fig. 5.1.

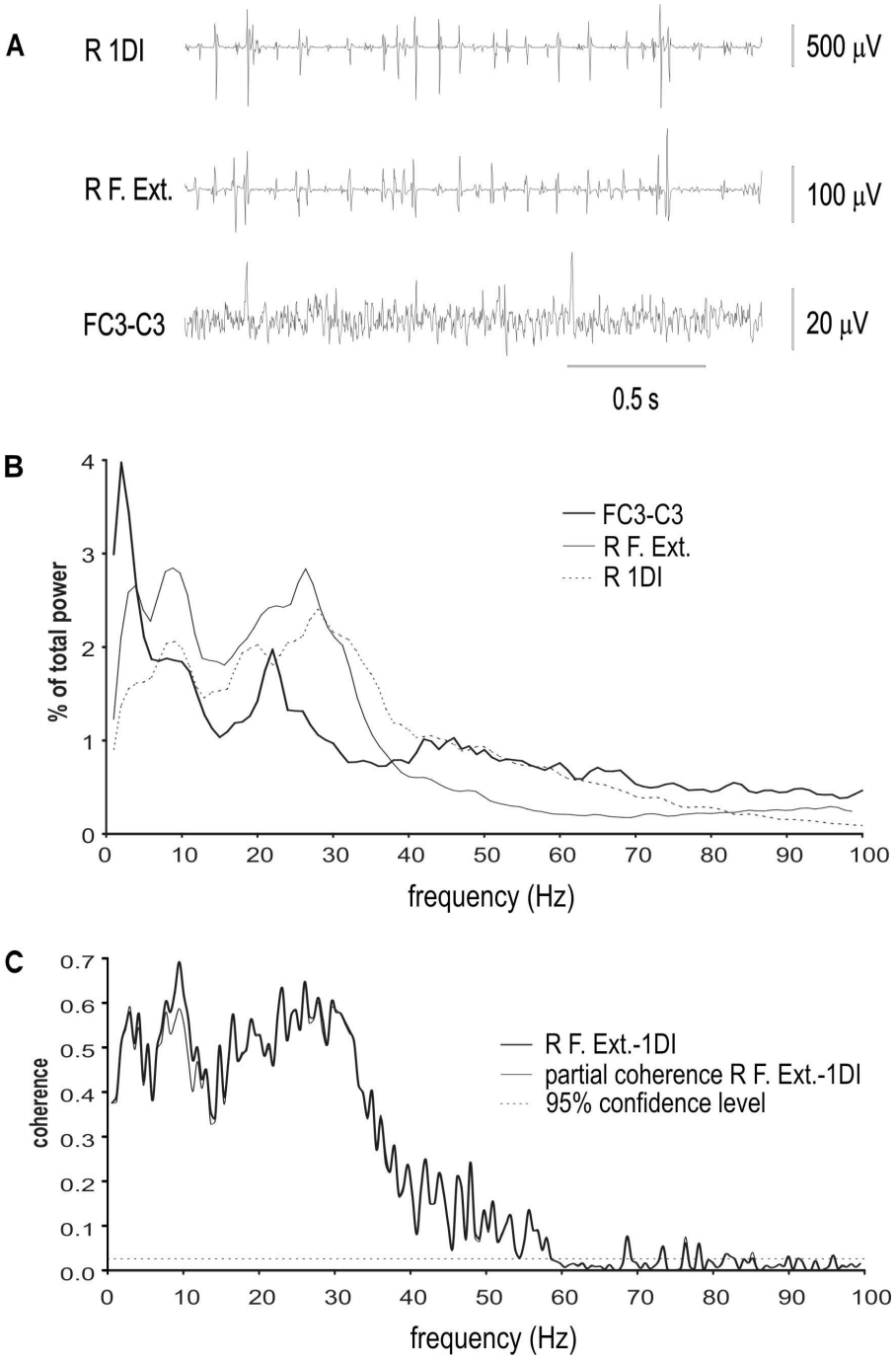

Fig. 5.1: (**A**): Raw EEG and EMG of case 1 exhibiting irrregular short myoclonic bursts at an average frequency of ~12 Hz during a postural contraction. (**B**) Normalised autospectra of EEG over FC3-C3 and EMG from finger extensor and 1DI. (**C**) Intermuscular coherence (thick line) between finger extensor and 1DI discloses exaggerated coherence up to 58 Hz. Note that the partial coherence between the two muscles (thin line) with the EEG as predictor is only slightly lower from 6 to 12 Hz.

Similar to case 1, all the remaining patients had abnormally inflated EMG-EMG coherence and the results of all 5 patients are pooled in Fig 5.2. Fig 5.2 A is the mean percentage total EEG power at each frequency in the five patients recorded over the sensorimotor area ipsilateral and contralateral to the affected limb, compared to that found in age-matched healthy subjects. The normal power increase in the beta range (15-30Hz) with a peak centered around 20 Hz is absent in the patients and there is a shift of EEG activity to the theta range, with a peak at ~8 Hz, which is, however, not statistically significant. Figures 5.2 B and 5.2C are the mean percentage total EMG power at each frequency for the forearm extensors and 1DI, respectively. The patients show a large peak centred around 15 Hz. Figure 5.2D is the mean transformed coherence between the ipsilateral forearm extensor and 1DI EMG signals in the five patients, compared to that in high frequency cortical myoclonus (Grosse et al., 2003) and healthy subjects. The five patients with CBD have a grossly inflated EMG-EMG coherence over a broad band that even exceeds that in the patients with established high-frequency cortical myoclonus. Transformed coherence reached up to 1.5 (range 0.4-1.5) and was above the 95%-confidence limit up to 60 Hz. Coherence for CBD patients was significantly different from normals ($p<0.001$) in both the 8-30 Hz (α and β bands) and 31-60 Hz (γ band), while patients with cortical myoclonus only differed form normals over the 8-30 Hz range ($p<0.05$) (Fig. 5.2E). In CBD, phase spectra suggested that EMG activity in the forearm extensors preceded that in 1DI by 5.5 ± 0.7 ms (range 3.1 –7.7 ms), consistent with synchronisation through an efferent drive and excluding volume conduction as an explanation for the high levels of EMG-EMG coherence (Fig. 5.2F). Similar lags were seen in cortical myoclonus and healthy subjects.

Fig. 5.2.

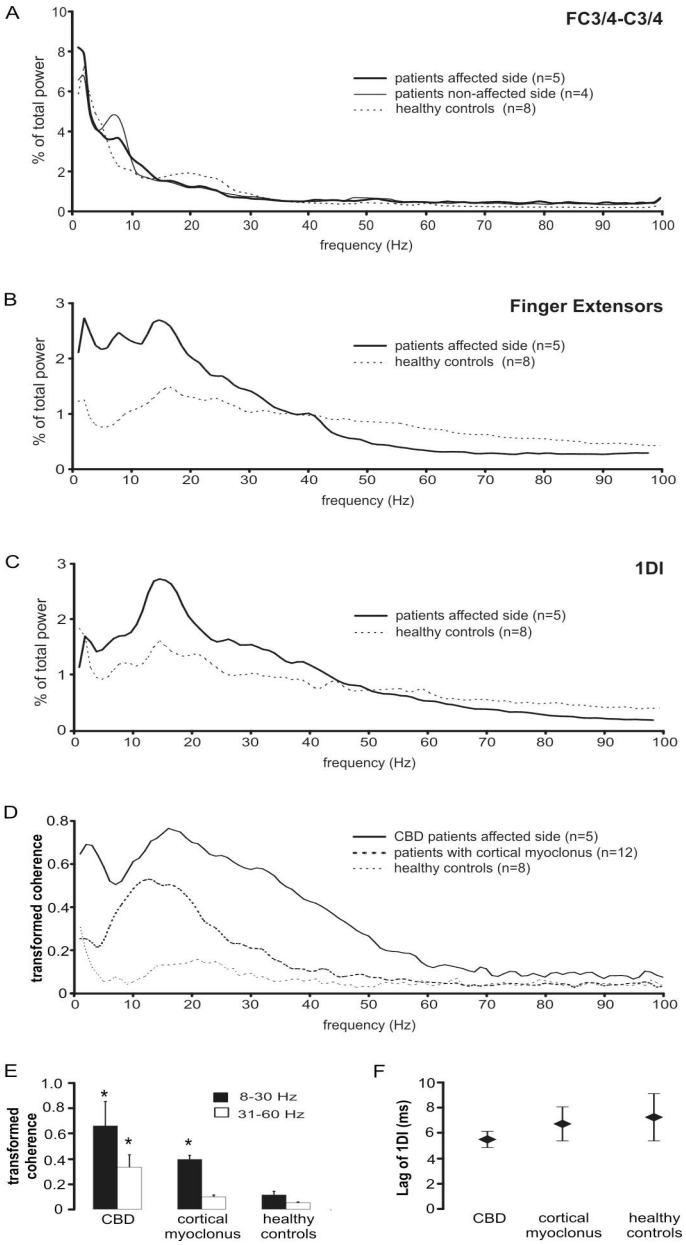

Fig. 5.2: Pooled results in the 5 patients compared to age-matched healthy subjects. Normalised power for EEG (**A**), finger extensor (**B**) and 1DI (**C**). Pooled transformed coherence for finger extensor and 1DI is inflated in the range up to 60 Hz with a peak centered around 15 Hz (**D**). Note that EMG-EMG coherence for patients with established high frequency cortical myoclonus is less exaggerated and occupies a narrower frequency band. (**E**) In CBD patients coherence is significantly different from both normals and patients with cortical myoclonus across 8-30 Hz and 31-60 Hz, while for patients with cortical myoclonus only the 8-30 Hz band is statistically different from normals. Error bars indicate standard error of the mean. (*=$p<0.05$). (**F**) Time delays between the two muscles for patients with CBD, patients with cortical myoclonus and healthy controls showing an appropriate delay between 1DI and finger extensors, thereby indicating that high levels of coherence were not due to volume conduction.

Despite the grossly inflated intermuscular coherence, significant cortico-muscular coherence was only found for both finger extensor and 1DI in case 1 and occurred over a narrow frequency range centred around 10 Hz (Fig 5.3 A) which corresponds to the drop in coherence when partialisation with EEG was performed (shown in Fig.5.1 C). On the affected side the phase spectrum was suggestive of an afferent drive, as 1DI EMG lead EEG by 51.7 ± 6.4 ms (Fig 5.3 B) and finger extensor EMG lead EEG by 58.2 ± 10.8 ms. In contrast, over the unaffected side EEG lead finger extensor EMG by 5.4 ± 2.6 ms, consistent with a predominantly cortico-spinal drive while phase for 1DI was not significant.

Fig.5.3.

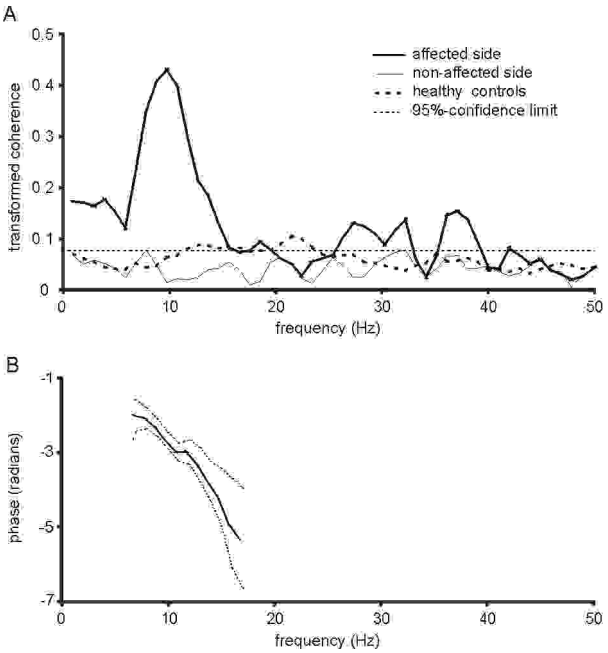

Fig. 5.3: (**A**) Transformed coherence between affected side (FC3/C3-right 1DI) and unaffected side (FC4/C4-left 1DI) in case 1 showing exaggerated coherence on the affected side up to 18 Hz with a distinct peak at 10 Hz which is neither present on the unaffected side nor in averaged coherence in normals. Compare this narrow EEG-EMG coherence with the broad band of EMG-EMG coherence in the same patient shown in Fig 1C. (**B**) Phase spectrum on the affected side discloses that right 1DI EMG leads EEG by 28.4 ± 7.7ms.

Back-averaged EEG and cumulant density estimates were negative or disclosed ambiguous results with no unequivocal EEG cortical correlate preceding the onset of averaged EMG.

5.3. Discussion

It can be shown that in five patients with the clinical diagnosis of probable CBD a distinctive pattern of inflated EMG-EMG coherence over a broad band without evidence of a comparably exaggerated EEG-EMG coherence was present. The very high levels of intermuscular coherence in the affected limb are indicative of an abnormally strong common drive to these muscles. There are several reasons for believing that this common drive might differ in some respects from other forms of cortical myoclonus which have been studied so far. Using similar techniques, exaggerated EMG-EMG coherence can be seen in rhythmic high-frequency cortical myoclonus, but in this condition this feature is accompanied by abnormal EEG-EMG coupling to finger extensors and 1DI over a common frequency range (Grosse et al., 2003), in which EEG phase leads EMG (Farmer et al., 1993). We found no significant EEG-EMG coherence in four of our patients, and, in the one patient in whom this activity was present, EMG lead EEG on the affected side, indicating reafference rather than corticospinal drive. Although motor cortex pathology is common in CBD, affecting most likely both cortico-cortical and efferent cortical projections (Armstrong et al., 2000; Armstrong et al., 2001) it is, however, unlikely that this could entirely obscure cortico-muscular coherence while leaving the structures generating myoclonus preserved (Grosse et al., 2003). Cortical myoclonus is the result of the synchronised discharge of pyramidal neurones in the motor cortex and it is depolarisation of these neurones that likely accounts for the scalp negative cortical correlate that underlies cortico-muscular coherence. High frequency cortical myoclonus is likely to represent an exaggeration of the physiological tendency of cortical pyramidal neurones to synchronise in the lower beta band (Grosse et al., 2003) and it is conspicuous that the normal peak at this frequency was absent from the EEG picked up over the sensorimotor cortex in our patients with CBD. By exclusion, then, it is possible to hypothesise that the elevated EMG-EMG coherence in the absence of any significant EEG-EMG coherence found in our patients was either subcortical in origin or that it reflects a disturbed interaction and gradual disintegration of the network between the sensorimotor cortex and subcortical structures as has been previously

suggested (Carella et al., 1997). The involvement of a subcortical generator of the myoclonus would be consistent with the exceptionally short latency of reflex myoclonus in CBD compared to typical cortical reflex myoclonus (Thompson et al., 1994; Lu et al., 1998).

6. Bilaterally synchronous oscillatory EMG-EMG activity evoked by the acoustic startle the healthy human

A major impetus to the study of motor control in both health and disease has been the realisation that the cortico-spinal system in the human tends to drive synchronisation of motor units over the 15-30 Hz band, to the extent that the coupling between EMG signals at this frequency may be taken as a surrogate marker of cortico-spinal activity (Farmer et al., 1993; Conway et al., 1995; Salenius et al., 1997; Baker et al., 1997; Mima et al., 1998b; Brown et al., 1998; Brown et al., 1999; Kilner et al., 1999; Halliday et al., 1998; Gross et al., 2000; Marsden et al., 2001; Forss et al., 2002; Grosse et al., 2003). In contrast, knowledge of reticulospinal function has been limited by the inaccessibility of this system, both in terms of recording and stimulating, and by the absence of a known surrogate measure in EMG, with the exception of the drive to motor units at above 60 Hz during breathing (Kirkwood et al, 1982; Carr et al, 1994). Here, we use the acoustic startle response (ASR) to demonstrate that some forms of reticulospinal activity in the human are associated with a characteristic pattern of bilaterally synchronous oscillations with a frequency of 10-20 Hz between motor units.

As in other animals there are several lines of evidence that the ASR in humans is relayed in the reticular formation of the lower brainstem and uses reticulospinal efferents (Hammond, 1973; Leitner et al, 1980; Davis et al, 1982; Lingenhöhl and Friauf, 1992; Lingenhöhl et al, 1992; Koch and Schnitzler, 1997; Koch, 1998; Yeomans and Frankland, 1996; Yeomans et al., 2002). Firstly, the startle reflex exists in anencephalic infants (Edinger and Fisher, 1913). Secondly, the caudo-rostral pattern of recruitment of cranial nerve innervated muscles suggests a generator in the caudal brainstem in the startle reflex (Brown et al., 1991a; Valldeoriola et al., 1997; Matsumoto et al., 1992). Thirdly, symptomatic cases of exaggerated startle involve brainstem pathology and sometimes responses at a latency only compatible with a brainstem relay (Brown et al., 1991b; Matsumoto et al., 1992). Finally, the startle reflex is diminished in the Steele-Richardson-Olszewski syndrome, in

which there are widespread pathological changes in the brainstem including degeneration of the pontine reticular formation with severe neuronal loss (Vidailhet et al., 1992).

We recorded EMG activity in proximal and distal upper extremity muscles during the physiological startle reflex in order to define any common drive to motoneurones from the reticulospinal system in the human. Given that the reticulospinal system projects bilaterally and preferentially innervates motoneurones of proximal muscles (Kuypers, 1981), we predicted that a reticulospinal drive would be evident as significant EMG-EMG coherence between homologous proximal muscle pairs, with less coupling between hand muscles on the two sides of the body.

6.1. Methods

6.1.1. Subjects and recording procedure

Healthy subjects gave their informed consent to the study which was approved by the by the Joint Research Ethics Committee of the National Hospital for Neurology and Neurosurgery and the Institute of Neurology. 28 subjects were recorded but only 15 had at least two auditory startle reflexes upon testing. Only the results in these subjects (13 female, 2 male; mean age: 29 yrs; range: 20-59 yrs) were therefore analysed. EMG was recorded from deltoid, biceps, finger flexor, and first dorsal interosseous (1DI) using surface electrodes (Ag-Ag, 9mm diameter) placed 3 cm apart on the muscle belly, with the exception of 1DI where the reference electrode was placed over the proximal metocarpo-phalangeal joint of the index finger. EMG was also recorded from sternocleidomastoid and the onset of activity in this muscle was used to trigger the selection of post-stimulation startle blocks (see later). Facial muscles, which are usually activated during the startle response such as orbicularis oculi, masseter or mentalis (Brown et al., 1991) were not recorded as significant cross-talk between these muscles was to be expected. Coherence between right and left sternocleidomastoid muscles was not evaluated for similar reasons.

Subjects sat on a chair and were asked to provide a gentle background contraction of deltoid, biceps, finger flexors and 1DI, bilaterally, while [1] unexpected acoustic stimuli (1 kHz tone of 50 ms duration at 98 dB) were delivered pseudorandomly and binaurally through headphones once every 5 minutes or so, or [2] they voluntarily mimicked a startle response at a rate of once every 10 s after an initial learning session. The voluntary startles served to show that any drive identified in the ASR was not related to background contraction, some non-specific feature of phasic movements or of the analytical approach utilised. However, given that the physiological cortico-spinal drive to motor units is attenuated during movement (Brown et al., 1998; Kilner et al., 1999), voluntary startles did not allow us to contrast the pattern of the corticospinal drive to muscles with that evident during reflex startles. We therefore [3] also asked the same subjects to tonically contract their deltoid, biceps and 1DI muscles bilaterally at a level under 50% maximal voluntary contraction for a period of about 60s.

EMG was band pass filtered between 53 and 1000 Hz and signals were amplified and digitised with 12-bit resolution by a CED 1401 analogue-to-digital converter. The sampling rate was 2 kHz. Signals were displayed and stored on a PC by a software package (CED Spike 2, version 4).

6.1.2. Analysis

Frequency analysis was performed upon the ASRs recorded in the 15 subjects. To this end the 0.92 s following the onset of each ASR (defined in sternocleidomastoid) was extracted from the recording. Only ASRs with a mean rectified EMG level in each block greater than thrice pre-stimulation background (in sternocleidomastoid, deltoid and biceps muscles) were analysed. In this way habituated startles were avoided. All the extracted ASRs were then concatenated to give a total record of 100 s, which was downsampled by averaging successive pairs of data points after digitally low pass filtering at 500Hz to avoid aliasing. Sham startle responses and submaximal voluntary contraction were processed in a

similar fashion, concatenating the same data lengths as used in the ASR from each subject. Table 1 shows how many ASRs individual subjects contributed to the whole sample.

Table 6.1: Number of startle blocks in each subject contributing to the entire ASR sample (block size: 0.92s)

number of startles	no. of individuals
2	4
3	2
5	1
6	2
9	2
13	1
14	1
15	1
17	1

Coherence and cumulant density estimates were estimated from rectified EMG using methods outlined in chapter II. The discrete Fourier transform and parameters derived from it were estimated by dividing the concatenated records into a number of disjoint sections of equal duration (512 data points), and estimating spectra by averaging across these discrete sections (Halliday *et al.*, 1995). The frequency resolution of all spectra was 2 Hz.

6.1.3. Statistics

The power in each bin of autospectra was expressed as the relative percentage of the total power of each autospectrum to facilitate comparison between muscles and subjects. The variance of the coherence was normalised as outlined in chapter II using the Fisher transform. To test normalised power and transformed EMG-EMG coherences for statistical significance a repeated measures general linear model was performed using the three contraction conditions and frequency band as the main effects. Separate models were performed for deltoid and 1DI and for deltoid-biceps and finger flexor-1DI, respectively. Where results were non-spherical, a Greenhouse-Geisser correction was used and when differences were significant a pair-wise Students-t-test was carried out.

6.2. Results

Fig.6.1 compares a typical ASR with a voluntary sham startle in one of the subjects. There is evidence of phasic discharges repeating every 70-80 ms in deltoid during the ASR but not the voluntary movement from the same subject.

Fig. 6.1.

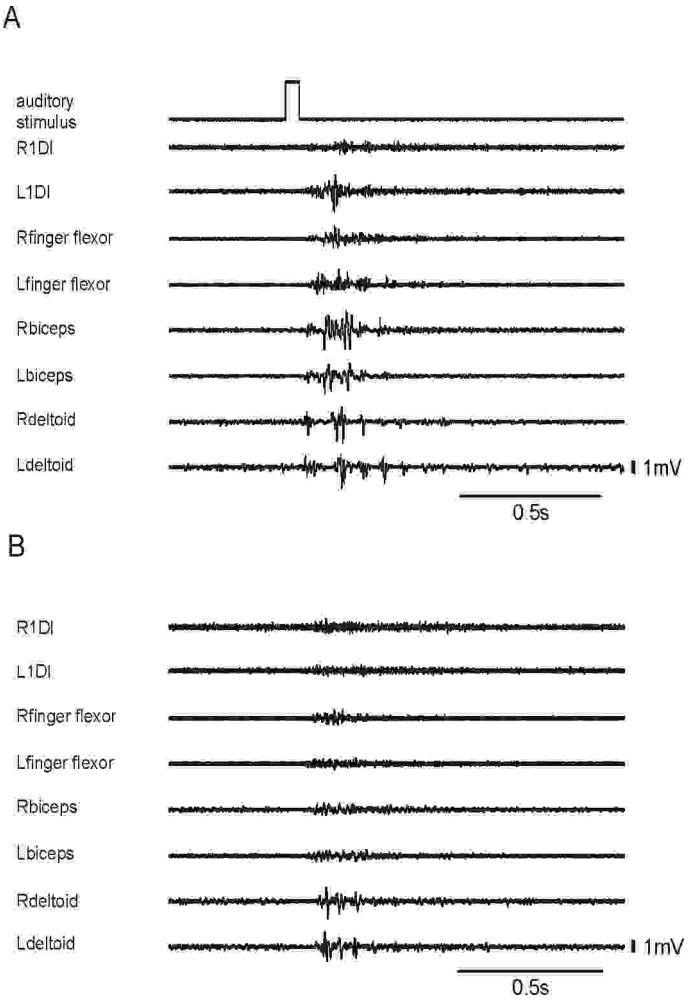

Fig. 6.1. EMG record of a typical reflex startle (**A**) and voluntary sham startle (**B**) in the same healthy subject. Note phasic discharges repeating every 70-80 ms in deltoid during the ASR.

Fig. 6.2 demonstrates the averaged spectra of the percentage total EMG power for deltoid, biceps and 1DI, with the pooled data from homologous muscles on the two sides of

the body. The results from ASR, voluntary sham startles and tonic voluntary contractions are illustrated. Deltoid EMG has a peak centred around 12-14 Hz during the ASR. A similar, albeit less distinct feature, is seen in the ASR spectrum from biceps. This feature is absent during voluntary sham startles and tonic voluntary contraction.

Fig. 6.2.

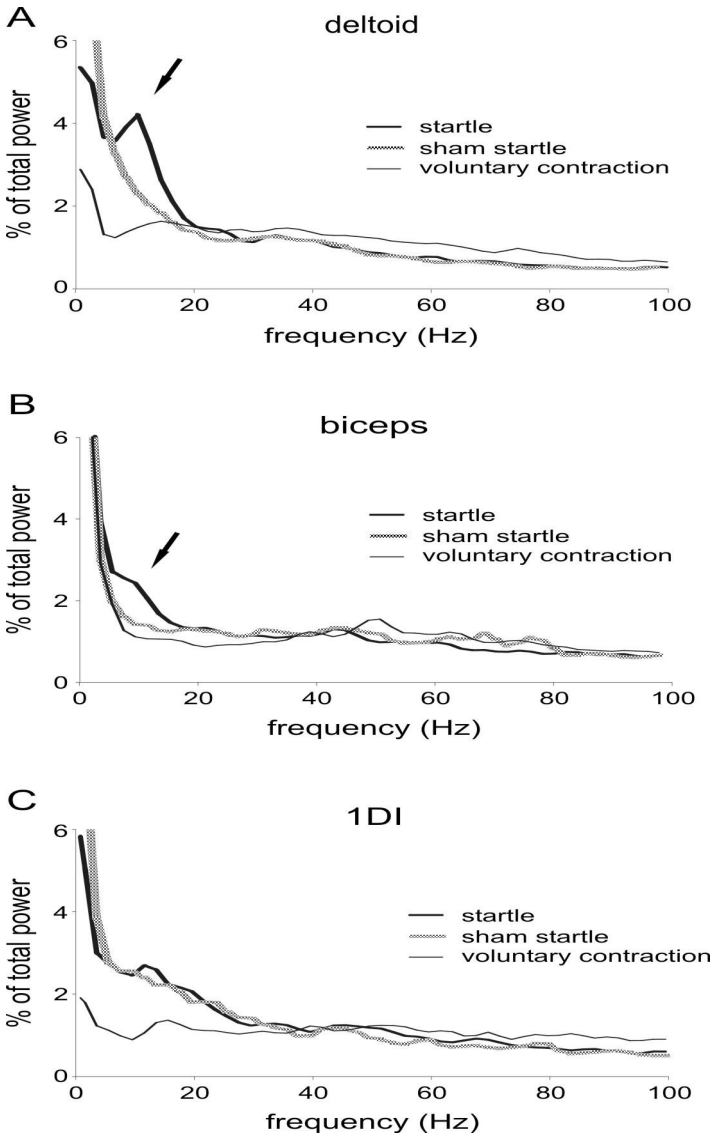

Fig. 6.2. Averaged spectra of the percentage total EMG power in ASR, voluntary sham startles and tonic voluntary contraction in deltoid (**A**), biceps (**B**) and 1DI (**C**). Homologous muscles from the two sides of the body have been pooled in 15 subjects to give 390 data blocks. Note the peak centred around 14 Hz during reflex startles in deltoid (arrowed).

The coherence spectra between right and left deltoid, biceps and 1DI during ASR, voluntary sham startles and tonic voluntary contractions are given in Fig 6.3A, C and E. The deltoid-deltoid and biceps-biceps EMG coherence during the ASR was above the 95%-significance level between 10 and 20 Hz and showed a discrete peak around 12-14 Hz. The peak was biggest in deltoid (Fig 6.3 A), where about 20 % of the activity at 12 Hz was synchronised between the two sides of the body. Conversely, in the voluntary sham startle and tonic voluntary contraction there was only minor coherence above 10 Hz. Note that 1DI-1DI coherence (Fig 6.3 E) was little different in the ASR, sham startle and tonic voluntary contraction. To check, whether volume conduction could account for the coherence between bilateral muscles we levelled the surface recorded analogue EMG signals and then performed frequency analysis on the two resulting point processes. The result for deltoid, the muscle with the shortest distance between itself and its homologue, is shown in Fig 6.3A (inset). There remains a clear peak at around 14 Hz in the point process coherence pooled across subjects. Note that, in line with the lower information content of the point process, the coherence was lower than between the analogue signals (Fig 6.3A).

Fig 6.3B, D and F are the cumulant density estimates for the ASR. The cumulant density estimate for deltoid has a broad central peak with side-lobes every 70-80 ms (Fig 6.3B). Side-lobes are much less distinct in biceps (Fig 6.3B) and absent in 1DI (Fig 6.3B). They were also absent during voluntary sham startles and tonic voluntary contractions (not shown) in all of the muscles. The cumulant density function was estimated from blocked and hanning windowed data. Note that the cross-correlograms between homologous muscles were almost identical to the cumulant density estimates (Fig 6.3B, D and F), so that the periodicity evident in the cumulant density estimates for homologous deltoid and biceps muscle pairs were not epiphenomena of the way in which data were blocked.

Fig. 6.3.

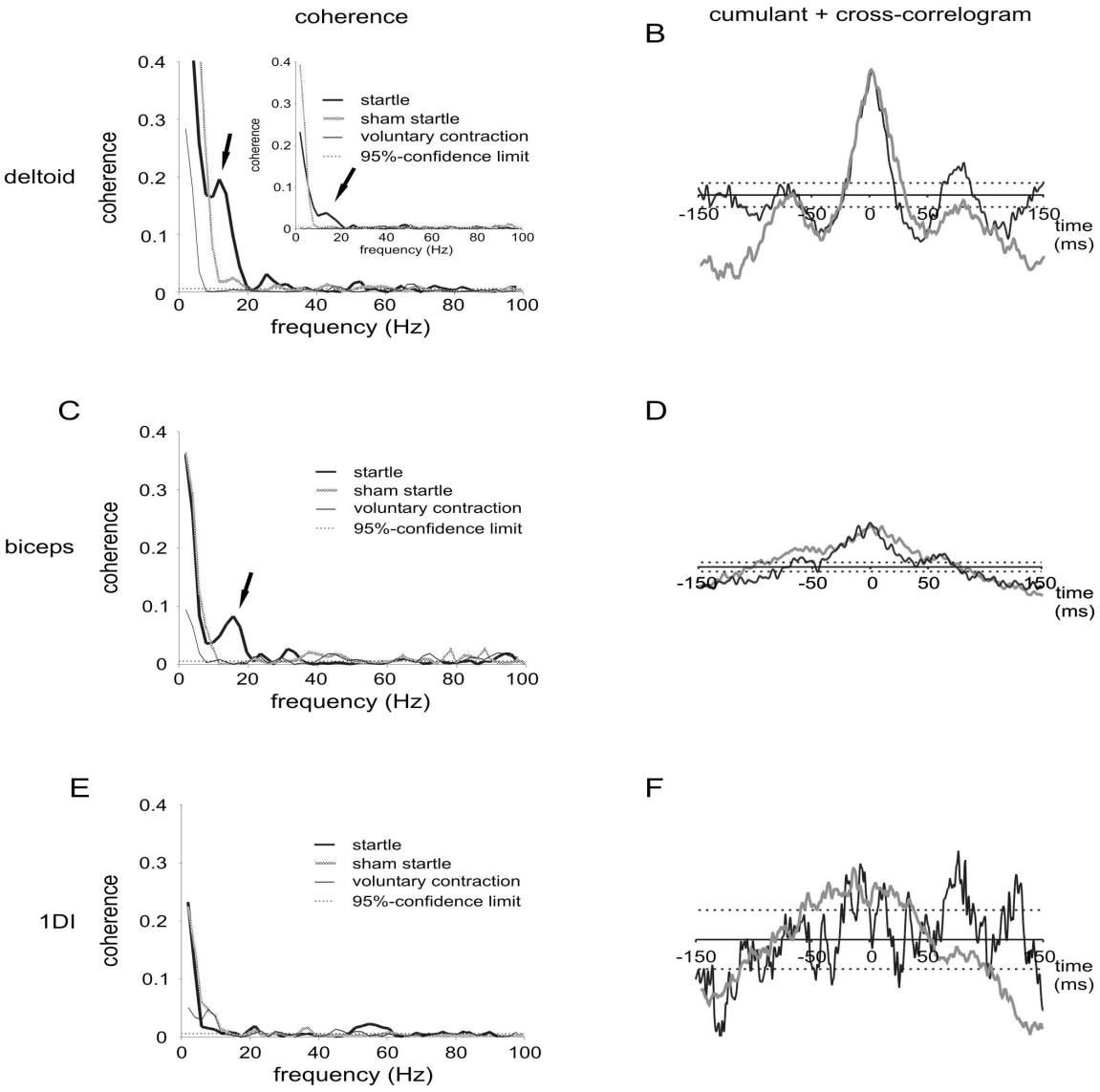

Fig. 6.3. Coherence spectra between right and left deltoid (**A**), biceps (**C**) and 1DI (**E**) during ASR, voluntary sham startles and tonic voluntary contraction and cumulant density estimates for the same muscles during the ASR (**B**, **D** and **F**). Only the spectra from the ASR in deltoid and biceps have a discrete peak in coherence around 14 Hz (arrows). The coherence spectrum for *levelled* deltoid-deltoid EMG pooled over 15 subjects is shown in the inset to (**A**). Note the peak at around 14 Hz (arrow) in the point process coherence in the ASR but not sham startles or voluntary contraction. There is also considerable coherence <10 Hz. This was diminished by detrending the data (not shown), although the latter did not affect the coherence in the 10-20 Hz band. The cumulant density estimate (black line) for deltoid (**B**) has a broad central peak with side-lobes every 70 ms during the ASR. Side-lobes are less distinct in biceps (**D**) and absent in 1DI (**F**). Cross-correlograms (grey lines in **B**, **D** and **F**) match the cumulant density estimates in deltoid and biceps (black lines in **B**, **D**, **F**). Peak-to-peak r-value in deltoid is 0.16; same scaling for biceps and 1DI. Dottes lines indicate 95% confidence limit of the cumlant density estimate. 100 s of data drawn from 15 subjects.

However, pooled coherence spectra, such as those shown in Fig 6.2 and Fig 6.3B, D and F can be relatively dominated by a few individuals with very high EMG-EMG coherence and confidence levels established across the whole spectrum (Halliday et al., 1995) do not necessarily take this into account. To corroborate the consistency of our findings across the subject group we therefore randomly divided the sample of 100 s of EMG from each condition into five segments consisting of 20 s. The percentage total power in each of the five segments was entered into a general linear model with conditions (3 levels: ASR, sham startle, voluntary contraction) and frequency (2 levels: 10-20 Hz, 20-30 Hz) as main effects. There was a significant interaction between condition and frequency in deltoid ($F[2;8] = 50.843$, $p < 0.001$) but not for 1DI. Post hoc analysis revealed a significant difference between the ASR and both the sham startles ($p=0.01$) and voluntary contraction ($p=0.017$) in the 10-20 Hz frequency band. Fig. 6.4 A shows the averaged normalised power across the five segments of 20 s.

Fig. 6.4.

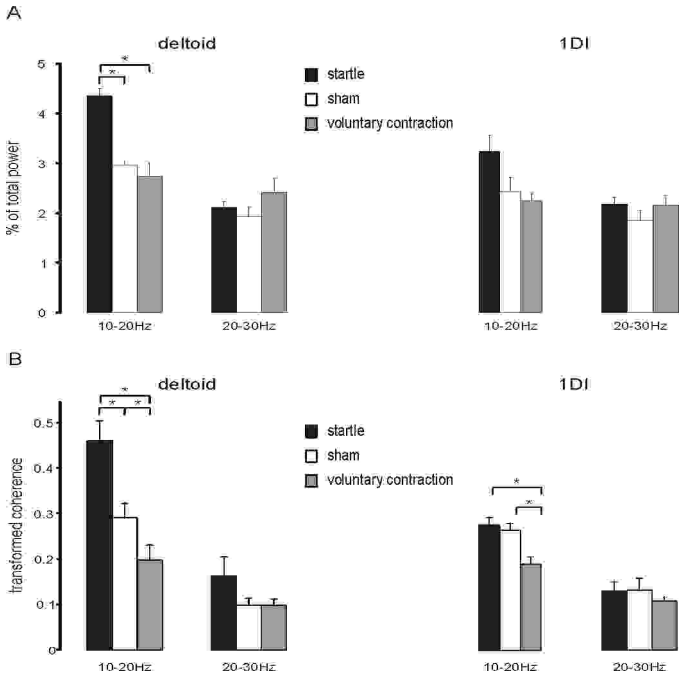

Fig. 6.4. Five blocks of 20 s of data have been analysed, the power normalised, the coherence transformed and averaged for the 10-20 and 20-30 Hz bands in deltoid and 1DI. (**A**) Normalised power. (**B**) Transformed coherences. Bars indicate standard error of the means. Asterixes indicate statistically significant differences between conditions ($p<0.05$).

Similarly, transformed coherences from the 20s segments were entered into a General Linear Model which also showed a significant main effect for frequency and condition only for deltoid ($F[2;8] = 27.948$, $p = 0.01$). Here, differences were significant between the ASR and both the sham startles ($p=0.006$) and voluntary contractions ($p<0.01$) as well as between sham startles and voluntary contractions ($p=0.03$) in the 10-20 Hz band. Averaged transformed coherence from the five 20 s segments are illustrated in Fig. 6.4B. Note that power and coherence in the 10-20 Hz band were both higher in deltoid in the ASR than in sham startles or tonic voluntary contraction, so that changes in coherence were not due to modulations in non-linearly related frequency components (Florian et al., 1998).

In addition, the pattern of pooled EMG-EMG coherence detailed in Fig 6.3 was represented individually among those subjects with more than 10 blocks of EMG during reflex startles (i.e. sufficient to estimate coherence). Figure 6.5 contrasts power and coherence spectra in reflex and voluntary startles in two such subjects.

Fig. 6.5.

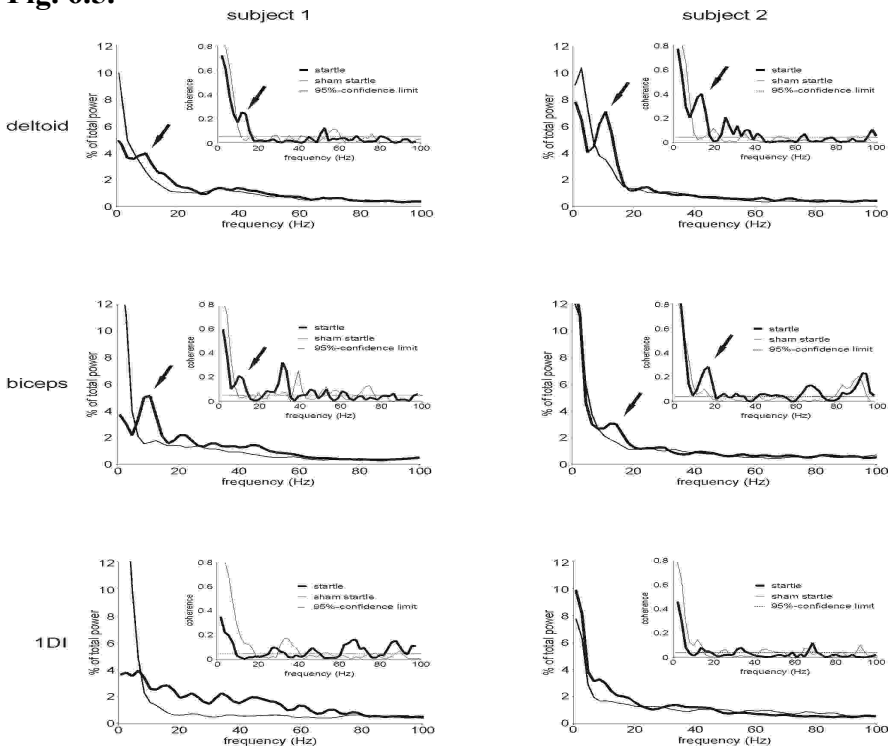

Fig. 6.5. Power and coherence spectra (insets) in reflex and voluntary sham startles in two subjects. **A**. 15 s concatenated data. **B**. 13s concatenated data. Note the spectral peaks at about 14 Hz (arrowed) in proximal muscle pairs in the ASR.

Finally it should be considered whether the coherence between homologous muscles at 10-20 Hz during the ASR could reflect the square wave nature of the acoustic stimulus. Could the stimulus have elicited a pulse of bilateral reflex EMG activity of similar duration, which then appeared in coherence spectra as a peak in coupling? Ordinarily we would expect a 50 ms acoustic stimulus to lead to an EMG burst of 50 ms duration and contaminate coherence spectra with a peak at 20 Hz, rather higher than seen here. Even if we were to consider a delay in the offset of the EMG pulse, to give a period of 70-80 ms appropriate for the frequencies detected in this study, there are several reasons for believing this to be an unlikely explanation. First, reflex EMG activity was elicited in several muscles but only coherence between deltoid and, to a lesser extent biceps, demonstrated a peak at 10-20 Hz. Second, both the raw EMG records (Fig 6.1A), the cumulant density estimates and the cross-correlograms of deltoid and biceps muscles (Fig 6.3) indicated that reflex EMG bursts at 70-80 ms were repetitive rather than single.

6.3. Discussion

It could be demonstrated that the normal acoustic startle reflex is associated with a tendency for motor units in homologous muscles on the two sides of the body to synchronously discharge in the 10-20 Hz band. The synchronising influence was strongest for the more proximal muscles of the upper limb, and was not an artefact of the analysis technique or of volume conduction. Thus, voluntary sham startles analysed in an identical fashion failed to demonstrate this feature and bilateral coherence was evident between homologous proximal muscles regardless of whether analogue or levelled EMG was analysed. Given the strong evidence that the startle reflex is mediated by the reticulospinal system this common oscillatory drive to the two sides of the body in the ASR can be ascribed to reticulospinal activity. This is supported by the finding of synchronised discharges in this frequency range between reticular neurones in the lower brainstem of dogs (Schulz et al., 1985). Interestingly, the tetanic fusion frequency of upper limb muscles is around 15 Hz, suggesting that the

reticulospinal drive at this frequency may have mechanically important effects (Nathan and Tavi, 1990).

Why should neurones in the primate motor cortex tend to synchronise at 20-30 Hz (Murthy and Fetz, 1996; Baker et al., 1997; Baker et al., 1999; Baker et al., 2001*)* whereas those giving rise to the reticulospinal drive following acoustic stimulation tend to synchronise at 10-20 Hz? On the one hand it seems possible that this reflects differences in the central network properties of the respective sites. On the other hand, differences in peripheral feedback delays are unlikely to account for the different synchronisation patterns. If anything the shorter peripheral conduction time to and from proximal muscles would favour a higher frequency drive to proximal than distal muscles, and yet the reticulospinal drive to proximal muscles causes synchronisation at lower frequency than the corticospinal drive preferentially distributed to distal upper limb muscles.

The reticulospinal drive demonstrated here can be contrasted in character with the corticospinal drive to muscle. The latter does not lead to bilateral synchronisation, preferentially involves distal limb muscles and results in EMG-EMG coherence at generally higher frequencies (Farmer et al., 1990; Carr et al., 1994; Farmer et al., 1993; Marsden et al., 1999). In voluntary tonic contractions of weak to moderate intensity cortical drive leads to contralateral EMG-EMG coherence over the 15-30 Hz band (Kilner et al., 1999), whereas during strong contractions or movement cortical drive tends to synchronise motor units in the Piper range of 30-60 Hz (Brown, 2000). Recently, corticomuscular coherence has been reported in the frequency range of physiological tremor (8-12 Hz). However, this coupling is generally weak and it is unclear whether it is afferent or efferent in origin (Marsden et al, 2001; Raethjen et al., 2000). In any case, physiological postural, action and force tremors are not bilaterally synchronous (Marsden et al., 1969; Vallbo and Wessberg, 1993), although, exceptionally, pathological tremors may exhibit synchronisation across the muscles of the two sides of the body (Lauk et al., 1999; Raethjen et al., 2000; O'Sullivan et al., 2002).

In particular, the bilaterally coherent muscle activity documented here is reminiscent of that seen in the pathological condition of primary orthostatic tremor. The latter is associa-

ted with strong synchronisation of muscle activity within and between limbs at around 13-18 Hz. Synchronisation is most evident upon standing, and characteristically abates during the swing phase of gait (Heilman, 1984; Britton et al., 1992; McManis and Sharbrough, 1993). The tremor frequency overlaps with the frequency of synchronisation seen in the ASR and it is interesting to note that reticulospinal neurones in the cat medullary and caudal pontine regions exhibit phasic modulation that is correlated to locomotor activity (Drew et al., 1986; Orlovsky, 1970; Perreault et al., 1993; Shimamura and Kogure, 1983; Shimamura et al., 1982). A similar phenomenon may be seen in humans where the 8-20 Hz drive to tibialis anterior motor units is suppressed during the mid-swing phase of walking (Halliday et al., 2003). Recently, Sharott et al (2002) showed that healthy subjects could develop a similar bilateral synchronisation at around 13-18 Hz in leg muscles when particularly unsteady. The possibility arises that the upper limb drive in the normal auditory startle reflex, pathological primary orthostatic tremor and the orthostatic tremor of posturally challenged healthy subjects involve a similar reticulospinal generator.

In summary, a specific pattern of EMG-EMG coherence that is associated with non-respiratory reticulospinal activity in the human. The challenge now is to define when this drive is manifest in health and how it may be deranged in disease.

7. Summary and perspectives

It can be shown in this work that distinct patterns of cortico-muscular and/or intermuscular coherence can be identfied in a variety of movement disorders (cortical myoclonus, limb dystonia, myoclonus of CBD). Additionally, it could be demonstrated that the assessment of the reticulospinal system is feasible by using intermuscular frequency analysis of homologous muscles, which might open up a new line of research of subcortical drives within the motor system.

In high frequency rhythmic myoclonus of cortical origin EEG-EMG and EMG-EMG frequency analysis has potential diagnostic value for distal muscles in providing a simple and sensitive measure of the strength of functional coupling between cortex and muscle. Detailed consideration of EEG-EMG and EMG-EMG phase spectra also provides important information regarding the mechanisms underlying myoclonic bursts in different muscles. In the hand, phase suggests that efferent pathways dominate and jerking seems to be an expression of spontaneous cortical discharges that are intrinsically rhythmic. In more proximal muscles phase relationships may be dominated by either efferent or afferent loops arguing that myoclonus may arise from spontaneous rhythmic cortical discharges or self-sustaining myoclonic activity through afferent-efferent loops.

In patients with limb dystonia due to a variety of etiologies there were relevant differences among etiologies. 10 out of 12 (83%) of symptomatic DYT1 patients had an excessive 4-7 Hz common drive to TA evident as an inflated coherence in this band. This drive also involved GC leading to co-contracting EMG bursts. In contrast, asymptomatic DYT1 carriers, patients with symptomatic dystonia, patients with fixed dystonia and healthy subjects showed no evidence of such a drive in the theta-frequency band nor any other distinguishing electrophysiological feature. Moreover, the pathological 4-7 Hz drive in symptomatic DYT1 patients was much less common in the upper limb, where it was only present in two out of six (33%) of patients with clinical involvement of the arms. It can therefore be concluded that the nature of the abnormal drive to dystonic muscles may vary according to the muscles under consideration and, particularly, with aetiology.

Patients with the myoclonus of CBD can exhibit dramatically inflated EMG-EMG coherence in the absence of any evidence of a pathological cortico-spinal drive as determined by EEG-EMG coherence, raising the possibility of involvement of subcortical motor systems in the myoclonus of CBD. However, given the relatively small size of the sample, more research is needed to define how representative the present findings are in patients with of CBD.

Intermuscular frequency analysis of muscle bursts elicted by the acoustic startle response demonstrated autospectral peaks at around 14 Hz in deltoid and biceps muscles only. Similarly, coherence spectra of the EMG recorded between homologous proximal upper limb muscles demonstrated a peak centred around 12-16 Hz during reflex startles. Coherence in the 10-20 Hz band was significantly greater in the startle reflex than during voluntary sham startles or voluntary tonic contraction for deltoid, but not first dorsal interosseous, muscles. Thus, the coherence at 10 to 20 Hz between EMGs from homologous muscles represents a potential surrogate measure of reticulospinal activity that may be useful in determining the contribution of the reticulospinal system to different types of movement in health and disease.

So far studies of the coherence between cortical activity and EMG or between EMG signals have focussed on long records of essentially stationary physiological activity, such as voluntary tonic contraction or records of persistent tremor. However, these paradigms are relatively limited. Many pathological conditions, such as hyperekplexia and paroxysmal dystonia, lead to involuntary muscle contractions that are brief. Wider adoption of MAR models may permit the determination of the pattern of descending drives in such conditions in the future. In other pathological conditions such as chorea, involuntary movement may be persistent, but vary in an unpredictable fashion.

In these more complex cases, it is not appropriate to apply the standard stationary FFT based spectral estimation techniques. For these types of signal, non-stationary models can capture much more of the true structure of the data. Non-stationary signals are those whose statistical moments, such as the mean and variance change in time through the signal. One

way of approaching non-stationary signals is to consider them as being composed of a number of smaller stationary states in which the statistical properties stay fairly constant. There are a number of standard models that can be employed to probabilistically determine these smaller stationary regimes (or states) and their respective spectral properties. Such an approach is particularly suitable for objectively segmenting signals into regimes corresponding to different states of muscle activation and rest (Cassidy and Brown, 2002). Periods of stationary activity detected on probabilistic grounds can then be averaged for better spectral estimates. This approach may therefore prove useful in the determination of the pattern of descending drive in conditions such as chorea. Alternatively, one can employ a model whose properties change dynamically though the data record. Such an approach would be more suitable where signals change gradually so that discrete state change times are hard to discern, as in event-related (de) synchronisation paradigms.

Advances need not be solely analytical. More work is necessary on the pharmacological underpinning of cortico-muscular and intermuscular coherence through the systematic investigation of drug effects and ligand-gated channelopathies, and normal ranges for EEG-EMG and EMG-EMG coherences at different frequencies clearly need to be established. Thus, at present there is still a considerable way to go before frequency analysis can provide an accessible and useful tool in the assessment of disorders of the motor system in a routine clinical practice.

References

Amstrong RA, Cairns NJ, Lantos PL. A quantitative study of the pathological lesions in the neocortex and hippocampus of twelve patients with corticobasal degeneration. Experimental Neurology 2000;163:348-356.

Amstrong RA, Lantos PL, Cairns NJ. The spatial patterns of pathological brain lesions in 12 patients with corticobasal degeneration. Pathophysiology 2001;8:47-53.

Baker SN, Kilner JM, Pinches EM, Lemon RN. The role of synchrony and oscillations in the motor output. Exp Brain Res 1999;128:109-117.

Baker SN, Olivier E, Lemon RN. Coherent oscillations in monkey motor cortex and hand muscle EMG show task-dependant modulation. J Physiol 1997;501:225-241.

Baker SN, Spinks R, Jackson A, Lemon RN. Synchronization in monkey motor cortex during a precision grip task. I. Task-dependent modulation in single-unit synchrony. J Neurophysiol 2001;85:869-885.

Berardelli A, Rothwell JC, Day BL, Marsden CD. Pathophysiology of blephrospasm and oromandibular dystonia. Brain 1985;108:593-608.

Berardelli A, Rothwell JC, Hallett M, Thomson PD, Manfredi M, Marsden CD. The pathophysiology of primary dystonia. Brain 1998;121:1195-1212.

Bhatia KP, Bhatt MH, Marsden CD. The causalgia-dystonia syndrome. Brain 1993;116:843-851.

Brillinger DR. Time Series-Data Analysis and theory (2nd ed.). San Francisco, CA: Holden Day, 1981.

Britton TC, Thompson PD, van der KW et al. Primary orthostatic tremor: further observations in six cases. J.Neurol 1992;239:209-217.

Brown P, Corcos D, Rothwell JC. Does parkinsonian action tremor contribute to muscle weakness in Parkinson's disease? Brain 1998a;120:401-408.

Brown P, Day BL, Rothwell JC, Thompson PD, Marsden CD. Intrahemispheric and interhemispheric spread of cerebral cortical activity and its relevance to epilepsy. Brain 1991;114:2333-2351.

Brown P, Day BL. Eye acceleration during large horizontal saccades in man. Exp Brain Res 1997b;113:153-157.

Brown P, Farmer SF, Halliday DM, Marsden JF, Rosenberg JR. Coherent cortical and muscle discharge in cortical myoclonus. Brain 1999;122:461-472.

Brown P, Marsden CD. Rhythmic cortical and muscle discharge in cortical myoclonus. Brain 1996;119:1307-1316.

Brown P, Marsden CD. What do the basal ganglia do? Lancet 1998b;351:1801-1804.

Brown P, Marsden JF. Cortical network resonance and motor activity in humans. Neuroscientist 2002;7:518-526.

Brown P, Rothwell JC, Thompson PD, Britton TC, Day BL, Marsden CD. New observations on the normal auditory startle reflex in man. Brain 1991a;114:1891-1902.

Brown P, Rothwell JC, Thompson PD, Britton TC, Day BL, Marsden CD. The hyperekplexias and their relationship to the normal startle reflex. Brain 1991b;114:1903-1928.

Brown P, Salenius S, Rothwell JC, Hari R. Cortical Correlate of the Piper Rhythm in Humans. J Neurophysiol 1998c;80:2911-2917.

Brown P. Muscle sounds in Parkinson's disease. Lancet 1997a;349:533-535.

Brown P. The Piper rhythm and related activities in man. Prog Neurobiol 2000;60:97-108.

Brunt ERP, Weerden T van, Prium J, Lakke JW. Unique myoclonic pattern in corticobasal degeneration. Mov Disord 1995;10:132-142.

Burke RE, Fahn S, Marsden CD, Bressman SB, Moskowitz C, Friedman J. Validity and reliability of a rating scale for the primary torsion dystinias. Neurology 1985;35:73-77.

Cantello R, Gianelli M, Civardi C, Mutani R. Focal subcortical reflex myoclonus. A clinical and neurophysiological study. Arch Neurol 1997;54:187-196.

Carr LJ, Harrison LM, Stephans JA. Evidence for bilateral innervation of certain homologous motoneurone pools in man. J Physiol 1994;475:217-227.

Cassidy MJ, Brown P. Hidden Markov based autoregressive analysis of stationary and non-stationary electrophysiological signals for functional coupling studies. J Neurosc Methods 2002;116:35-53.

Cassidy MJ, Penny WD. Bayesian nonstationary autoregressive models for biomedical signal analysis. IEEE Trans Biomed Eng 2002;49:1142-1152.

Ceballos-Baumann AO, Passingham CD, Marsden CD, Brooks DJ. Motor reorganisation in acquired hemidystonia: a PET activation study. Ann Neurol 1995b;37:746-757.

Ceballos-Baumann AO, Passingham CD, Marsden CD, Brooks DJ. Overactivity of prefortal and underactivity of motor cortical areas in idiopathic dystonia. Ann Neurol 1995a;37:363-372.

Challis RE, Kitney RI. Biomedical signal processing (in four parts). Part 1: Time-domain methods. Med Biol Eng Comput 1990;28:509-524.

Challis RE, Kitney RI. Biomedical signal processing (in four parts). Part 3: The power spectrum and coherence function. Med Biol Eng Comput 1991;29:225-241.

Christakos CN. On the detection and measurement of synchrony in neural populations by coherence analysis. J Neurophysiol 1997;78:3453-3459.

Colebatch JG, Gandevia SC. The distribution of muscular weakness in upper motor neuron lesions affecting the arm. Brain 1989;112:749-763.

Conners BW, Amitai Y. Making waves in the neocortex. Neuron 2001;18:347-349.

Conway BA, Farmer SF, Halliday DM, Rosenberg, JR. On the relation between motor-unit discharge and physiological tremor. In: Taylor A, Gladden MH, Durbaba R, editors. Alpha and Gamma motor systems. New York: Plenium Press, 1995a:596-598.

Conway BA, Halliday DM, Farmer SF, Shahani U, Maas P, Weir AI, Rosenberg JR. Synchronization between motor cortex and spinal motoneuronal pool during the performance of a maintained motor task in man. J Physiol 1995b;489:917-924.

Coubes P, Roubertie A, Vayssiere N, Hemm S, Echenne B. Treatment of DYT1-generalised dystonia by stimulation of the internal globus pallidus. Lancet. 2000;355:2220-2221.

Davis M, Gendelman DS, Tischler MD, Gendelman PM. Primary acoustic startle circuit: lesion and stimulation studies. J Neurosci 1982;2:791-805.

DeLuca CJ, Erim Z. Common drive of motor units in regulation of muscle force. Trends Neurosci 1994;17:299-304.

DeLuca CJ, LeFever RS, McCue MP, Xenakis AP. Control scheme governing concurrently active human motor units during voluntary contractions. J Physiol 1982;329:129-142.

Deuschl G, Seifert G, Heinen F, Illert M, Lücking CH. Reciprocal inhibition of forearm flexor muscles in spasmodic torticollis. J. Neurol Sci 1992;113:85-90.

Drew T, Dubuc R, and Rossignol S. Discharge patterns of reticulospinal and other reticular neurons in chronic, unrestrained cats walking on a treadmill. J Neurophysiol 1986;55:375-401.

Edinger L, Fisher B. Ein Mensch ohne Großhirn. Pflügers Arch Ges Physiol 1913;152:535-562.

Eisen A, Shytbel W. Clinical experience with transcranial magnetic stimulation. Muscle Nerve 1990;13:995-1011.

Fahn S. Psychogenic movement disorders. In: Marsden CD, Fahn S, eds. Movement disorders. Oxford: Butterworth-Heinemann, 1994:359-372.

Farmer SF, Bremner FD, Halliday DM, Rosenberg JR, Stephans JA. The frequency content of common synaptic inputs to motoneurons studies during isometric voluntary contraction in man. J Physiol 1993;470:127-155.

Farmer SF, Ingram DA, Stephens JA. Mirror movements studied in a patient with Klippel-Feil syndrome. J Physiol 1990;428:467-484.

Farmer SF, Sheean GL, Mayston MJ, Rothwell JC, Marsden CD, Conway BA, Halliday DM, Rosenberg JR, Stephens JA. Abnormal motor unit synchronization of antagonist muscles underlies pathological co-contraction in upper limb dystonia. Brain 1998b;121:801-814.

Farmer SF. Rhythmicity, synchronization and binding in human and primate motor systems. J Physiol 1998a;509:3-14.

Feige B, Aertsen A, Kristeva-Feige R. Dynamic synchronisation between multiple cortical motor areas and muscle activity in phasic voluntary movements. J Neurophysiol 2000;84:2622-2629.

Ferbert A, Caramia D, Priori A, Bertolasi L, Rothwell JC. Cortical projection to erector spinae muscles in man as assessed by focal transcranial magnetic stimulation. Electroencephaplogr Clin Neurophysiol 1992;85:382-387.

Florian, G, Andrew C, Pfurtscheller G. Do changes in coherence always reflect changes in functional coupling. Electroencephalogr Clin Neurophysiol 1998;106:87-91.

Gotman J. Measurement of small time differences between EEG channels: method and application to epileptic seizure propagation. Electroenceph clin Neurophysiol 1983;56:501-514.

Gross J, Tass PA, Salenius S, Hari R, Freund HJ, Schnitzler A. Cortico-muscular synchronization during isometric muscle contraction in humans as revealed by magnetoencephalography. J Physiol 2000;527:623-631.

Grosse P, Guerrini R, Parmeggiani L, Bonani P, Pogosyan A, Brown P. Abnormal corticomuscular and intermuscular coupling in high-frequency rhythmic myoclonus. Brain 2003;126:326-342.

Guerrini R, Bonanni P, Patrignani A, Brown P, Parmeggiani L, Grosse P, Brovedani P, Moro F, Aridon P, Carrozzo R, Casari G. Autosomal dominant cortical myoclonus and epilepsy (ADCME) with complex partial and generalized seizures: a newly recognized epilepsy syndrome with linkage to chromosome 2p11.1-q12.2. Brain 2001;124:2459-2475.

Guerrini R, De Lorey TM, Bonanni P, Moncla, Dravet C, Suisse G, Livet MO, Bureau M, Malzac P, Genton P, Thomas P, Sartucci F, Simi P, Serratosa JM. Cortical Myoclonus in Angelman Syndrome. Ann Neurol

1996;40:39-48.

Hallett M, Wilkins DE. Myoclonus in Alzheimer's disease and minipolymyoclonus. Adv Neurol 1986;43:399-405.

Halliday DM, Conway BA, Christensen LOD, Hansen NL, Petersen NP, Nielsen JB. Functional coupling of Motor Units is modulated during walking in Human subjects. J Neurophysiol 2003;89:960-968.

Halliday DM, Conway BA, Farmer SF, Rosenberg JR. Load-independent contributions from motor-unit synchronisation to human physiological tremor. J Neurophysiol 1999;82:664-675.

Halliday DM, Conway BA, Farmer SF, Rosenberg JR. Using electroencephalography to study functional coupling between cortical activity and electromyograms during voluntary contractions in humans. Neurosci Lett 1998;241:5-8.

Halliday DM, Conway BA, Farmer SF, Shahnani U, Russell AJC, Rosenberg JR. Coherence between low-frequency activation of the motor cortex and tremor in patients with essential tremor. Lancet 2000;355:1149-1153.

Halliday DM, Rosenberg JR, Amjad AM, Breeze P, Conway BA, Farmer SF. A framework for the analysis of mixed time series/point process data - theory and application to the study of physiological tremor, single motor unit discharges and electromyograms. Prog Biophys molec Biol 1995;64:237-278.

Hamdy S, Rothwell JC. Gut feelings about recovery after stroke: the organization and reorganization of human swallowing motor cortex. Trends Neurosci 1998;21:278-282.

Hammond GR. Lesions of the pontine and medullary reticular formation and prestimulus inhibition of the acoustic startle reaction in rats. Physiol Behav 1973;10:239-243.

Hansen S, Hansen NL, Christensen LOD, Petersen NT, Nielsen JB. Coupling of antagonistic ankle muscles during co-contraction in humans. Exp Brain Res 2002;146:282-292.

Heilman KM. Orthostatic tremor. Arch.Neurol 1984;41:880-881.

Hellwig B, Häußler S, Lauk M, Guschlbauer B, Köster B, Kristeva-Feige R, Timmer J, Lücking CH. Tremor correlated cortical activity detected by electroencephalography. Clin Neurophysiol 2000;111:806-809.

Hellwig B, Häußler S, Schelter B, Lauk M, Guschlbauer B, Timmer J, Lücking CH. Tremor-correlated cortical activity in essential tremor. Lancet 2001;357:519-523.

Hjorth B. An on-line transformation of EEG scalp potentials into orthogonal source derivations. Electroencephalogr Clin Neurophysiol 1975;39:526-530.

Hurtado JM, Gray CM, Tamas LB, Sigvardt KA. Dynamics of tremor-related oscillations in the human globus pallidus: A single case study. Proc Natl Acad Sci USA 1999;96:1674-1679.

Ikeda A, Kakigi R, Funai N, Neshige R, Kuroda Y, Shibasaki H. Cortical tremor: A variant of cortical reflex myoclonus. Neurology 1990;40:1561-1565.

Ikoma K, Samii A, Mercuri B, Wassermann EM, Hallett M. Abnormal cortical motor excitability in dystonia. Neurology 1996;46:1371-1376.

Jankovic J, Van der Linden C. Dystonia and tremor induced by peripheral trauma: predesposing factors. J Neurol, Neurosurg Psychiatry 1988;51:1512-1519.

Jedynak CP, Bonnet AM, Agid Y. Tremor and Idiopathic Dystonia. Mov Disord 1991;6:230-236.

Jefferys JGR, Traub RD, Whittington MA. Neuronal networks for induced ‘40Hz’ rhythms. Trends Neurosci

1996;19:202-208.

Kamen G, DeLuca CJ. Firing rate interactions among human orbicularis oris motor units. Int J Neurosci 1992;64:167-175.

Kaminski M, Blinowska KJ. A new method of the description of the information flow in the structures. Biological cybernetics 1991;65:203-210.

Kilner JM, Baker SN, Salenius S, Jousmaki V, Hari R, Lemon RN. Task-dependent modulation of 15-30 Hz coherence between rectified EMGs from human hand and forearm muscles. J Physiol 1999;516:559-570.

Kirkwood PA, Sears TA, Tuck DL, Westgaard RH. Variations in the time course of the synchronisation of intercostal motoneurones in the cat. J Physiol 1982;327:105-135.

Koch M, Lingenhöhl K, Pilz PKD. Loss of the acoustic startle response following neurotoxic lesions of the caudal pontine reticular formation: possible role of giant neurones. Neuroscience 1992;49:617-625.

Koch M, Schnitzler HU. The acoustic startle response in rats-circuits mediating evocation, inhibition and potentiation. Behav Brain Res 1997;89:35-49.

Koch M. The Neurobiology of startle. Prog Neurobiol 1999;59:107-128.

Kompoliti K, Goetz CG, Boeve BF, Maraganore DM, Ahlskog JE, Marsden CD, Bhatia KP, Greene PE, Przedborski S, Seal EC, Burns RS, Hauser RA, Gauger LL, Factor SA, Molho ES, Riley DE. Clinical presentation and pharmacological therapy in corticobasal degeneration. Arch Neurol 1998;55:957-961.

Köster B, Lauk M, Timmer J, Winter T, Guschlbauer B, Glocker FX, Danek A, Deuschl G, Lücking CH. Central mechanisms in human enhanced physiological tremor. Neurosci Lett 1998;241:135-138.

Kostic VS, Stojanovic-Svetel M, Kacar A. Symptomatic dystonia associated with structural brain lesions: report of 16 cases. Can J Neurol Sci 1996;23:53-56.

Kuypers HGJM. Anatomy of the descending pathways. In: Handbook of Physiology - The Nervous System. Motor Control. Bethesda, MD: Am. Physiol Soc, sect. 1, pt II, 597-666.

Lachaux J, Lutz A, Rudauf D, Cosmelli D, LeVanQuyen M, Martinerie J, Varela F. Estimating the time-course of coherence between single trial brain signals: an introduction to wavelet coherence. Neurophysiol Clin 2002;32:157-174.

Lance JW, Schwab RS, Peterson EA. Action tremor and the cogwheel phenomenon in Parkinson's disease. Brain 1963; 86:95-110.

Lang AE. Psychogenic dystonia: a review of 18 cases. Can J Neurol Sci 1995;22:136-143.

Lauk M, Koster B, Timmer J, Guschlbauer B, Deuschl G, Lücking CH. Side-to-side correlation of muscle activity in physiological and pathological human tremors. Clin Neurophysiol 1999;110:1774-1783.

Leitner DS, Powers AS, Hoffman HS. The neural substrate of the startle response. Physiol Behav 1980;25:291-297.

Lemstra AW, Vernhagen Metman L, Lee JI, Dougherty PM, Lenz FA. Tremor-frequency (3-6 Hz) activity in the sensorimotor arm representation of the internal segment of the globus pallidus in patients with Parkinson's disease. Neurosci Lett 1999;267:129-132.

Leocani L, Comi G. EEG coherence in pathological conditions. J Clin Neurophysiol 1999;16:548-555.

Lingenhöhl K, Friauf E. Giant neurons in the caudal pontine reticular formation receive short latency acoustic

input: an intracellular recording and HRP-study in the rat. J Comp Neurol 1992;325:473-492.

Liu X, Griffin IC, Parkin SG, Miall RC, Rowe JG, Gregory RP, Scott RB, Aziz TZ. Involvement of the medial pallidum in focal myoclonic dystonia: a clinical and neurophysiological case study. Mov Disord 2002;17:346-353.

Llinàs R, Pare D. Role of intrinsic neuronal oscillations and network ensembles in the genesis of normal and pathological tremor. In: Findley LJ, W.C. Koller WC, eds. Handbook of tremor disorders. New York: Marcel Dekker, 1995:7-36.

Llinàs R, Volkind R. The olivocerebellar system: functional properties as revealed by harmaline-induced tremor. Exp Brain Res 1973;18:69-87.

Lopes da Silva F, Pijn JP, Boeijinga P. Interdependence of EEG signals: linear vs nonlinear associations and the significance of time delays and phase shifts. Brain Topogr 1989;2:9-18.

Lu CS, Ikeda A, Terada K, Mima T, Nagamine T, Fukuyama H, Kohara N, Kojima Y, Yonekura Y, Chen RS, Tsai CH, Chu NS, Kimura J, Shibasaki H. Electrophysiological studies of early stage corticobasal degeneration. Mov Disord 1998;13:140-146.

Markus HS, Lees AJ, Lennox G Marsden CD, Costa DC. Patterns of regional cerebral blood flow in corticobasal degeneration studies using HMPAO SPECT -comparison with Parkinson's disease and normal controls. Mov Disord 1995;10:179-187.

Marsden CD, Meadows JC, Lange GW, Watson RS. The relation between physiological tremor of the two hands in healthy subjects. Electroencephalogr Clin Neurophysiol 1969;27:179-185.

Marsden CD, Obeso JA, Traub MM, Rothwell JC, Kranz H, La Cruz F. Muscle spasm associated with Sudeck' s atrophy after injury. BMJ 1984;288:173-176.

Marsden CD, Obeso JA, Zarranz JJ, Lang AE. The anatomical basis of symptomatic hemidystonia. Brain 1985;108:463-483.

Marsden JF, Limousin-Dowsey P, Ashby P, Pollak P, Brown P. Subthalamic nucleus, sensorimotor cortex and muscle interrelationships in Parkinson's disease. Brain 2001c:124:378-388.

Marsden J, Limousin-Dowsey P, Fraix V, Pollak P, Odin P, Brown P. Intermuscular coherence in Parkinson's disease: Effects of subthalamic nucleus stimulation. Neuroreport 2001b;12:1113-1117.

Marsden JF, Brown P, Salenius S. Involvement of the sensorimotor cortex in physiological force and action tremor. Neuroreport 2001a;12:1937-1941.

Marsden JF, Ashby P, Rothwell JC, Brown P. Phase relationship between cortical and muscle oscillations in cortical myoclonus: electrocorticographic assessment in a single case. Clin Neurophysiol 2000b;111:2170-2174.

Marsden JF, Werhahn KJ, Ashby P, Rothwell J, Noachtar S, Brown P. Organization of cortical activities related to movement in humans. J Neurosci 2000a;20:2307-2314.

Marsden JF, Farmer SF, Halliday DM, Rosenberg JR, Brown P. The unilateral and bilateral control of motor unit pairs in the first dorsal interosseus and paraspinal muscles in man. J Physiol 1999;521:553-564.

Matsumoto J, Fuhr P, Nigro M, Hallett M. Physiological abnormalities in hereditary hyperekplexia. Ann Neurol 1992;32:41-50.

Mayston MJ, Harrison LM, Stephens JA, Farmer SF. Physiological tremor in human subjects with X-linked Kallmann's syndrome and mirror movements. J Physiol 2001;530:551-563.

McAuley JH, Britton TC, Rothwell JC, Findley LJ, Marsden CD. The timing of primary orthostatic tremor bursts has a task-specific plasticity. Brain 2000;123:254-266.

McAuley JH, Rothwell JC, Marsden CD. Frequency peaks of tremor, muscle vibration and electromyographic activity at 10 Hz, 20Hz and 40 Hz during human finger muscle contraction may reflect rhythmicities of central neural firing. Exp Brain Res 1997;114:525-541.

McLachlan RS, Leung L. A movement-associated fast rolandic rhythm. J Can Sci Neurol 1991;18:333-336.

McManis PG, Sharbrough FW. Orthostatic tremor: clinical and electrophysiologic characteristics. Muscle Nerve 1993;16:1254-1260.

Mima T, Gerloff C, Steger J, Hallett M. Frequency-coding of motor control system-coherence and phase estimation between cortical rhythm and motoneuronal firing in humans. Soc Neurosci Abstr 1998;24:1768.

Mima T, Goldstein S, Toma K, Ragbir S, Hallett M. The lack of cortico-muscular coherence coupling of 8-12 Hz central component of physiological tremor. Mov Disord 2000;15, supplement 3:78.

Mima T, Hallett M. Corticomuscular coherence: a review. J Clin Neurophysiol 1999a;16:501-511.

Mima T, Hallett M. Electroencephalographic analysis of cortico-muscular coherence: reference effect, volume conduction and generator mechanism. Clin Neurophysiol 1999;110:1892-1899.

Mima T, Keiichiro T, Koshy B. Coherence between cortical and muscular activities after subcortical stroke. Stroke 2001b;32:2597-2601.

Mima T, Matsuoka T, Hallett M. Functional coupling of human right and left cortical motor areas demonstrated with partial coherence analysis. Neurosci Lett 2000;287:93-96.

Mima T, Matsuoka T, Hallett M. Information flow from the sensorimotor cortex to muscle in humans. Clin Neurophysiol 2001a;112:122-126.

Mima T, Nagamini T, Ikeda A, Yazawa S, Kimura J, Shibasaki H. Pathogenesis of cortical myoclonus studied by magnetoencephalography. Ann Neurol 998;43:598-607.

Murayama N, Lin YY, Salenius S, Hari R. Oscillatory interaction between human motor cortex and trunc muscles during isometric contraction. Neuroimage 2001;14:206-1213.

Murthy VN, Fetz EE. Coherent 25- to 35-Hz oscillations in the sensorimotor cortex of awake behaving monkeys. Proc Natl Acad Sci USA 1992;89:5670-5674.

Murthy VN, Fetz EE. Synchronizaton of neurones during local field potential oscillations in sensorimotor cortex of awake monkeys. J Neurophysiol 1996b76:3968-3982.

Murthy VN, Fetz EE. Oscillatory activity in sensorimotor cortex of awake monkeys: Synchronisation of local field potentials and relation to behaviour. J Neurophysiol 1996a;76:3949-3967.

Nakashima K, Rothwell JC, Thompson PD, Day BL, Berardelli A, Agostino R, Artieda J, Papas SM, Obeso JA, Marsden CD. The blink reflex in patients with idiopathic torsion dystonia. Arch Neurol 1990;47:413-416.

Nardocci N, Zorzi G, Grisoli M, Rumi V, Broggi G, Angelini L. Acquired Hemidystonia in Childhood. A Clinical and Neuroradiological Study of Thirteen Patients. Pediatric Neurology 1996;15:108-113.

Nathan R, Tavi M. The influence of stimulation pulse frequenvy on the generation of joint moments in the upper limb. IEEE Transactions on biomedical engeneering 1990;39:317-322.

Németh A. The genetics of primary dystonia and related disorders. Brain 2002;125:695-721.

Nielsen J, Kagamihara Y. Synchronisation of human leg motor units during co-contraction in man. Exp Brain Res 1994;102:84-94.

O'Sullivan JD, Rothwell J, Lees AJ, Brown P. Bilaterally coherent tremor resembling enhanced physiologcal tremor: report of three cases. Mov Disord 2002;17:387-391.

Obeso JA, Rothwell JC, Lang AE, Marsden CD. Myoclonic dystonia. Neurology 1983;33:825-830.

Ohara S, Nagamine T, Ikeda A, Kunieda T, Matsumoto R, Taki W, Hashimoto N, Baba K, Mihara, T, Salenius S, Shibasaki H. Electrocorticogram-electromyogram coherence during isometric contraction of hand muscle in human. Clin Neurophysiol 2000;111:2014-2024.

Orlovsky GN. Work of the reticulo-spinal neurons during locomotion. Biophysics (USSR) 1970;15:761-771.

Palmer E, Ashby P. Corticospinal projections to upper limb motoneurones in humans. J Physiol 1992;448:397-412.

Panizza M, Lelli S, Nilsson J, Hallett M. H-reflex recovery curve and reciprocal inhibition of H-reflex in different kinds of dystonia. Neurology 1990;40:824-828.

Perreault MC, Drew T, Rossignol S. Activity of medullary reticulospinal neurons during fictive locomotion. J Neurophysiol 1993;69:2232-2247.

Pettigrew LC, Jankovic J. Hemidystonia: a report of 22 patients and a review of the literature. J Neurol Neurosurg Psychiatry 1985;48:650-657.

Pfurtscheller G, Cooper R. Frequency dependence of the transmission of the EEG from cortex to scalp. Electroencephalogr Clin Neurophysiol 1975;38:93-96.

Piper HE. Elektrophysiologie menschlicher Muskeln. Springer, Berlin 1912.

Piper HE. Über den willkürlichen Muskeltetanus. Pflügers Gesamte Physiologie des Menschen und der Tiere 1907;119:301-338.

Raethjen J, Lindemann M, Dumplemann M, Stolze H, Wenzelburger R, Pfister G, Elger CE, Timmer J, Deuschl G. Cortical correlates of physiological tremor. Mov Disord 2000a;15 supplement 3:90.

Raethjen J, Lindemann M, Schmaljohann H, Wenzelburger R, Pfister G, Deuschl G. Multiple oscillators are causing Parkinisonian and essential tremor. Mov disord 2000;15:84-94.

Ridding MC, Sheehan G, Rothwell JC, Inzelberg R, Kujirai T. Changes in the balance between motor cortical excitation and inhibition in focal, task-specific dystonia. J. Neurol Neurosurg Psychiatry 1995;59:493-498.

Riley DE, Lang AE. Clinical diagnostic criteria. In: Litvan I, Goetz CG, Lang AE, eds. Corticobasal Degeneration. Philadelphia: Lipincott Williams & Wilkins 2000:29-34.

Rosenberg JR, Amjad AM, Breeze P, Brillinger DR, Halliday DM. The Fourier approach to the identification of functional coupling between neuronal spike trains. Progress in biophysics and molecular biology 1989;53:1-31.

Rosenberg JR, Halliday DM, Breeze P, Conway B.A. Identification of patterns of neuronal activity, partial spectra, partial coherence, and neuronal interactions. J Neurosci Methods 1998;83:57-72.

Rothwell JC, Thompson PD, Day BL, Boyd S, Marsden CD. Stimulation of the human motor cortex through the scalp. Exp Physiol 1991;76:159-200.

Salenius S, Avikainen S, Kaakkola S, Hari R, Brown P. Defective cortical drive to muscle in Parkinson's disease and its improvement with levodopa. Brain 2002;125:491-500.

Salenius S, Forss N, Hari R. Rhythmicity of descending motor commands covaries with the amount of motor cortex 20-30 Hz rhythms. Soc Neurosci Abstr 1997b;23:1948.

Salenius S, Portin K, Kajola M, Salmelin R, Hari R. Cortical control of human motoneuron firing during isometric contraction. J Neurophysiol 1997;77:3401-3405.

Sanes JN, Donoghue JP. Oscillations in local field potentials of the primate motor cortex. Proc Natl Acad Sci USA 1993;90:4470-4474.

Sawle GV, Brooks DJ, Marsden CD, Frackowiak RSJ. Corticobasal degeneration: a unique pattern of regional cortical oxygen metabolism and striatal fluorodopa up-take demonstrated by positron emission tomography. Brain 1991;114:541-556.

Schultz G, Lambertz B, Schultz B, Langhorst P, Krienke B. Reticular formation of the lower brainstem. A common system for cardio-repiratory and somatomotor functions. Cross-correlation analysis of discharge patterns of neighbouring neurones. J Auton Nerv Syst 1985;12:35-62.

Schwartzman RJ, Kerrigan J. The movement disorder of reflex sympathetic dystrophy. Neurology 1990;40:57-61.

Sharott A, Marsden J, Brown P. Primary orthostatic tremor is an exaggeration of a physiological response to instability. Mov Disord 2003;18:195-199.

Shibasaki H, Kuroiwa Y. Electroencephalographic correlates of myoclonus. Electroenceph clin Neurophysiol 1975;39:455-463.

Shimamura M, Kogure I, Wada SI. Reticular neuron activities associated with locomotion in thalamic cats. Brain Res 1982; 231:51-62.

Shimamura M, Kogure I. Discharge patterns of reticulospinal neurons corresponding with quadrupedal leg movements in thalamic cats. Brain Res 1983;260:27-34.

Spauschus A, Marsden J, Halliday DM, Rosenberg JR, Brown P. The origin of ocular microtremor in man. Exp Brain Res 1999;126:556-562.

Spauschus A, Marsden JF, Halliday DM, Rosenberg JR, Brown P. The origin of ocular microtremor in man. Exp Brain Res 1999;126:556-562.

Srinivasan R, Nunez PL, Silberstein RB. Spatial filtering and neocortical dynamics: estimates of EEG coherence. IEEE Trans Biomed Eng 1998;45:814-826.

Steriade M, Curro-Dossi R, Contreras D. Electrophysiological properties of intralaminarthalamocortical cells discharging rhythmic (~40 Hz) spike bursts at (~1000 Hz) during waking and rapid eye movements. Neuroscience 1993;56:1-9.

Storey E, Lichtenstein M, Desmond P, Lloyd J. Clinical features and SPECT scanning in presumed corticobasal ganglionic degeneration. Journal of Clinical Neuroscience 1995;2:321-328.

Tanosaki M, Okushima T, Ozaki I, Baba M, Matsungaga M. A case of clinically diagnosed corticobasal degeneration with unilateral cortical refle myoconus showing so-called giant SEP. Rinsho Shinkeigaku 1999;39:711-716.

Terada K, Ikeda A, Mima T, Kimura K, Nagahama Y, Kamioka Y, Murone I, Kimura J, Shibasaki H. Familial Cortical Myoclonic Tremor as a Unique Form of Cortical Reflex Myoclonus. Mov Disord 1997;12:370-377.

Thompson PD, Bhatia KP, Brown P, Davis MB, Pires M, Quinn NP, Luthert P, Honovar M, O'Brian MD, Marsden CD, Harding AE. Cortical myoclonus in Huntington's disease. Mov Disord 1994;9:633-641.

Thompson PD, Day BL, Rothwell JC, Brown P, Britton TC, Marsden CD. The myoclonus in corticobasal degeneration. Brain 1994;117:1197-1207.

Tijssen MAJ, Marsden JF, Brown P. Frequency analysis of EMG activity in patients with idiopathic torticollis. Brain 2000;123:677-686.

Tijssen MAJ, Münchau A, Marsden JF, Lees AJ, Brown P. Descending control of muscles in patients with cervical dystonia. Mov Disord 2002;17:493-500.

Tolosa E. Montserrat L, Bayes A. Blink reflex studies in focal dystonias: enhanced excitability of brainstem interneurones in cranial dystonia and spasmodic torticollis. Mov Disord 1988;3:61-69.

Toro C, Pascual-Leone A, Deuschl G, Tate E, Pranzatelli MR, Hallett M. Cortical tremor. A common manifestation of cortical myoclonus. Neurology 1993;43:2346-2353.

Turton A, Lemon RN. The contribution of fast corticospinal input to the voluntary activation of proximal muscles in normal subjects and in stroke patients. Exp Brain Res 1999;129:559-572.

Vallbo AB, Wessberg J. Proprioceptive mechanisms and the control of finger movements. In: Wing AM, Haggard P, Flanagan JR, eds. Hand and brain: the neurophysiology and psychology of hand movements. London: Academic Press Inc., 1996:363-379.

Vallbo AB, Wessberg, J. Organisation of motor output in slow finger movements in man. J Physiol 1993;469:673-691.

Valldeoriola F, Valls-Solé J, Tolosa E, Nobbe FA, Muñoz JE, Martí J. The acoustic startle response is normal in patients with multiple system atrophy. Mov Disord 1997;12:697-700.

Vidailhet M, Rothwell JC, Thompson PD, Lees AJ, Marsden CD. The auditory startle response in the Steele-Richardson-Olszewski syndrome and Parkinson's disease. Brain 1992;115:1181-1192.

Volkmann J, Joliot M, Mogilner A, Ioannides AA, Lado F, Fazzini E, Ribary U, Llinas, R. Central motor loop oscillations in parkinsonian resting tremor revealed by magnetoencephalography. Neurology 1996;46:1359-1370.

Wilkens DE, Hallett M, Erba G. Primary generalised epileptic myoclonus: a frequent manifestation of minipolymyoclonus of central origin. J Neurol Neurosurg Psychiat 1985:48:506-516.

Wilson M, Bower JM. Cortical oscillations and temporal interactions in a computer simulation of piriform cortex. J Neurophysiol 1992;67:981-995.

Wollaston WH. On the duration of muscle action. Philosophical Transactions of the Royal Society of London 1810:1-5.

Yanagisawa N, Goto A. Dystonia Musculorum Deformans. Analysis with Electromyography. Journal of the Neurological Sciences 1971;13:39-65.

Yeomans JS, Frankland PW. The acoustic startle reflex: neurons and connections. Brain Res Rev 1996;21:301-314.

Yeomans JS, Li L, Scott BW, Frankland PW. Tactile, acoustic and vestiblar systems sum to elicit the startle reflex. Neurosci Biobehav Rev 2002;26:1-11.

Yeomans JS, Rosen JB, Barbeau J, Davis M. Double-pulse stimulation of startle-like responses in rats: refractory periods and temporal summation. Brain Res 1989;486:147-158.